Functional characterisation of neuropeptides that act as ligands for both calcitonin-type and pigment-dispersing factor-type receptors in a deuterostome

Xiao Cong [1, 2, #], Huachen Liu [1, #], Lihua Liu [1], Nayeli Escudero Castelán [3], Kite G.E. Jones [3], Michaela Egertová [3], Maurice R. Elphick [3, *] and Muyan Chen [1, *]

1 The Key Laboratory of Mariculture, Ministry of Education, Ocean University of China, Qingdao, China

2 Yantai Institute of Coastal Zone Research, Chinese Academy of Sciences, Yantai, China

3 School of Biological & Behavioural Sciences, Queen Mary University of London, London, United Kingdom

* Correspondence: m.r.elphick@qmul.ac.uk; chenmuyan@ouc.edu.cn;

# These authors contributed equally to this work.

Abstract

The calcitonin (CT) family of related peptides exerts diverse physiological effects in mammals via two G-protein coupled receptors: CTR and the CTR-like receptor CLR. Phylogenetic analysis of CT-type signaling has revealed the presence of CT-type peptides and CTR/CLR-type proteins in both deuterostome and protostome invertebrates. Furthermore, experimental studies have demonstrated that in the protostome *Drosophila melanogaster* the CT-like peptide DH_{31} can act as a ligand for a CTR/CLR-type receptor and a pigment-dispersing factor (PDF) receptor. Here we investigated the signaling mechanisms and functions of CT-type neuropeptides in a deuterostome invertebrate, the sea cucumber *Apostichopus japonicus* (phylum Echinodermata). In *A. japonicus*, a single gene encodes two CT-type peptides (AjCT1 and AjCT2) and both peptides act as ligands for a CTR/CLR-type receptor (AjCTR) and two PDF-type receptors (AjPDFR1, AjPDFR2), but with differential activation of downstream cAMP/PKA, Gαq/Ca^{2+}/PKC and ERK1/2 signaling pathways. AjCT1/AjCT2-encoding transcripts were detected in the central nervous system and a variety of organ systems and neuropeptide expression was visualized immunohistochemically using an antiserum to a starfish CT-type peptide (ArCT). *In vitro* pharmacological experiments demonstrated that AjCT1 and/or AjCT2 cause dose-dependent relaxation of longitudinal muscle and intestine preparations. Furthermore, *in vivo* pharmacological experiments, combined with gain- and loss-of-function experiments, revealed a potential physiological role for AjCT2/AjPDFR2 signaling in promoting feeding and growth in *A. japonicus*. To our knowledge, this is the first study to obtain evidence that CT-type peptides can act as ligands for both CTR/CLR-type and PDF-type receptors in a deuterostome. Moreover, it provides the first evidence for appetite-stimulating and growth-promoting effects of CT-type neuropeptides in bilaterians. Given the economic importance of *A. japonicus* as a foodstuff, the discovery of CT-type peptides as potential regulators of feeding and growth in this species may offer novel strategies for aquaculture applications.

Graphical abstract

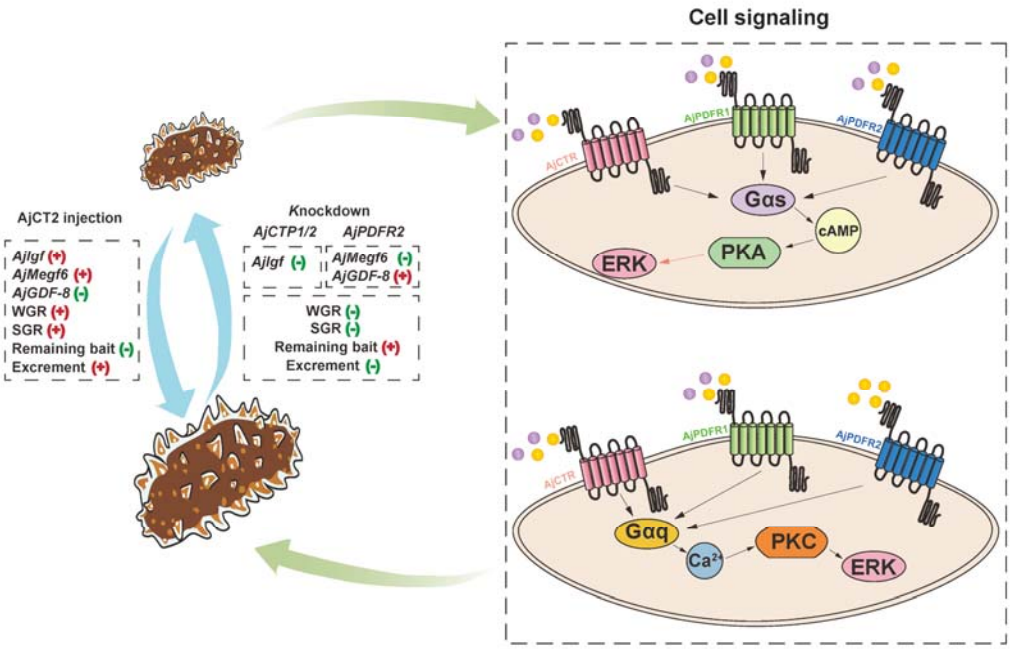

A schematic showing proposed molecular mechanisms by which CT-type signaling regulates feeding and growth in *A. japonicus*. AjCT1 and AjCT2 are represented by purple and yellow circles, respectively. For cell signaling, black arrows indicate that this process is activated, whilst the pink arrow indicates that ERK1/2 is activated in the AjCT1/AjPDFR1, AjCT2/AjPDFR1 and AjCT2/AjPDFR2 signaling pathways.

Keywords: calcitonin; neuropeptide; echinoderm; sea cucumber; calcitonin receptor; pigment-dispersing factor receptor; feeding; growth

1. Introduction

The peptide calcitonin (CT) was first identified as a hormone that regulates blood calcium levels and subsequently a family of CT-related neuropeptides was discovered in mammals, including calcitonin gene related peptides (CGRPs), amylin (AMY), adrenomedullin (AM), and CT receptor-stimulating peptide (CRSP) (Copp et al., 1962; Sekiguchi et al., 2009; Sekiguchi et al., 2016). Members of the CT-type family of peptides typically have a disulfide bond in their N-terminal region (Cai et al., 2018) and exert their physiological effects in mammals by binding to two related G protein-coupled receptors: CTR (CT receptor) and CLR (CTR-like receptor) (Martins et al., 2014). However, receptor activity-modifying proteins (RAMPs) acting as accessory proteins are key determinants of ligand selectivity for CTR and CLR (Mclatchie et al., 1998). Thus, formation of a complex with a RAMP is essential for CLR function, whereas RAMPs are not required for CTR ligand recognition (Kuwasako et al., 2011; Bomberger et al., 2012). Furthermore, binding of CT to CTR in the absence of RAMPs (Katafuchi et al., 2009) can activate signaling via several downstream pathways, including cAMP accumulation, Ca^{2+} mobilization, and ERK activation (Chen et al., 1998; Pondel, 2000; Walker et al., 2010; Andreassen et al., 2014).

Transcriptome/genome sequencing has enabled analysis of the phylogenetic distribution of CT-type signaling systems, indicating that the evolutionary origin of CT-type peptides and CTR/CLR-related receptors can be traced back to the urbilaterian common ancestor of deuterostomes and protostomes (Furuya et al., 2000; Johnson et al., 2005; Jékely, 2013; Mirabeau and Joly, 2013). Furthermore, in protostomes two different types of CT-related peptides have been identified. Firstly, peptides that are structurally similar to vertebrate CT-type peptides in having an N-terminal disulphide bridge and secondly, CT-like diuretic hormone 31 (DH_{31})-type peptides that lack an N-terminal disulphide bridge (Furuya et al., 2000; Conzelmann et al., 2013). Furthermore, phylogenetic analysis indicates that gene duplication in a common ancestor of the protostomes gave rise to genes encoding CT-type peptides with a disulphide bridge and DH_{31}-type peptides, which were then differentially retained in protostome taxa (Conzelmann et al., 2013; Cai et al., 2018).

Receptors for CT-type peptides with a disulphide bridge have been characterised in a molluscan species, the oyster *Crassostrea gigas* (now known as *Magallana gigas*), which has seven CTR/CLR-type receptors. Two of these receptors, named Cg-CT-R and Cragi-CTR2, were shown to be specifically activated by the CT-type neuropeptides Cragi-CT1b and Cragi-CT2, respectively, thereby mediating intracellular Ca^{2+} mobilization and cAMP accumulation (Schwartz *et al.*, 2019). CT-type peptides with a disulphide bridge are not present in the insect *Drosophila melanogaster.* However, receptors that are activated by DH_{31} have been identified in this species and, interestingly, DH_{31} can act as a ligand for two types of receptors. Thus, DH_{31} acts as a ligand for a CTR/CLR-related protein (CG17415), but it also acts as a ligand for a protein (CG13758) that is the receptor for pigment-dispersing factor (PDF) (Johnson et al., 2005; Mertens et al., 2005; Shafer et al., 2008). Furthermore, the functional significance of the existence of dual receptor signaling pathways for DH_{31} in *Drosophila* has been investigated extensively (Johnson et al., 2005; Goda et al., 2019).

Currently, relatively little is known about CT-type signaling systems in deuterostome invertebrates. Analysis of transcriptome/genome sequence data has enabled identification of genes/transcripts encoding CT-type peptides and candidate CTR/CLR-type receptors for these peptides in several deuterostome invertebrate taxa, including urochordates (e.g. *Ciona intestinalis*), cephalochordates (e.g. *Branchiostoma floridae*), hemichordates (e.g. *Saccoglossus kowalevskii*) and echinoderms (e.g. *Strongylocentrotus purpuratus*) (Burke et al., 2006; Sekiguchi et al., 2009; Sekiguchi et al., 2016; Rowe and Elphick, 2012; Martins et al., 2014). Furthermore, analysis of the expression and action of CT-type peptides identified in the starfish *Asterias rubens* and *Patiria pectinifera* has revealed that they act as muscle relaxants (Cai et al., 2018; Semmens et al., 2016). However, experimental confirmation of ligand-receptor partners has thus far only been reported for the cephalochordate *B. floridae*, where three CT-type peptides were shown to act as ligands for a CTR/CLR-type receptor when it is co-expressed with RAMP-type proteins (Sekiguchi et al., 2016). To gain further insights into the mechanisms of CT-

type signaling in invertebrate deuterostomes, the aim of this study was to functionally characterise CT-type peptides and their receptors in an echinoderm – the sea cucumber *Apostichopus japonicus*.

A. japonicus is an economically important species in Asian aquaculture (Pangestuti and Arifin, 2018; Guo et al., 2020) and a species representative of the phylum Echinodermata. As a phylum of deuterostome invertebrates, echinoderms form a sister clade to the chordates together with hemichordates and xenoturbellids (Bromham and Degnan, 1999; Bourlat et al., 2006; Dunn et al., 2008) and as such they occupy a key "intermediate" phylogenetic position relative to the protostome invertebrates and vertebrates (Zandawala et al., 2017), which make them attractive as experimental systems to address evolutionary questions. In our previous studies, we have established this species as a model system to obtain insights into the evolutionary history and comparative physiology of neuropeptide signaling systems in bilaterians (Chen et al., 2019; Li et al., 2022; Zheng et al., 2022; Cong et al., 2023; Zheng et al., 2024). A gene encoding two CT-type peptides (AjCT1 and AjCT2) has been identified in *A. japonicus* (Chen et al., 2019) and a candidate receptor (AjCTR) for these peptides has also been predicted (Huang et al., 2021). Furthermore, relevant to the discovery that the CT-like peptide DH_{31} can act as a ligand for both a CTR/CLR-type receptor and a PDF-type receptor in *Drosophila*, the sequences of two PDF-type receptors have been identified in *A. japonicus* (AjPDFR1 and AjPDFR2) (Huang et al., 2021).

The first aim of this study was to investigate if AjCT1 and/or AjCT2 act as ligands for AjCTR, AjPDFR1 and AjPDFR2 and to characterise the downstream signaling pathways that are activated when AjCT1 and/or AjCT2 bind to their receptor(s). The second aim was to investigate the physiological roles of AjCT1 and AjCT2 in *A. japonicus* by analysing the expression of the gene encoding these peptides, investigating CT-type neuropeptide expression using immunohistochemistry, examining the *in vitro* and *in vivo* pharmacological effects of these peptides and performing loss-of-function tests. The functional characterisation of CT-type signaling in *A. japonicus* reported in this study provides new insights into the evolution and

comparative physiology of neuropeptides and a basis for application of neuropeptide-based strategies to improve aquaculture methods for this economically important species.

2. Results

2.1 Characterization and phylogenetic analysis of AjCT1/2

The complete cDNA sequences of the CT-type neuropeptide precursors *AjCTP1* and *AjCTP2* were confirmed. The coding sequence of *AjCTP2* is shorter than *AjCTP1* (Figure 1A) but both transcripts encode precursor proteins that comprise the same predicted 23-residue N-terminal signal peptide (Figure 1-figure supplement 1A). *AjCTP1* encodes both putative CT-type neuropeptides (AjCT1 and AjCT2), while *AjCTP2* only encodes AjCT2 (Figure 1A, Figure 1-figure supplement 1A and 1B). Exon and intron structure analysis showed that *AjCTP1* comprises four exons, with AjCT1 and AjCT2 encoded in the third and fourth exons, respectively. *AjCTP2* comprises three exons, excluding the third exon that encodes AjCT1 (Figure 1A). Phylogenetic analysis revealed that AjCTP1 and AjCTP2 are closely related to CT-type precursors from other sea cucumbers (*Holothuria glaberrima* and *Holothuria scabra*), and are positioned within a clade that also contains CT-type precursors from other echinoderms (sea urchin *S. purpuratus*, starfish *A. rubens*). Furthermore, the echinoderm CT-type precursors are positioned within a clade that also comprises CT-type precursors from chordates, whilst DH_{31}/CT-type precursors from protostomes are positioned in a separate clade (Figure 1B). Sequence alignment of CT-related neuropeptides revealed that, with the exception of DH_{31}-type peptides, the N-terminal region of CT-related peptides has a pair of conserved cysteine residues that are known or predicted to form a disulfide bond. Another conserved feature is a C-terminal proline residue, with the exception of CGRPs (Figure 1-figure supplement 2). Accordingly, both AjCT1 and AjCT2 have these conserved characteristics.

2.2 Characterization and phylogenetic analysis of three candidate receptors for AjCT1/2

The sequences of three candidate receptors for AjCT1 and AjCT2 were obtained

by RACE and phosphorylation sites were predicted, as shown in Figure 2-figure supplement 1A, 1B, and 1C. Phylogenetic analysis revealed that CTR/CLR-related receptors divided into three clades and an *A. japonicus* CTR/CLR-type receptor (AjCTR) was positioned in a clade with other deuterostome CTR/CLR-type receptors, including human CTR and CLR. The other two clades comprised protostome DH31-type receptors, which include the *Drosophila* receptor that has been identified experimentally as the receptor for DH31, and other protostome CTR/CLR-related receptors (Cluster A), including two receptors in the mollusc *Magallana gigas* that have been identified experimentally as receptors for CT-like peptides with a disulphide bridge. The phylogenetic analysis also revealed that two *A. japonicus* PDF-type receptors (AjPDFR1 and AjPDFR2) were positioned in a clade comprising PDF-type receptors, with one branch containing PDF-type receptors from deuterostomes (including AjPDFR1 and AjPDFR2) and another branch containing PDF-type receptors from protostomes (including the *Drosophila* PDF receptor) (Figure 2). Domain prediction of the candidate receptors showed that AjCTR had HRM (Hormone receptor) and 7tm_GPCRs (seven-transmembrane G protein-coupled receptor) superfamily domains (Figure 2-figure supplement 2A), whereas AjPDFR1 and AjPDFR2 only presented the 7tm_GPCRs superfamily domain (Figure 2-figure supplement 2B). To further investigate an orthologous relationship of the candidate receptors with homologous receptors in other echinoderms, we conducted a gene synteny analysis in *A. japonicus*, *A. rubens* and *L. variegatus*. The neighboring genes of *AjCTR* included *GOLGA4*, *NeuroD*, *CRF2*, *ppGalNAc-T*, *URB3*, *SLC40A1*, *CMAH* and *MAGP*. The relative positions of these genes were different from those in *A. rubens* and *L. variegatus* (Figure 2-figure supplement 2C). The same situation was also observed for the synteny analysis of PDFRs.

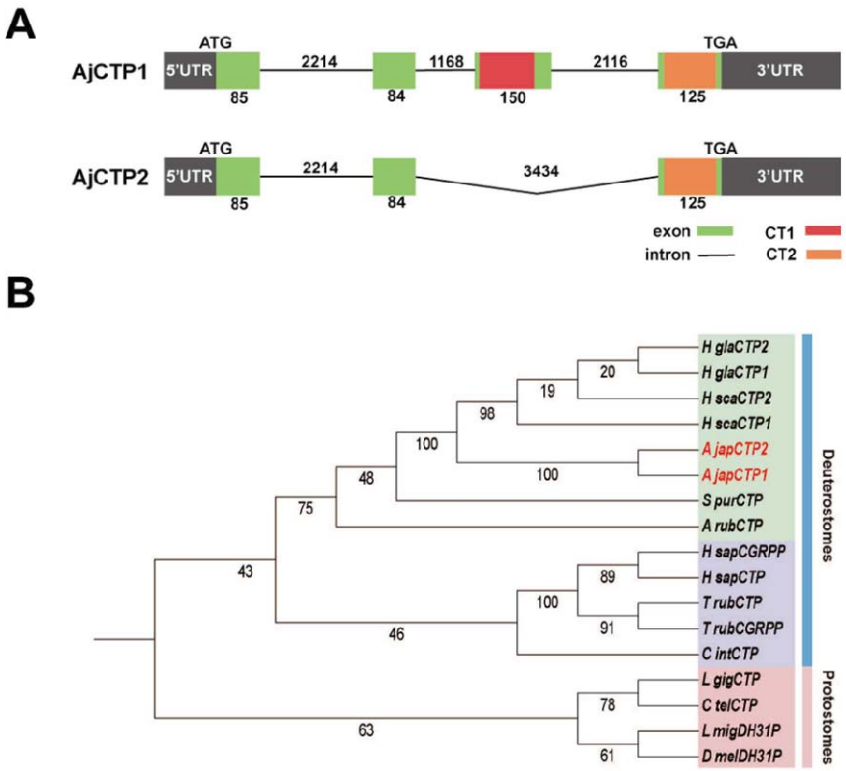

Figure 1. CT-type neuropeptide precursors and candidate receptors for CT-type peptides in *A. japonicus.* (A) Alternative splicing schematic of *AjCTP1* and *AjCTP2*. Exons are represented by green rectangles, introns are represented by lines, AjCT1 and AjCT2 are represented by red and orange rectangles respectively, upstream and downstream non-coding regions are represented by gray rectangles. The numbers represent the length of exons or introns. (B) Phylogenetic analysis of AjCTP1 and AjCTP2 and CT-related neuropeptide precursors from other bilaterians. CT-type precursors from deuterostomes are shown in green (echinoderms) and purple (chordates), CT-type precursors from protostomes are shown in pink. Full species names and accession numbers are listed in Supplementary table 1.

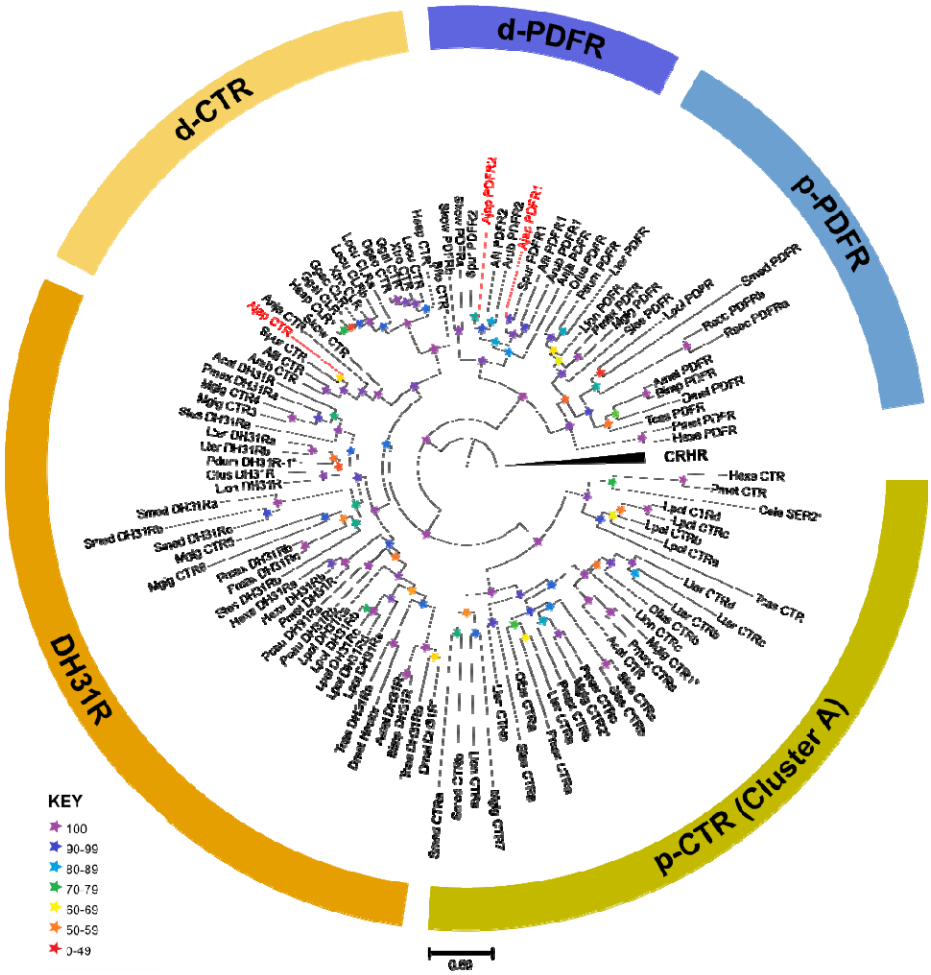

Figure 2. Maximum-likelihood phylogenetic tree of bilaterian CT-type and PDF-type receptor families, including those found in *A. japonicus*, rooted with CRH-type receptors. The tree comprises distinct CT-type receptor and PDF-type receptor clades with bootstrap support >90. The CT-type receptor clade is subdivided into a deuterostome-specific clade (dCTR, yellow), which includes the *A. japonicus* CTR (AjCTR), and two protostome receptor clades. One comprises DH31 receptors (DH31R, orange), and the other comprises protostome-specific CTRs (p-CTR (Cluster A), green). The name 'Cluster A' is referenced for consistency with Cardoso et al., 2024. The PDF-type receptors are subdivided into protostome (p-PDFR, blue) and deuterostome (d-PDFR, purple) clades, with the latter including the two *A. japonicus* PDFRs (AjPDFR1, AjPDFR2). The stars represent branch support (bootstrap 1000 replicates, see key). The scale bar indicates amino acid substitutions per site. The *A. japonicus* receptors characterised in this paper are highlighted in red, and CT-type family receptors for which ligands have been identified experimentally in other published studies are indicated with an asterisk (Gorn et al., 1992; McLatchie et al., 1998; Johnson et al., 2005; Bauknecht & Jekely, 2015; Sekiguchi et al., 2016; Schwartz et al., 2019; Beets et al., 2023; Huang et al., 2024). Species names are abbreviated as follows: Acal (*Aplysia californica*), Afil (*Amphiura filiformis*), Ajap (*Apostichopus japonicus*), Amel (*Apis mellifera*), Anja (*Anneissia japonica*), Arub (*Asterias rubens*), Bflo (*Branchiostoma*

floridae), Bimp (*Bombus impatiens*), Cele (*Caenorhabditis elegans*), Cint (*Ciona intestinalis*), Dmel (*Drosophila melanogaster*), Ggal (*Gallus gallus*), Ggec (*Gekko gecko*), Hexe (*Hypsibius exemplaris*), Hsap (*Homo sapiens*), Llon (*Lineus longissimus*), Locu (*Lepisosteus oculatus*), Lpol (*Limulus polyphemus*), Lter (*Lumbricus terrestris*), Mgig (*Magallana gigas*), Ofus (*Owenia fusiformis*), Pcau (*Priapulus caudatus*), Pdum (*Platynereis dumerilii*), Pmax (*Pecten maximus*), Pmet (*Paramacrobiotus metropolita*), Rsoc (*Rotaria socialis*), Scla (*Styela clava*), Skow (*Saccoglossus kowalevskii*), Sles (*Sepioteuthis laessoniana*), Smed (*Schmidtea mediterranea*), Spur (*Strongylocentrotrus purpuratus*), Tcas (*Tribolium castaneum*), Xtro (*Xenopus tropicalis*). Sequence accession numbers are listed in supplementary table 2.

2.3 AjCT1 and AjCT2 act as ligands for AjCTR, AjPDFR1 and AjPDFR2

To investigate if AjCT1 and/or AjCT2 act as ligands for AjCTR, AjPDFR1 and AjPDFR2, here, two receptor assay methods were employed. As shown in Figure 3A, both AjCT1 and AjCT2 (10^{-6} M) caused a significant increase in CRE luciferase activity in HEK293T cells transfected with AjCTR, AjPDFR1 or AjPDFR2. Furthermore, this effect was inhibited by pre-incubation of cells with the PKA inhibitor H89. The intracellular accumulation of cAMP was also measured, and this showed that AjCT1 and AjCT2 (10^{-9} – 10^{-5} M) caused a dose-dependent increase in cAMP in HEK293T cells transfected with AjCTR, AjPDFR1 or AjPDFR2 (Figure 3B). However, when exposed to AjCT1 or AjCT2, the maximum accumulation of intracellular cAMP was higher in cells transfected with AjCTR than in cells transfected with AjPDFR1 and AjPDFR2 (Figure 3B). Measurement of SRE luciferase activity revealed that AjCT1 and AjCT2 (10^{-6} M) administration evoked an increase in activity in HEK293T cells transfected with AjCTR and AjPDFR1 (Figure 4A). However, in HEK293T cells transfected with AjPDFR2, an increase in SRE luciferase activity was only observed with AjCT2, not with AjCT1. Furthermore, as shown in Figure 4A, AjCT1- and AjCT2-induced increases in SRE luciferase activity were not observed in cells that had been pre-incubated with FR900359 (Gαq protein inhibitor) and Gö 6983 (PKC inhibitor). As shown in Figure 4-figure supplement 1, receptors localized in the cell membrane, but after exposure to AjCT1 and AjCT2 (10^{-6} M) for 15 min, internalization of pEGFP-N1/*AjCTR*, pEGFP-N1/*AjPDFR1* and pEGFP-N1/*AjPDFR2* was observed in transfected HEK293T cells (Figure 4B). Taken together, all these findings indicate that AjCT1 and AjCT2 can act as ligands for the

three candidate receptors and then activate cAMP/PKA signaling and Gαq/Ca^{2+}/PKC signaling in all combinations, with the exception of AjCT1/AjPDFR2 which only activates the cAMP/PKA cascade.

To investigate whether the activated signaling pathways may exert downstream effects via the ERK–MAPK pathway, the phosphorylation levels of ERK1/2 were analysed in transfected HEK293T cells. pERK1/2 levels in cells transfected with AjCTR or AjPDFR1, but not AjPDFR2, were significantly increased after a 5 min incubation with AjCT1 (Figure 5A). Furthermore, this effect was blocked by the PKC inhibitor in AjCTR-expressing cells, and this effect was blocked by both PKA and PKC inhibitors in AjPDFR1-expressing cells (Figure 5-figure supplement 1A). pERK1/2 levels in cells transfected with AjCTR or AjPDFR1 or AjPDFR2, were significantly increased after a 5 min incubation with AjCT2 (Figure 5B). Moreover, this effect persisted until 15 min after exposure to AjCT in both AjCTR-transfected cells and AjPDFR1-transfected cells but not in AjPDFR2-transfected cells (Figure 5B, Table 1). Furthermore, these effects were blocked by PKA and PKC inhibitors in AjPDFR1 and AjPDFR2 expressing cells, whereas in AjCTR expressing cells, peptide-induced pERK1/2 activity was only blocked by a PKC inhibitor (Figure 5-figure supplement 1B). These results indicate that, with the exception of AjCT1/AjPDFR2, both AjCT1 and AjCT2 can activate the ERK1/2 cascade by binding to the candidate receptors.

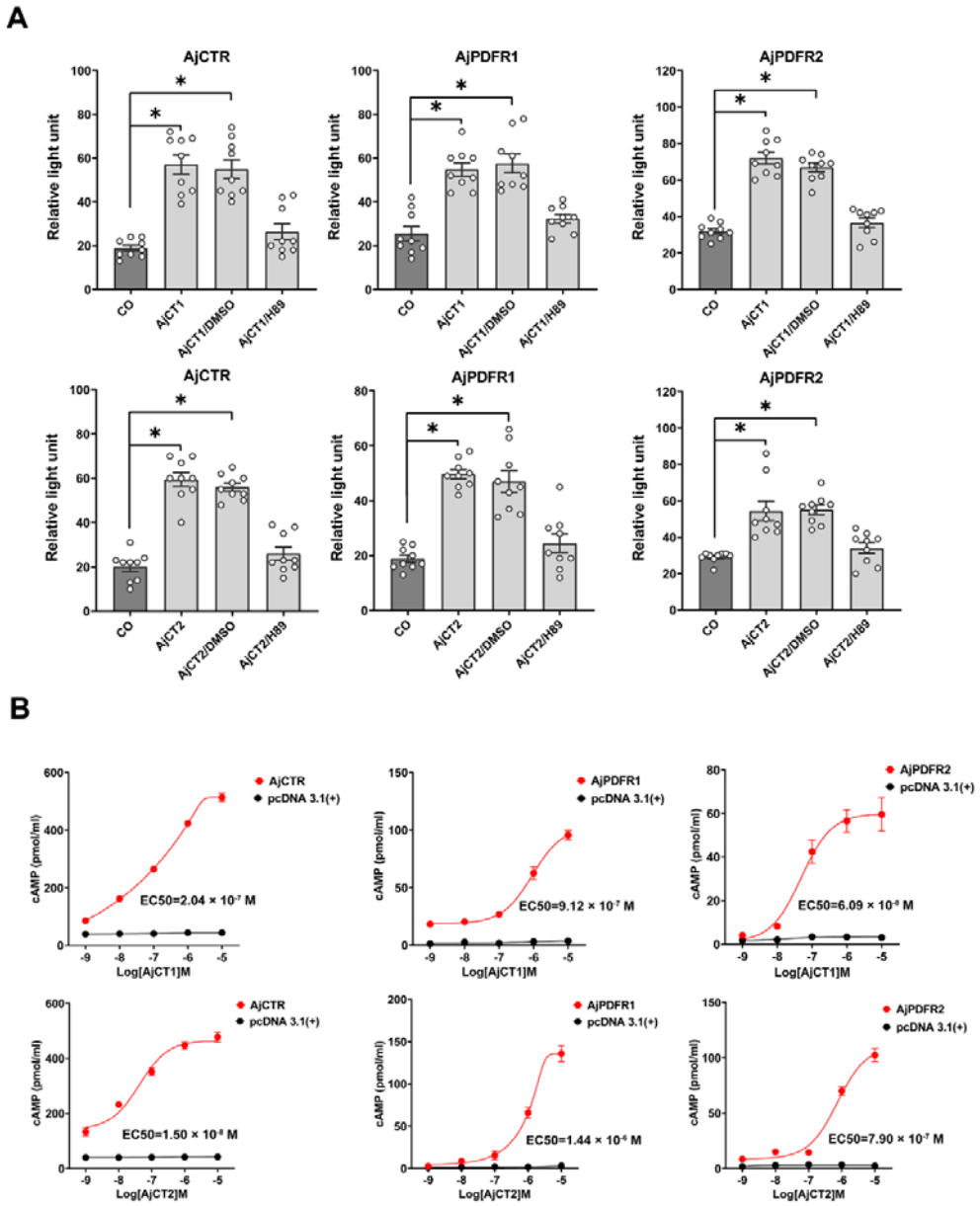

Figure 3. Pharmacological characterisation of AjCT1 and AjCT2 as ligands for the *A. japonicus* receptors AjCTR, AjPDFR1 and AjPDFR2. (A) CRE-driven luciferase activity measured in HEK293T cells transfected with one of the three candidate receptors after exposure to AjCT1 or AjCT2 or neuropeptide + DMSO or neuropeptide + H89 (10 μM) or serum-free DMEM (CO, negative control). The neuropeptide concentration used here was 10^{-6} M. Mean values with standard deviations (n = 9) are shown. * indicates a statistically significant difference with $p < 0.05$. (B) Measurement of cAMP accumulation after exposure to AjCT1 or AjCT2 (10^{-9} – 10^{-5} M). No cAMP elevation is observed in control experiments where HEK293T cells were transfected with empty pcDNA 3.1(+) (black circle). The estimated EC_{50} of AjCT1 for AjCTR, AjPDFR1 and AjPDFR2 were 2.04 × 10^{-7} M (95% CI: 1.06 × 10^{-7} -8.69 × 10^{-7} M), 9.12 × 10^{-7} M (95% CI: 5.56

× 10^{-7} -4.45 × 10^{-6} M) and 6.09 × 10^{-8} M (95% CI: 2.23 × 10^{-8} -2.84 × 10^{-7} M) respectively. The estimated EC_{50} of AjCT2 for AjCTR, AjPDFR1 and AjPDFR2 were 1.50 × 10^{-8} M (95% CI: 1.03 × 10^{-9} -3.89 × 10^{-8} M), 1.44 × 10^{-6} M (95% CI: 1.04 × 10^{-6} -1.99 × 10^{-6} M) and 7.90 × 10^{-7} M (95% CI: 5.73 × 10^{-7} -1.06 × 10^{-6} M) respectively. Error bars represent SEM for three independent experiments.

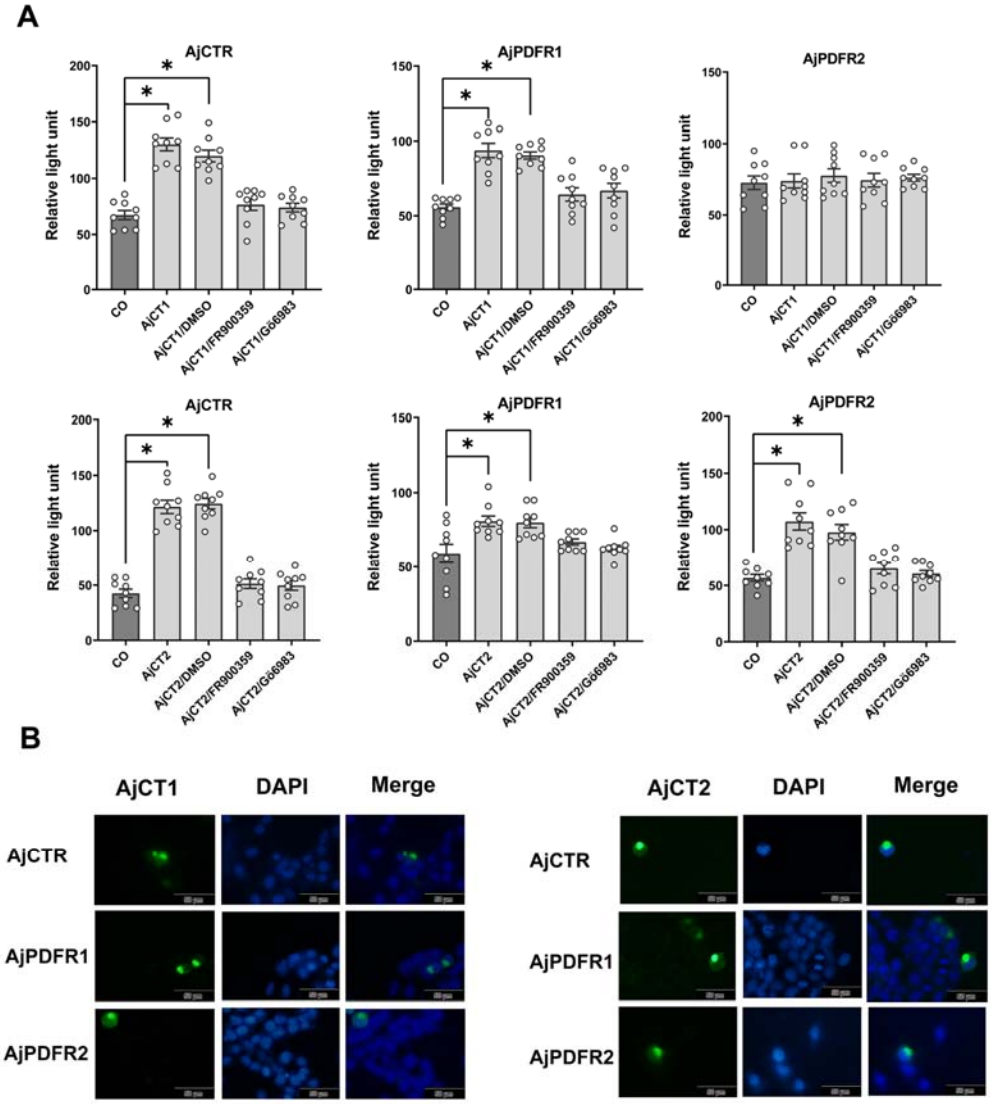

Figure 4. SRE-driven luciferase activity and receptor internalization in cells transfected with AjCTR, AjPDFR1 or AjPDFR2 and exposed to AjCT1 or AjCT2. (A) SRE-driven luciferase activity measured after incubation with neuropeptide (10^{-6} M AjCT1 or AjCT2)/DMSO, neuropeptide (10^{-6} M)/FR900359 (1uM) and neuropeptide (10^{-6} M)/Gö 6983 (1 μM). Mean values with standard deviations (n = 9) are shown. * indicates a statistically significant difference with *p*

< 0.05. (B) Internalization of AjCTR, AjPDFR1 and AjPDFR2 after 15 min treatment with 10^{-6} M AjCT1 or AjCT2. Green fluorescence represents the localization of pEGFP-N1/receptors in cells. The cell nucleus probe (DAPI) was used for cell nucleus staining. Scale bar: 50 μm. All pictures are representative of three independent experiments.

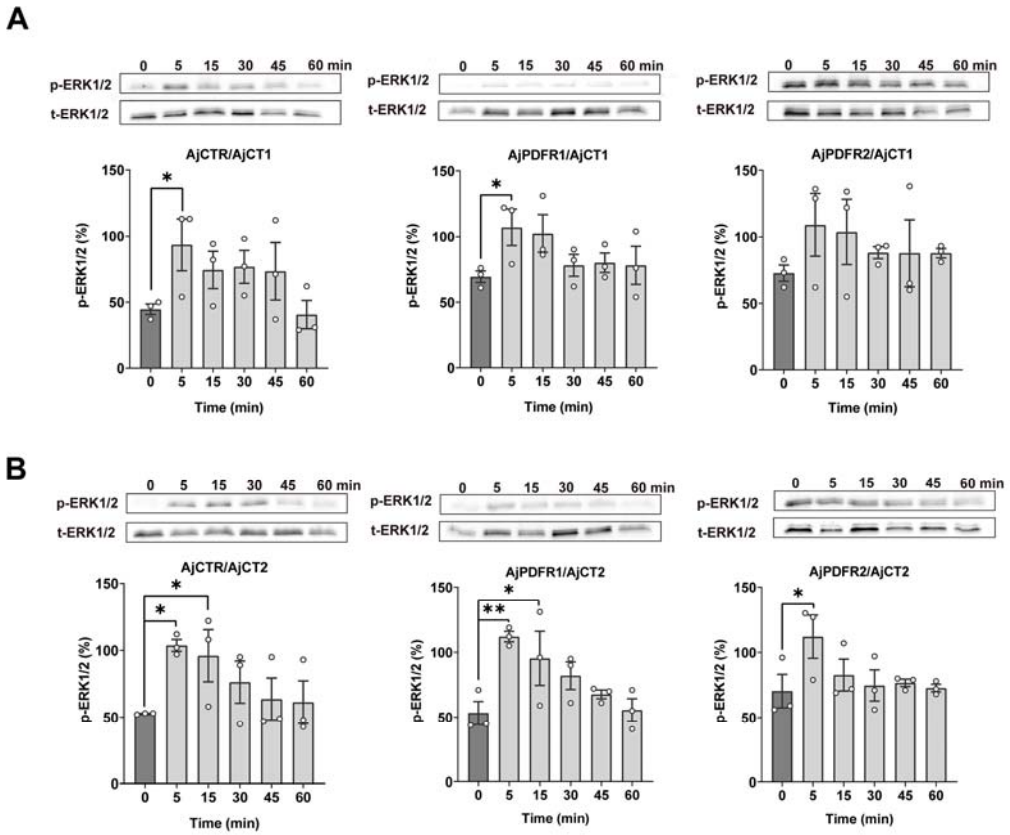

Figure 5. ERK1/2 activity in cells transfected with AjCTR, AjPDFR1 or AjPDFR2 and exposed to AjCT1 or AjCT2. (A) and (B) show the immunoblot intensity of representative phosphorylation bands. The transfected HEK293T cells were incubated with AjCT1 (10^{-6} M) or AjCT2 (10^{-6} M) for 0, 5, 15, 30, 45 and 60 min. The p-ERK1/2 was normalized based on t-ERK1/2. All images are representative of three independent experiments. Error bars represent SEM for three independent experiments. Statistically significant differences are indicated as follows: *: $p < 0.05$, **: $p < 0.01$.

Table 1. Activation of signaling pathways

Assays / Receptors	cAMP/PKA/ERK1/2		Gαq/Ca^{2+}/PKC/ERK1/2	
	AjCT1	AjCT2	AjCT1	AjCT2
AjCTR	×*	×*	√	√
AjPDFR1	√	√	√	√
AjPDFR2	×*	√	×	√

A tick indicates cAMP/PKA/ERK1/2 or Gαq/Ca^{2+}/PKC/ERK1/2 activation, the cross indicates no

activation, the cross with * indicates that the cAMP/PKA pathway is activated, while the ERK1/2 pathway is not activated.

2.4 Expression profile of AjCTP1/2 and its receptors in A. japonicus

qRT-PCR analysis revealed that *AjCTP1/2* had the highest expression level in the circumoral nervous system (CNS) (Figure 6A). The expression levels of three receptors differed from those of *AjCTP1/2*. *AjCTR* (Figure 6B) and *AjPDFR1* (Figure 6C) showed the highest expression level in CNS and longitudinal muscle, whereas *AjPDFR2* exhibited highest expression in the respiratory tree (Figure 6D).

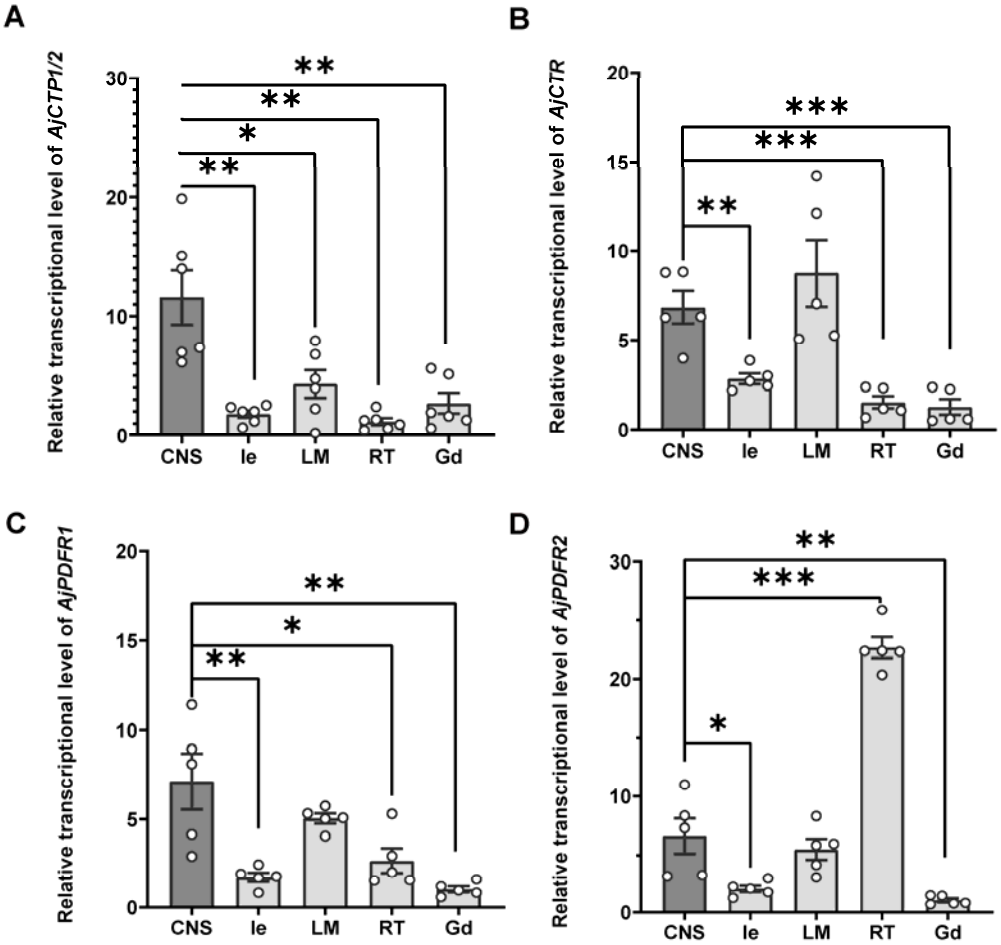

Figure 6. The relative expression level of *AjCTP1/2* (A), *AjCTR* (B), *AjPDFR1* (C) and *AjPDFR2* (D) in different tissues. The circumoral nervous system was selected as the control group. Values are means ± SEM (*AjCTP1/2*, n = 6; *AjCTR*, *AjPDFR1* and *AjPDFR2*, n = 5). Asterisks represent significant differences as follows: *: $p < 0.05$, **: $p < 0.01$, ***: $p < 0.001$. CNS, circumoral

nervous system; Gd, gonad; Ie, intestine; LM, longitudinal muscle; RT, respiratory tree.

To investigate the distribution of CT-type neuropeptides in *A. japonicus* using immunohistochemistry we employed an antiserum to the starfish (*Asterias rubens*) CT-type neuropeptide ArCT, which has been used previously for visualization of the expression of ArCT in *A. rubens* (Cai et al., 2018) and a CT-type neuropeptide in the feather star *Antedon mediterranea* (AmCT; Aleotti et al., 2022). The antigen peptide that was used to generate the ArCT antiserum (KYNSPFGASGP-NH_2) shares a C-terminal FGxxGP-NH_2 (where X is variable) motif with both AjCT1 (FGSAGP-NH_2) and AjCT2 (FGSGGP-NH_2) and therefore antibodies to ArCT may cross-react with AjCT1 and/or AjCT2. Accordingly, the ArCT antiserum revealed immunostaining in the central nervous system (radial nerve cords and circumoral nerve ring) (Figure 7A–F), which was abolished by pre-incubation of the antiserum with the ArCT antigen peptide (Figure 7-figure supplement 1). More specifically, high magnification images revealed immunostaining was localised in the ectoneural region, but not in the hyponeural region, of the radial nerve cords, with bilaterally symmetrical immunostained cells (neuronal somata) present in the ectoneural epithelium (Figure 7C). Likewise, immunostained cells were revealed in the ectoneural region of the circumoral nerve ring (Figure 7D-F). Furthermore, immunostaining was also revealed in tentacle nerves, which emanate from the circumoral nerve ring (Figure 7D-F), and in several regions of the digestive system, including the pharynx/stomach (Figure 7G), intestine (Figure 7H) and cloaca (Figure 7I). No immunostaining was observed in the longitudinal muscles (Figure 7A, B).

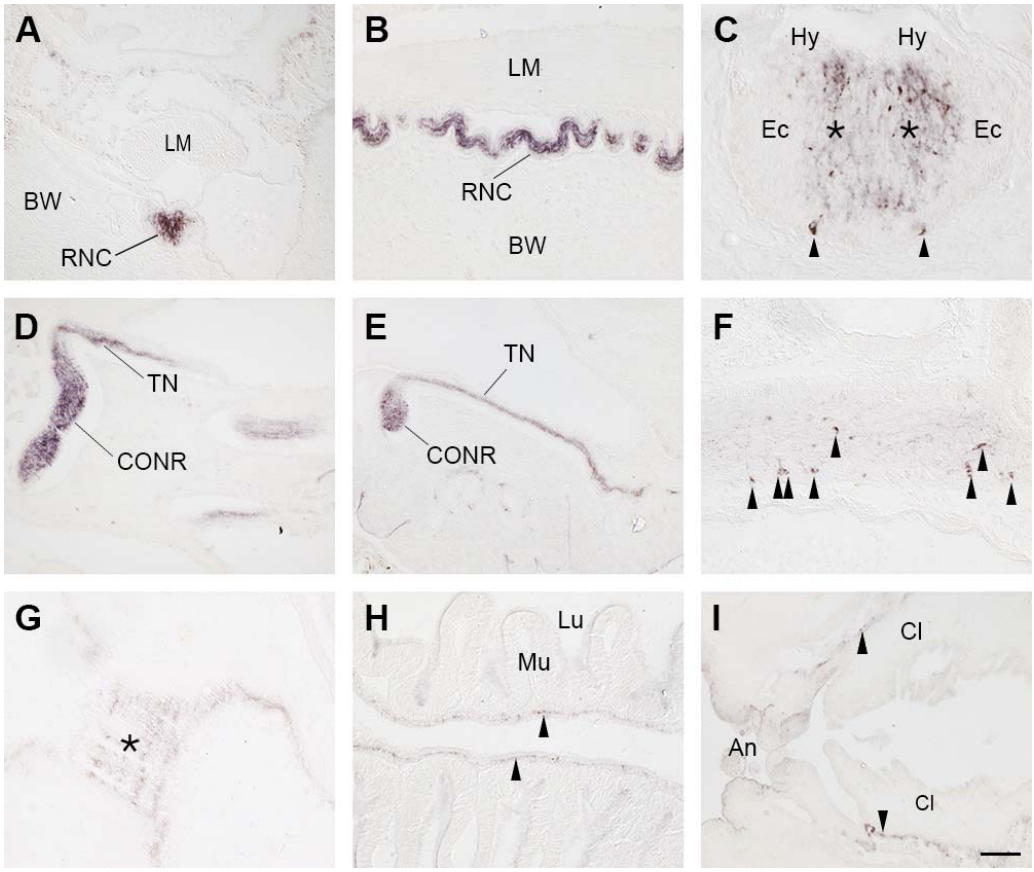

Figure 7. Immunohistochemical localization of CT-type neuropeptide expression in *A. japonicus* using antibodies to the starfish CT-type neuropeptide ArCT. A. Transverse section showing immunostaining in the radial nerve cord. B. Longitudinal section showing immunostaining in the radial nerve cord. C. High magnification image of a transverse section showing immunostained cells (arrowheads) and immunostained fibers in the neuropile (asterisks) of the ectoneural region of the radial nerve cord. Note the absence of immunostaining in the hyponeural region. D, E. Longitudinal sections showing immunostaining in the circumoral nerve ring and in tentacle nerves that emanate from the circumoral nerve ring. F. High magnification image of a transverse section showing immunostained cells (arrowheads) in the circumoral nerve ring. G. Longitudinal section showing immunostained fibers (asterisk) at the junction between the pharynx and the stomach. H. Longitudinal section showing immunostained fibers (arrowheads) in the intestine. I. Longitudinal section showing immunostained fibers (arrowheads) in the cloaca. Abbreviations: An, anus; BW, body wall; Cl, cloaca; CONR, circumoral nerve ring; Ec, Ectoneural region of the radial nerve cord; Hy, hyponeural region of the radial nerve cord; LM, longitudinal muscle; Lu, lumen; Mu, mucosa; RNC, radial nerve cord; TN, tentacle nerve. Scale bar, as shown in panel I, is 100 µm in A, B, D, E, I; 50 µm in F, G, H; 25 µm in C.

2.5 AjCT1 and AjCT2 causes dose-dependent relaxation of longitudinal muscle and intestine preparations from A. japonicus

Both AjCT1 and AjCT2 caused dose-dependent relaxation of longitudinal

muscles from *A. japonicus* at 10^{-10}–10^{-6} M (Figure 8). The maximum relaxant effects of AjCT2 (10^{-6} M) on longitudinal muscles are illustrated in Figure 8-figure supplement 1A. At the highest concentration tested (10^{-6} M), AjCT1 and AjCT2 caused 30.07 ± 7.49% and 32.50 ± 14.49% reversal of acetylcholine (ACh)-induced contraction, respectively (Figure 8A, 8B). AjCT1 had no effect on the contractile state of intestine preparations, even at concentrations as high as 10^{-5} M (Figure 8C). Unlike AjCT1, AjCT2 caused dose-dependent relaxation of intestine preparations, with 26.33 ± 8.75% reversal of ACh-induced contraction observed at 10^{-5} M (Figure 8D). Control experiments in which ACh-induced contraction was recorded without addition of CT-type peptides showed that ACh-induced contraction of longitudinal muscles and intestinal preparations persisted for ≥15 minutes, confirming that relaxation effects observed could be attributed to addition of AjCT1 or AjCT2 (Figure 8-figure supplement 1B, 1C).

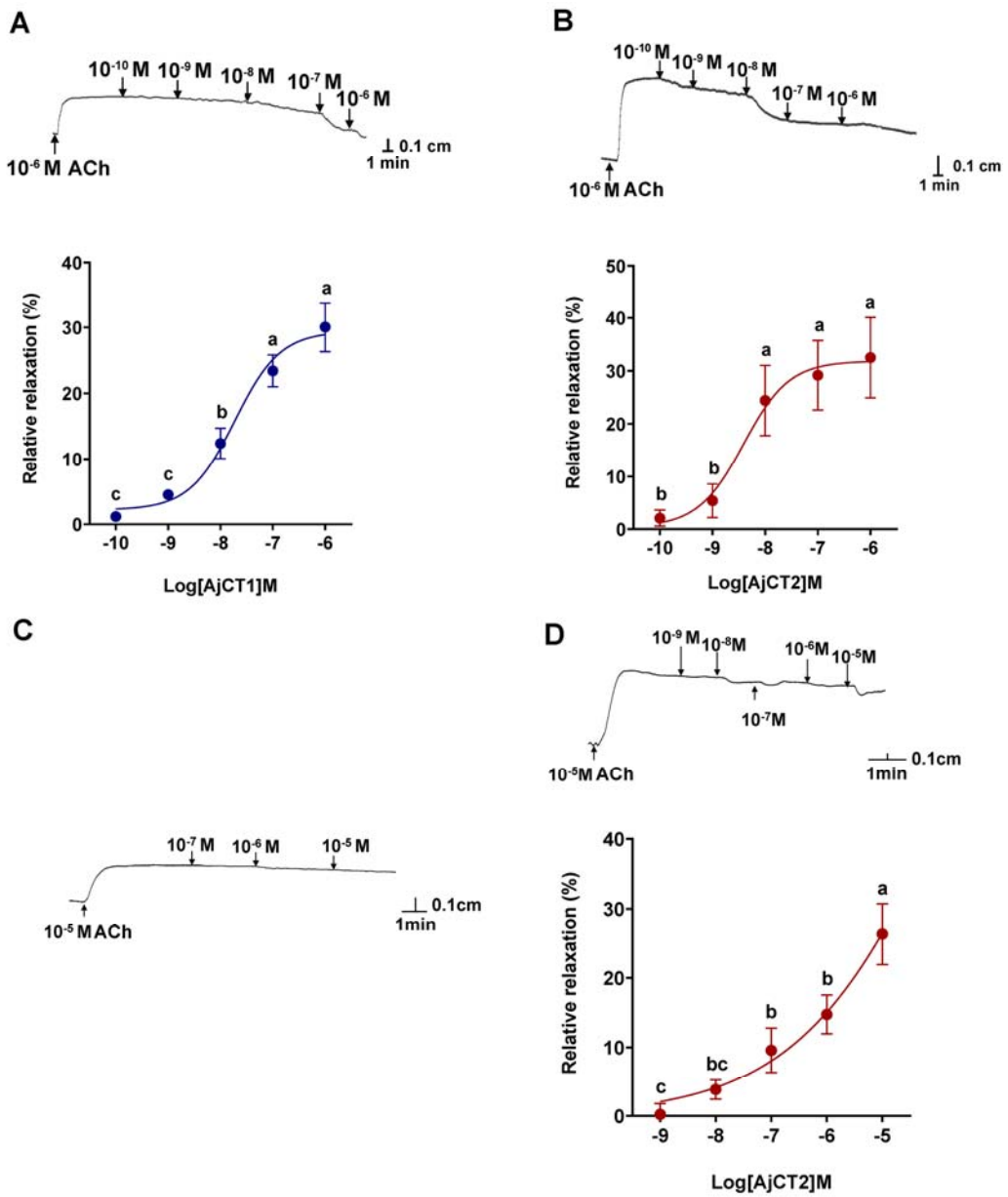

Figure 8. Pharmacological effects of AjCT1 and AjCT2 on longitudinal muscle and intestine preparations from *A. japonicus.* (A) and (B) show representative recordings of the relaxing effects of AjCT1 and AjCT2 on longitudinal muscle preparations. The graphs show the dose-dependent relaxing effects of AjCT1 and AjCT2 (10^{-10} – 10^{-6} M), calculated as the percentage reversal of the contracting effect of 10^{-6} M ACh. (C) and (D) show representative recordings of experiments in which AjCT1 (10^{-7} – 10^{-5} M) and AjCT2 (10^{-9} – 10^{-5} M) were tested on intestine preparations. AjCT1 had no effect, but AjCT2 caused relaxation and the graph shows the dose-dependent relaxing effect of AjCT2 (10^{-9} – 10^{-5} M), calculated as the percentage reversal of the contracting effect of 10^{-5} M ACh. All recordings shown are representative of three independent experiments.

Mean values ± SEM were determined from three preparations. Lowercase letters a, b and c above

columns indicate the statistical difference at $p < 0.05$, whilst there is no significant difference between bc and c.

2.6 AjCT2 affects feeding and growth in A. japonicus

To investigate the effects of AjCT1 and AjCT2 *in vivo*, a long-term injection experiment was carried out at concentrations of 5×10^{-3} mg/mL (low-dose group) and 5×10^{-1} mg/mL (high-dose group), with the injection volume calculated based on the wet weight of sea cucumbers at 1 μL/g. As shown in Figure 9A, there were no significant changes in weight gain rate (WGR) and specific growth rate (SGR) in the AjCT1 low concentration group (CT1L), AjCT1 high concentration group (CT1H) and AjCT2 low concentration group (CT2L) ($p \geq 0.05$), but in the AjCT2 high concentration group (CT2H) there was a significant increase in WGR and SGR in comparison with the control group (CO) ($p < 0.05$). Correspondingly, the mass of feces increased and the residual bait mass decreased (Figure 9A-figure supplement 1). Furthermore, the relative intestinal expression levels of several growth factors were investigated and the results showed that *AjGDF-8*, a growth inhibitory factor (Li et al., 2016), was significantly down-regulated in all the experimental groups. In contrast, the relative expression levels of *AjIgf* and *AjMegf6*, growth promoting factors (Párrizas and LeRoith, 1997; Deribe et al., 2009), were significantly up-regulated in intestines (Figure 9B).

Subsequently, the relative intestinal expression levels of AjCT1 and AjCT2 receptors were further tested for the CT2H group. The results showed that the relative expression levels of all three receptors were significantly up-regulated, with the ranked fold change being *AjCTR* > *AjPDFR1* > *AjPDFR2* (Figure 9C). Conversely, the relative expression levels of the three receptor genes were significantly down-regulated in *siAjCTP1/2*-1 treated animals (Figure 10A, 10B and 10C). The interference rate for si*AjCTP1/2*-1 was 66 % (Figure 10-figure supplement 1).

In long-term AjCT2 loss-of-function studies, the si*AjCTP1/2*-1 group exhibited significant reductions in WGR and SGR compared to the control group (siNC) ($p < 0.05$, Figure 11A). Correspondingly, except for phase I, the si*AjCTP1/2*-1 group

showed significantly increased remaining bait and decreased excrement across phases II-VI (Figure 11B). Furthermore, the growth inhibitory factor *AjGDF-8* was significantly up-regulated and the growth promoting factor *AjMegf6* was significantly down-regulated in the si*AjCTP1/2*-1 group (Figure 11C).

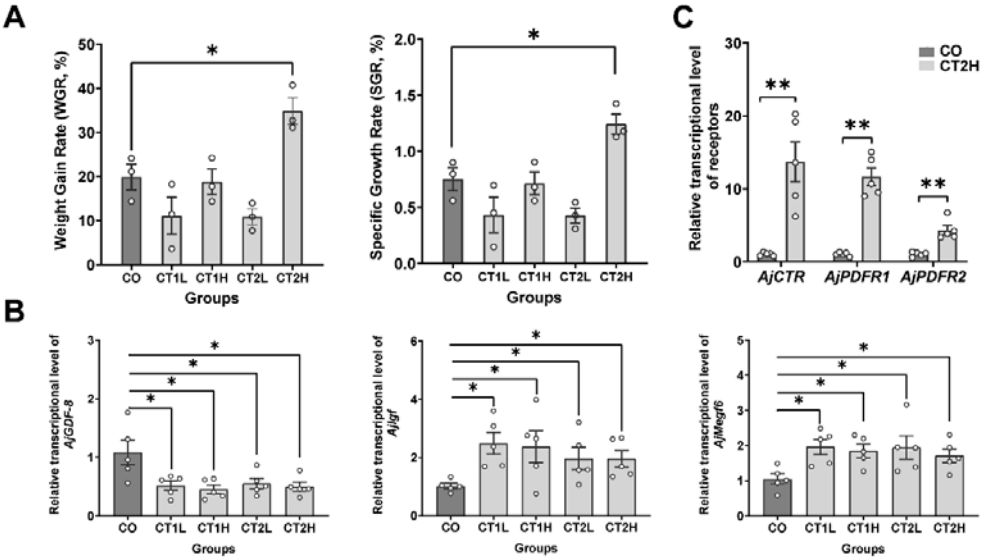

Figure 9. *In vivo* pharmacological tests revealed that AjCT1 and AjCT2 affect feeding and growth-related gene expression in *A. japonicus*. (A) Weight gain rate (WGR) and specific growth rate (SGR) in experimental and control groups. Values are means ± SEM (n = 3, representing three parallel experiments of each group). (B) The relative intestinal transcript expression levels of *AjGDF-8*, *AjIgf* and *AjMegf6* in different groups after injection of AjCT1 or AjCT2 or sterilized seawater (CO) *in A. japonicus*. Values are means ± SEM (n = 5 biological duplication). (C) The relative intestinal expression levels of AjCT1/2 receptors (*AjCTR*, *AjPDFR1* and *AjPDFR2*) in CT2H and CO groups after 24 days injection experiment. Values are means ± SEM (n = 5 biological duplication). CO: control group (sterilized seawater); CT1L/CT2L: AjCT1/AjCT2 low concentration group (5×10^{-3} mg/mL); CT1H/CT2H: AjCT1/AjCT2 high concentration group (5×10^{-1} mg/mL). * indicates statistically significant differences with $p < 0.05$, ** indicates statistically significant differences with $p < 0.01$.

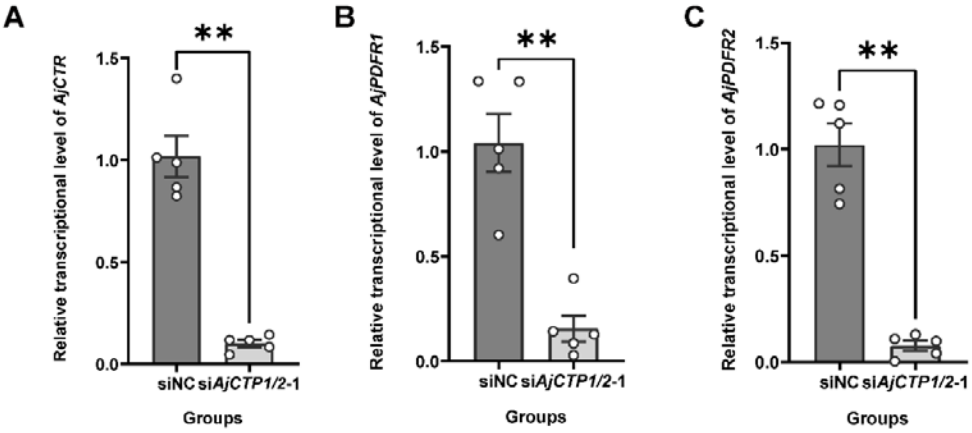

Figure 10. The relative intestinal expression levels of AjCT1/2 receptors after *AjCTP1/2*-1 knockdown. (A), (B) and (C) show the relative expression levels of *AjCTR*, *AjPDFR1* and *AjPDFR2* respectively. Values are means ± SEM (n = 5). ** indicates statistically significant differences with $p < 0.01$.

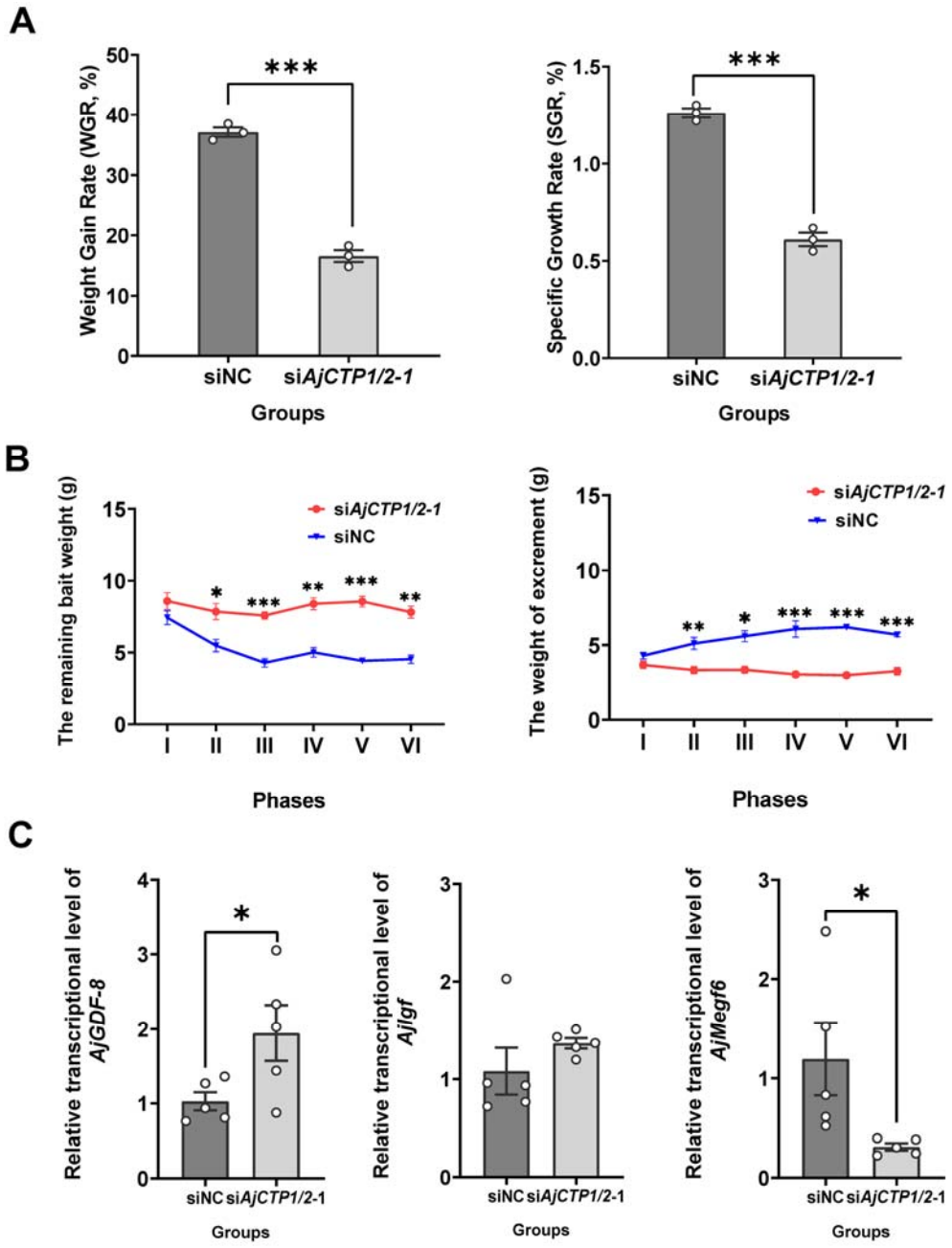

Figure 11. Effects of 24-day *AjCTP1/2*-1 knockdown *in vivo* on feeding and growth in *A. japonicus*. (A) Weight gain rate (WGR) and specific growth rate (SGR) in siNC and *siAjCTP1/2*-1 groups. Values are means ± SEM (n = 3, representing three parallel experiments for each group). (B) Calculation of the remaining bait and excrement mass in different phases. The 24-day experiment was divided into six phases (I-VI), with each phase comprising four days. Values are means ± SEM (n = 3, representing three parallel experiments for each group). (C) The relative intestinal transcript expression levels of *AjGDF-8*, *AjIgf* and *AjMegf6* in siNC and *siAjCTP1/2*-1 groups. Values are means ± SEM (n = 5 biological duplication). siNC: negative control group; si*AjCTP1/2*-1: effectively experimental groups targeting *AjCTP1/2*. Asterisks represent statistically significant differences as follows: *: $p < 0.05$, **: $p < 0.01$, ***: $p < 0.001$.

2.7 AjPDFR2 mediates CT-type signaling-induced feeding and growth promotion in A. japonicus

The differential activation of signaling pathways and associated physiological outcomes between AjCT2 and AjCT1 suggested that AjCT2 may promote feeding and growth via AjPDFR2-mediated mechanisms. To investigate this hypothesis, we performed long term knockdown experiments targeting AjPDFR2. As shown in Figure 12A, si*AjPDFR2-1* effectively knocked down the expression of *AjPDFR2*. In the si*AjPDFR2-1* group, both WGR and SGR were significantly decreased compared to siNC group (Figure 12B). Correspondingly, the remaining bait weight was significantly increased in si*AjPDFR2-1* group (except during phase I), and the weight of excrement was significantly decreased in phase V and VI (Figure 12C). Additionally, the growth promoting factor *AjIgf* was significantly down-regulated in the si*AjPDFR2-1* group (Figure 12D).

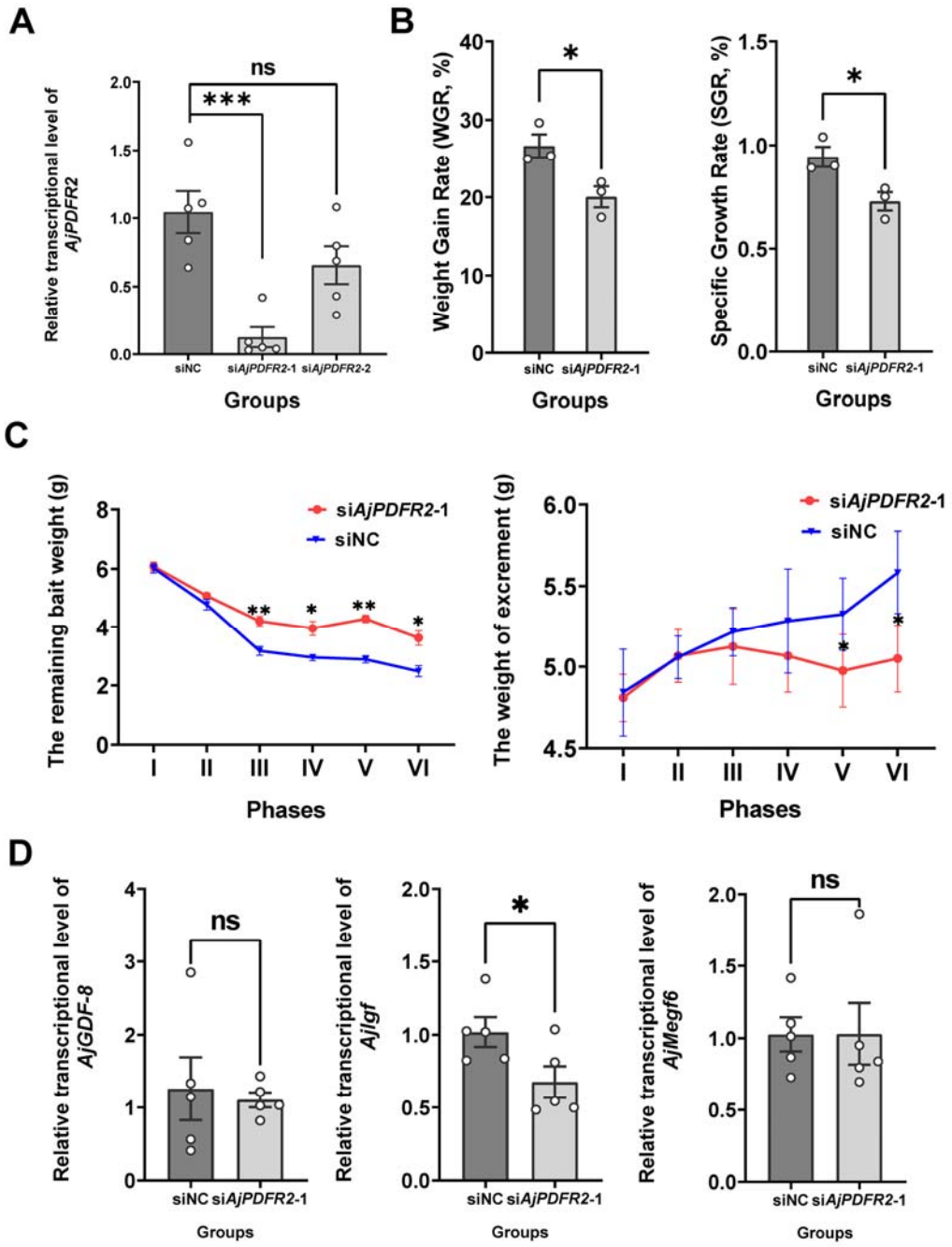

Figure 12. Effects of *AjPDFR2*-1 knockdown *in vivo* on feeding and growth in *A. japonicus*. (A) The relative expression level of *AjPDFR2* in siNC, si*AjPDFR2*-1 and si*AjPDFR2*-2. (B) Weight gain rate (WGR) and specific growth rate (SGR) in siNC and *siAjPDFR2*-1 groups. Values are means ± SEM (n = 3, representing three parallel experiments for each group). (C) The remaining bait and excrement weight in different phases. The 24-day experiment was divided into six phases (I-VI), with each phase comprising four days. Values are means ± SEM (n = 3, representing three parallel experiments of each group). (D) The relative intestinal transcript expression levels of *AjGDF-8*, *AjIgf* and *AjMegf6* in siNC and *siAjPDFR2*-1 groups. Values are means ± SEM (n = 5 biological duplication). siNC: negative control group; siA*jPDFR2*-1 and siA*jPDFR2*-2:

experimental groups targeting A*jPDFR2*. Asterisks represent statistically significant differences as follows: *: $p < 0.05$, **: $p < 0.01$, ***: $p < 0.001$. ns: not significant.

3. Discussion

Previous studies have revealed that the CT-type neuropeptide DH_{31} can act as a ligand for a CTR/CLR-type receptor and a pigment-dispersing factor (PDF) receptor in a protostome – the insect *D. melanogaster* (Mertens et al., 2005; Shafer et al., 2008; Schwartz et al., 2019). Here we show that two CT-type peptides (AjCT1 and AjCT2) act as ligands for a CTR/CLR-type receptor and two pigment-dispersing factor (PDF) type receptors in a deuterostome – the sea cucumber *A. japonicus* (phylum Echinodermata). This is an important finding because it indicates that the ability of CT-type neuropeptides to act as ligands for both CTR/CLR-type receptors and PDF-type receptors may be an evolutionarily ancient property that originated in a common ancestor of the Bilateria. Alternatively, the ability of CT-type neuropeptides to act as ligands for PDF-type receptors in *D. melanogaster* and *A. japonicus* may have evolved independently. Further studies on a wider variety of both protostome (e.g. molluscs, annelids) and deuterostome taxa (e.g. other echinoderms, hemichordates) are needed to address this issue. Here, we also investigated the signal transduction pathways that are activated by AjCT1 and AjCT2 when these peptides bind to their receptors and then proceeded to investigate the expression and actions of these peptides to gain insights into their physiological/behavioral roles in *A. japonicus*, as discussed below.

3.1 Alternative RNA splicing gives rise to transcripts encoding one (AjCT2) or two (AjCT1, AjCT2) CT-type neuropeptides in A. japonicus

In vertebrates, alternative RNA splicing gives rise to transcripts encoding CT or CGRP (Amara et al., 1982; Morris et al., 1984). Analysis of transcriptome/genome sequence data from *A. japonicus* has revealed that in this species alternative RNA splicing gives rise to transcripts encoding one (AjCT2) or two (AjCT1, AjCT2) CT-type neuropeptides (Rowe et al., 2014; Zandawala et al., 2017; Chen et al., 2019; this study). A similar pattern of alternative RNA splicing has been reported for CT-type

precursors in other sea cucumbers (*H. scabra* and *H. glaberrima*; class Holothuroidea) and in brittle stars (*Amphiura filiformis* and *Ophiopsila Aranea*; class Ophiuroidea) (Zandawala et al., 2017; Suwansa-Ard et al., 2018). In contrast, CT-type precursors identified in other echinoderm classes (Asteroidea, Echinoidea and Crinoidea) comprise a single CT-type neuropeptide (Rowe and Elphick, 2012; Mirabeau and Joly, 2013; Rowe et al., 2014; Semmens et al., 2016; Cai et al., 2018; Aleotti et al., 2022). However, it remains to be determined if this feature of CT-type precursors in sea cucumbers and brittle stars evolved independently or originated in a common ancestor of eleutherozoan echinoderms but with subsequent loss in Asteroidea and Echinoidea (Figure 13).

Analysis of the sequences of AjCT1 and AjCT2 revealed the presence of two cysteine residues in their N-terminal regions, which is an evolutionarily conserved feature of CT-type peptides. Structural analysis of CT-type peptides in vertebrates and in starfish has revealed that these cysteines form a disulphide bridge in the mature peptides (Cai et al., 2018) and therefore it is inferred that this post-translational modification also occurs in AjCT1 and AjCT2. Furthermore, the C-terminal residue of AjCT1 and ACT2 is predicted to be an amidated proline, which is a conserved post-translational modification of CT/DH31-type peptides in many taxa, but not vertebrate CGRPs (Cai et al., 2018).

3.2 Identification and characterisation of receptors for CT-type neuropeptides in A. japonicus

Informed by previous genome-wide analysis of GPCRs in *A. japonicus* (Huang et al., 2021), we identified three candidate receptors for AjCT1 and/or AjCT2. Firstly, AjCTR, which is a homolog of CT/DH_{31}-type receptors that have been identified in other taxa, including vertebrates and insects (Garelja et al., 2022; Johnson et al., 2005; Toribio et al., 2003). Secondly, AjPDFR1 and AjPDF2, which are homologs of the PDF-type receptor that has been shown to be activated by DH_{31} in *D. melanogaster* (Mertens et al., 2005; Zandawala, 2012).

In mammals, CTR and CLR mediate effects of all CT-related neuropeptides, but

their ligand specificity relies on the presence and types of receptor activity-modifying proteins (RAMPs) (McLatchie et al., 1998; Purdue et al., 2002; Conner et al., 2004; Hay et al., 2018). Thus, CTR acts as a functional receptor for CT-type peptides without an associated RAMP (Katafuchi et al., 2009), whereas activation of downstream signaling via CLR requires an associated RAMP (Hay et al., 2018). Here, we investigated the occurrence of RAMPs in *A. japonicus* using the tblastn method employed by Sekiguchi *et al.*, (2016), which enabled identification of RAMPs in the cephalochordate *B. floridae*. However, no RAMPs were identified in *A. japonicus*, suggesting that AjCTR may be functionally more similar to CTR than CLR. Accordingly, tblastn analysis of other available echinoderm genomes (*A. rubens*, *S. purpuratus* and *Anneissia japonica*), as well as transcriptome databases for brittle stars (*O. victoriae*, *O. aranea* and *A. filiformis*), also failed to identify RAMPs. Likewise, RAMPs have also not been found in protostomes (Schwartz et al., 2019). Therefore, RAMPs may be unique to chordates, although interestingly RAMPs have also not been identified in the urochordate *C. intestinalis* (Sekiguchi et al., 2009) (Figure 13).

As highlighted above, here we show that the CT-type peptides AjCT1 and AjCT2 both act as ligands for a CTR/CLR-type receptor (AjCTR) and two PDF-type receptors (AjPDFR1, AjPDFR2) in *A. japonicus*. Furthermore, characterization of downstream signaling mechanisms revealed that both AjCT1 and AjCT2 trigger AjCTR-mediated cAMP accumulation, Ca^{2+} mobilization, and ERK signaling. These findings are consistent with previous studies on CT-type receptors in vertebrates and in the mollusc *Magallana gigas* (Pondel, 2000; Walker et al., 2010; Andreassen et al., 2014; Schwartz et al., 2019). Both AjCT1 and AjCT2 trigger cAMP accumulation, Ca^{2+} mobilization, and ERK signaling mediated by AjPDFR1. Both AjCT1 and AjCT2 triggered cAMP accumulation mediated by AjPDFR2, but only AjCT2 (not AjCT1) triggered Ca^{2+} mobilization and ERK signaling mediated by AjPDFR2. These differences in the signal transduction mechanisms activated by AjCT1 and AjCT2 may account for differences in the pharmacological activities and physiological roles of these peptides, as discussed below.

3.3 AjCT1 and AjCT2 act as muscle relaxants in A. japonicus

Analysis of the expression of the gene encoding the precursors comprising AjCT2 or AjCT1 and AjCT2 revealed the occurrence of transcripts in the circumoral nervous system as well as in peripheral tissues/organs, including the longitudinal muscle, digestive system and gonads. Immunohistochemical analysis using an antiserum to the starfish (*A. rubens*) CT-type neuropeptide ArCT enabled visualisation of CT-type neuropeptide(s) in juvenile specimens of *A. japonicus*. Intense and extensive immunostaining was revealed in the ectoneural region of the radial nerve cords and circumoral nerve ring, consistent with the high levels *AjCTP1/2* transcripts detected in circumoral nervous tissue. Immunostained nerve fibers were also observed in the digestive system (including the intestine), consistent with the detection *AjCTP1/2* transcripts in intestine. However, no immunostaining was observed in longitudinal muscles, which is inconsistent with the detection of *AjCTP1/2* transcripts this tissue. This may reflect differences in the detection sensitivity of the techniques used. In accordance with the expression pattern of AjCTP1/2 in *A. japonicus*, analysis of CT-type neuropeptide expression in other echinoderms has revealed a widespread pattern of expression in larval and adult starfish (*A. rubens*) and in juvenile and adult featherstars (*Antedon mediterranea*) (Mayorova et al., 2016; Cai et al., 2018; Aleotti et al., 2022).

Several CT-related peptides act as muscle relaxants in vertebrates (Steiner et al., 1991; Pinto et al., 1996; Yoshimoto et al., 1998; Edvinsson et al., 2001; Golpon et al., 2001; Kandilci et al., 2008) and, accordingly, previous studies have revealed that CT-type neuropeptides cause relaxation of muscle preparations in starfish, including locomotory organs (tube feet) and the apical muscle, which is functionally similar to the longitudinal muscle in sea cucumbers (Cai et al., 2018). Therefore, it was of interest to investigate if AjCT1 and/or AjCT2 act as muscle relaxants in *A. japonicus*. Both AjCT1 and AjCT2 caused dose-dependent relaxation of longitudinal muscle preparations, consistent with the relaxing effect of CT-type peptides on starfish apical muscle preparations. It is worth noting that while AjCT2 at 10^{-6} M exhibited the

maximum efficacy in reversing ACh-induced contraction, its relaxing effect weakened compared to the 10□□ M treatment when applied at progressively higher concentrations. This diminished efficacy likely stems from receptor desensitization, induced by repeated AjCT2 application to longitudinal muscle preparations (Tsurumaki et al., 2003; Arrowsmith and Wray, 2014). Furthermore, AjCT2, but not AjCT1, caused dose-dependent relaxation of intestine preparations from *A. japonicus*. Interestingly, the CT-type peptide ArCT does not to cause relaxation of cardiac stomach preparations from the starfish *A. rubens* (Cai et al., 2018). Therefore, from a functional perspective ArCT is more like AjCT1 than AjCT2 and we speculate that this may reflect loss of an exon encoding a AjCT2-like peptide in the Asteroidea lineage. Further insights into this issue and the evolution of CT-type neuropeptide function echinoderms could be obtained by investigation of the actions of CT-type peptides in brittle stars and sea urchins. Differences in the effects of AjCT1 and AjCT2 on the intestine may be explained by differences in their signal transduction mechanisms. Thus, only AjCT2, not AjCT1, triggered AjPDFR2-mediated activation of Ca^{2+} mobilization and ERK signaling and therefore we speculate that the relaxing effect of AjCT2 on the intestine may be mediated by activation of AjPDFR2.

3.4 AjCT2/AjPDFR2 stimulates feeding and growth in A. japonicus

In vivo pharmacological assays demonstrated that only high concentrations of AjCT2 significantly enhanced feeding and growth rates in *A. japonicus*. In contrast, neither a low concentration of AjCT2 nor any concentration of AjCT1 (low or high) induced detectable effects. Furthermore, long-term knockdown of *AjCTP1/2* further validated the essential role of AjCT2 in regulating feeding and growth in this species. To elucidate the receptor mediating AjCT2's feeding- and growth-promoting effects, we selected AjPDFR2 based on its distinct activation profile: AjCT2 selectively activated AjPDFR2, inducing downstream ERK1/2 phosphorylation, whereas AjCT1 exhibited no activity toward this receptor. Given this receptor specificity, we performed *AjPDFR2* knockdown experiments, which revealed phenotypic changes consistent with those in *AjCTP1/2* knockdown animals, including significantly

reduced WGR and SGR, alongside increased remaining bait accumulation and diminished excrement output compared to control. Collectively, these results support a model wherein AjCT2 promotes feeding and growth in *A. japonicus* via AjPDFR2-dependent activation of the cAMP/PKA/ERK1/2 and Gαq/Ca^{2+}/PKC/ERK1/2 cascades. Considering the inherent complexity of neuropeptide signaling systems, which involve multiple GPCR subtypes coupled to diverse signaling cascades, ligands bound to the same receptor may activate distinct G protein subforms within a single cell (Møller et al., 2003; Mendel et al., 2020). Receptor activation modes may be modulated by structural polymorphisms or binding site diversity (Wong et al., 2000; Changeux, 2010), as well as by the differential efficacy of peptides in activating receptors *in vivo*.

Collectively, these findings indicate that AjCT2 has a physiological role in stimulating feeding and growth in *A. japonicus*. To the best of our knowledge, this is the first study to report orexigenic and growth-promoting effects of a CT-type neuropeptide in bilaterian animals. Interestingly, previous studies have reported the expression of CT-type neuropeptides in the digestive system of invertebrate chordates (Sekiguchi et al., 2009; Sekiguchi et al., 2016). However, in contrast to the stimulatory effect of AjCT2 on feeding/growth in *A. japonicus*, CT-type neuropeptides have been found to inhibit feeding and growth in vertebrates (Del et al., 2002; Hay et al., 2018; Nakamura et al., 2018). Thus, it appears that opposing roles of CT-type neuropeptide signaling systems as regulators for feeding/growth have evolved in deuterostomes, with a stimulatory role reported here in an echinoderm and an inhibitory role reported previously in vertebrates (Figure 13). Further research is now needed to investigate if the stimulatory effect of AjCT2 on feeding/growth observed here in *A. japonicus* also applies to other sea cucumber species. Moreover, our discovery of this effect of AjCT2 on *A. japonicus* may provide a basis for development of novel approaches to improve aquaculture of this economically important species.

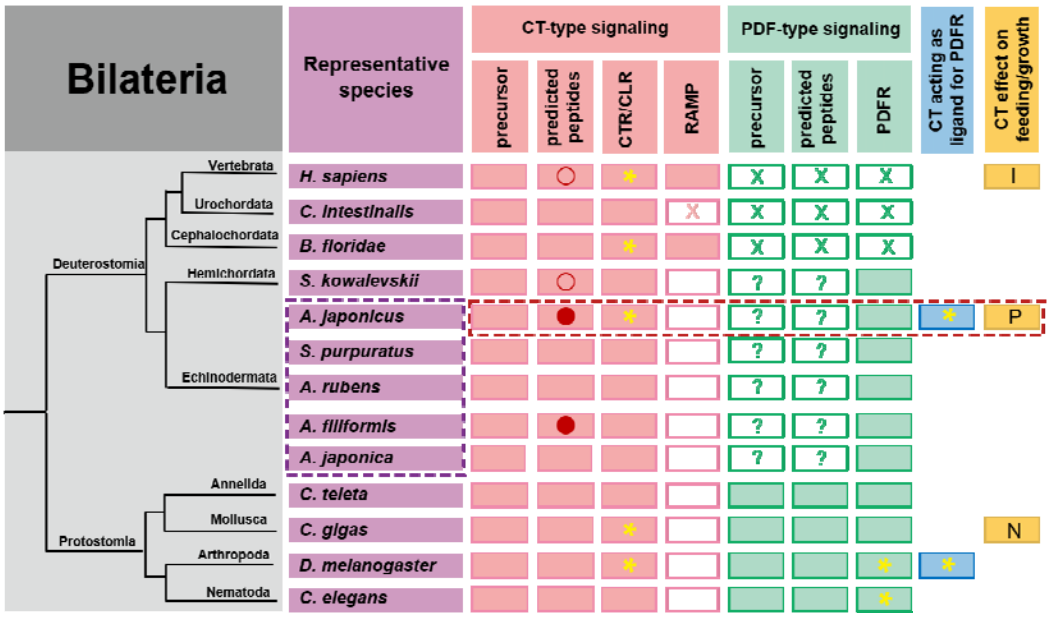

Figure 13. Phylogenetic summary of the occurrence and properties of CT-type and PDF-type signaling systems and effects of CT-type peptides on feeding/growth regulation in representative species. Echinoderms are boxed in purple with dashed lines and *A. japonicus*, the focus of this study, is framed in red with dashed lines. Pink filled rectangles indicate the occurrence of CT-type precursors/neuropeptides, CTR/CLR-type receptors and RAMPs. Green filled rectangles indicate the occurrence of PDF-type precursors/neuropeptides and receptors. Blue filled rectangles indicate species in which CT-type peptides have been shown to act as ligands for PDF-type receptors. Yellow filled rectangles indicate species in which effects or lack of effects of CT-type peptides on feeding/growth have been reported (I: Inhibition; P: Promotion; N: No effect). Red circles indicate that neuropeptides are generated by alternative splicing of precursor transcripts, with an unfilled circle indicating that transcripts encode one neuropeptide and with a filled circle indicating that transcripts can encode two neuropeptides in tandem. A yellow asterisk marks species in which neuropeptides have been shown to act as ligands for receptors experimentally. Unfilled rectangles indicate the absence of a protein. Unfilled rectanges containing a cross (X) indicate loss of a protein during evolution. Unfilled rectangles containing a question mark (?) indicate the existence of precursors/peptides that have yet to be identified.

4. Materials and methods

Key Resources Table				
Reagent type (species) or resource	Designation	Source or reference	Identifiers	Additional information
Cell line (*Homo sapiens*)	HEK293 cell line	Procell	CL-0005	
Antibody	phosphorylated ERK1/2 kinases (Thr202/Tyr204) (goat)	Cell Signaling Technology	CAT#4930	IF (1:2000)
Antibody	ERK1/2 kinases (137F5) (goat)	Cell Signaling Technology	CAT#4695T	IF (1:1000)
Antibody	HRP-conjugated goat anti-rabbit IgG (goat)	Absin	Abs20040ss	IF (1:2000)
sequence-based reagent	Primers for pcDNA3.1(+) plasmid construction--AjCTR	This paper	PCR PRIMER	FORWARD CGCGGATCCAAAATGCAGGAGAACGATTC BamH □
sequence-based reagent	Primers for pcDNA3.1(+) plasmid construction--AjCTR	This paper	PCR PRIMER	REVERSE CCGGAATTCTTAAACTACCGTTGTTTTAT EcoR □
sequence-based reagent	Primers for pcDNA3.1(+) plasmid construction—AjPDFR1	This paper	PCR PRIMER	FORWARD CGCGGATCCACAATGAGTGTCGGGAACGT BamH □
sequence-based reagent	Primers for pcDNA3.1(+) plasmid	This paper	PCR PRIMER	REVERSE CCGGAATTCTCATTTCCCACCCCACTCAC

	construction—AjPDFR1			EcoR □
sequence-based reagent	Primers for pcDNA3.1(+) plasmid construction—AjPDFR2	This paper	PCR PRIMER	FORWARD CGCGGATCCAAGATGGCGAACAATGAAAC BamH □
sequence-based reagent	Primers for pcDNA3.1(+) plasmid construction—AjPDFR2	This paper	PCR PRIMER	REVERSE CCGGAATTCTCATTCATTAAATTTGCCGT EcoR □
sequence-based reagent	Plasmid construction AjCTR–EGFP	This paper	PCR PRIMER	FORWARD CCGGAATTCTGAAAATGCAGGAGAACGATTC EcoR □
sequence-based reagent	Plasmid construction AjCTR–EGFP	This paper	PCR PRIMER	REVERSE CGCGGATCCCGAACTACCGTTGTTTTATCTG BamH □
sequence-based reagent	Plasmid construction AjPDFR1–EGFP			CCGGAATTCTGACAATGAGTGTCGGGAACGT EcoR □
sequence-based reagent	Plasmid construction AjPDFR1–EGFP			CGCGGATCCCGTTTCCCACCCCACTCACTGT BamH □
sequence-based reagent	Plasmid construction AjPDFR2–EGFP			CCGGAATTCTGAAGATGGCGAACAATGAAAC EcoR □
sequence-based reagent	Plasmid construction AjPDFR2–EGFP			CGCGGATCCCGTTCATTAAATTTGCCGTTCA BamH □
sequence-based reagent	Primers for qPCR assays *β*-Actin	This paper	PCR PRIMER	FORWARD AAGGTTATGCTCTTCCTCACGCT
sequence-based reagent	Primers for qPCR assays *β*-Actin	This paper	PCR PRIMER	REVERSE GATGTCACGGACGATTTCACG

sequence-based reagent	Primers for qPCR assays *β*-Tubulin	This paper	PCR PRIMER	FORWARD GAAAGCCTTACGACGGAACA
sequence-based reagent	Primers for qPCR assays *β*-Tubulin	This paper	PCR PRIMER	REVERSE CACCACGTGGACTCAAAATG
sequence-based reagent	Primers for qPCR assays *AjCTP1/2*	This paper	PCR PRIMER	FORWARD GTTTGGCGGTACCCATTAC
sequence-based reagent	Primers for qPCR assays *AjCTP1/2*	This paper	PCR PRIMER	REVERSE GGCGTTCGGTCTGTTAATAG
sequence-based reagent	Primers for qPCR assays *AjMegf6*	This paper	PCR PRIMER	FORWARD CGGTCCTTACTGTGCGGAGA
sequence-based reagent	Primers for qPCR assays *AjMegf6*	This paper	PCR PRIMER	REVERSE CGTCCTCCCAGCTGGACATC
sequence-based reagent	Primers for qPCR assays *AjIgf*	This paper	PCR PRIMER	FORWARD TGGAAGGCAGTAAGGCTA
sequence-based reagent	Primers for qPCR assays *AjIgf*	This paper	PCR PRIMER	REVERSE TAGGCTGATGTGGTTGGA
sequence-based reagent	Primers for qPCR assays *AjGDF-8*	This paper	PCR PRIMER	FORWARD ATACGCCCATACTCACATCC
sequence-based reagent	Primers for qPCR assays *AjGDF-8*	This paper	PCR PRIMER	REVERSE TGGCAGGAGTCAACCTTCAT
sequence-based reagent	Primers for qPCR assays *AjCTR*	This paper	PCR PRIMER	FORWARD GACGAATGGAGGAGAAGG
sequence-based reagent	Primers for qPCR assays *AjCTR*	This paper	PCR PRIMER	REVERSE CGCCGCAATTAGAGTAGT

sequence-based reagent	Primers for qPCR assays *AjPDFR1*	This paper	PCR PRIMER	FORWARD TTATCAACCGCCGTCTTC
sequence-based reagent	Primers for qPCR assays *AjPDFR1*	This paper	PCR PRIMER	REVERSE CAGGAGGAGGAACACATTC
sequence-based reagent	Primers for qPCR assays *AjPDFR2*	This paper	PCR PRIMER	FORWARD TGTTCTCCTGCCTCTTCT
sequence-based reagent	Primers for qPCR assays *AjPDFR2*	This paper	PCR PRIMER	REVERSE GTCCTTCTCATCGGTGTG
sequence-based reagent	Primers for 3’RACE *AjCTP1* *AjCTP2*	This paper	PCR PRIMER	GATTACGCCAAGCTTCGAGCTG TGTCGATAACATTACGCATGG
sequence-based reagent	Primers for 3’RACE AjPDFR1	This paper	PCR PRIMER	GATTACGCCAAGCTTGAGGGAA AGCCAAACCAGCGAGACG
sequence-based reagent	Primers for 3’RACE AjPDFR2	This paper	PCR PRIMER	GATTACGCCAAGCTTGTGCAAC CGGACGAAGATCCACGTG
sequence-based reagent	Primers for 5’RACE AjPDFR1	This paper	PCR PRIMER	GATTACGCCAAGCTTCGTCTCG CTGGTTTGGCTTTCCCTC
sequence-based reagent	Primers for 5’RACE AjPDFR2	This paper	PCR PRIMER	GATTACGCCAAGCTTGCCTTCC ACAAACATCCATGCGAACGC
sequence-based reagent	Primers for 5’RACE AjCTR	This paper	PCR PRIMER	GATTACGCCAAGCTTACGCCGG GCTCTCAAGAAGTCATTC
sequence	RNAi	This paper	si*AjCTP1*-1	GGAAUUAUCAAGACAGUAU (dT)(dT) AUACUGUCUUGAUAAUUCC (dT)(dT)
sequence	RNAi	This paper	si*AjCTP1*-2	GAAAGUCGCUAAUGCAGUA (dT)(dT) UACUGCAUUAGCGACUUUC

				(dT)(dT)
sequence	RNAi	This paper	si*AjPDFR2*-1	GUAGCGAUUGGUCGAAUAA (dT)(dT) UUAUUCGACCAAUCGCUAC (dT)(dT)
sequence	RNAi	This paper	si*AjPDFR2*-2	CAGUCAUUGUUAUCUACCA (dT)(dT) UGGUAGAUAACAAUGACUG (dT)(dT)
sequence	RNAi	This paper	siNC	UUCUCCGAACGUGUCACGU (dT)(dT) ACGUGACACGUUCGGAGAA (dT)(dT)
commercial assay or kit	SMARTer RACE 5'/3' Kit	Takara	Cat No. 634858	
commercial assay or kit	FastPure Gel DNA Extraction Mini Kit	Vazyme	DC301-01	
commercial assay or kit	Hifair® □ 1st Strand cDNA Synthesis SuperMix	YEASEN	Cat No. 11141ES60	
commercial assay or kit	Hieff UNICON Universal Blue qPCR SYBR Green Master Mix	YEASEN	Cat No. 11184ES08	
commercial assay or kit	Firefly luciferase reporter gene assay kit	MK	MF4001	
commercial assay or kit	cAMP Assay kit	R&D systems	Cat No. KGE002B	

686

687 ***4.1 Animals***

688 Adult sea cucumbers were collected from an aquaculture breeding farm in

Weihai, Shandong, China. All the animals were acclimated in breeding aquaria (18 □, 32 ppt) for at least seven days and fed daily with a commercially formulated diet. Tissues used for cDNA cloning and qRT-PCR were obtained from six adult *A. japonicus* (~120 g) and kept at -80 □ until use. Juvenile specimens of *A. japonicus* (~15 mm in length) were used for immunohistochemical analysis of CT-type neuropeptide expression. *In vitro* functional analysis and *in vivo* experiments were carried out using adult sea cucumbers with body masses of ~120 g and ~20 g, respectively.

Ethical approval

All methods were carried out in accordance with the ARRIVE guidelines (https://arriveguidelines.org) for animal experiments. All animal care and use procedures were approved by the Institutional Animal Care and Use Committee of Ocean University of China (Permit Number: 20141201). They were performed according to the Chinese Guidelines for the Care and Use of Laboratory Animals (GB/T 35892-2018).

4.2 Molecular structure and phylogenetic analysis of CT-type neuropeptides and precursors

A. japonicus CT-type neuropeptide precursor sequences (*AjCTP1*, GenBank accession number: MF401985; *AjCTP2*, GenBank accession number: MF401986) were identified in our previous study (Chen et al., 2019). Based on the published sequences, transcript-specific primers for *AjCTP1* and *AjCTP2* (Key resources table) were designed using Primer3Plus (https://www.primer3plus.com/) and sequence accuracy was confirmed by SMARTer RACE 5'/3' Kit (TaKaRa, Kusatsu, Japan) according to the manufacturer's instruction. A sequence translation tool (https://web.expasy.org/translate/) was used to obtain the corresponding amino acid sequences encoded by the cloned cDNAs. To identify the conserved features of CT-type neuropeptides in Bilateria, sequences were aligned using Clustal-X with default settings and then predicted using the online tool Multiple Sequence Comparison

Display Tool (http://www.bio-soft.net/sms/index.html). To investigate relationships of AjCTP1, AjCTP2 and CT-type precursors from other Bilateria, phylogenetic analyses were performed using the Neighbor joining method. The precursor sequences were aligned using the MUSCLE plugin (iterative, 10 iterations, UPGMB as clustering method), a phylogenetic tree was generated using the neighbor joining method with MEGA7 (v.7170509) and bootstrap values were calculated from 1000 replicate analysis and then modified using iTOL (https://itol.embl.de/login.cgi). The accession numbers or citations for all sequences used for analysis are listed in Supplementary table 1.

4.3 Cloning, sequence analysis and phylogenetic tree construction for candidate AjCT1/2 receptors in A. japonicus

Five potential receptors for AjCT1 and AjCT2 in *A. japonicus* (GenBank accession number: PIK49998.1, PIK49999.1, PIK49604.1, PIK34007.1 and PIK62458.1) were identified based on genome-wide analysis (Huang et al., 2021). Sequence comparison revealed that both PIK49998.1 and PIK62458.1 were partial sequences of PIK34007.1. Thus, three candidate receptors belonging to Class B (Secretin-like) GPCRs named as *AjCTR* (Calcitonin receptor, GenBank accession number: PIK49604.1), *AjPDFR1* (Pigment-dispersing factor receptor 1, GenBank accession number: PIK34007.1), and *AjPDFR2* (Pigment-dispersing factor receptor 2, GenBank accession number: PIK49999.1) were predicted and then analyzed. To confirm the accuracy of these sequences, cDNAs were cloned using the SMARTer RACE 5'/3' Kit (Takara, Cat No. 634858) and then sequenced (Beijing Genomics Institute, China).

Phylogenetic relationships of AjCTR, AjPDFR1 and AjPDFR2 with GPCRs belonging to the CT-type (including DH31 and Cluster A) and PDF-type receptor families in other bilaterian animals were investigated, with CRH-type receptors used as an outgroup. Receptor sequences (see supplementary table 2) were aligned using MUSCLE 5.1 with the PPP algorithm (Edgar, 2022). The alignment was trimmed with the gappyout option using trimAl 1.2rev59 (Capella-Gutiérrez et al., 2009), and

maximum-likelihood phylogenetic trees were generated with IQ-tree 2.0.7 for Linux 64-bit using the SH-aLRT and ultrafast bootstrap (UFBoot) methods with nearest neighbor interchange (NNI) correction tests (Guindon and Gascuel, 2003; Guindon et al., 2010; Hoang et al., 2018; Minh et al., 2020; Nguyen et al., 2015). The VT+F+I+G4 amino acid substitution model was selected, with branch support of 1000 bootstrap replicates. The tree was rooted using CRH-type receptors as the outgroup, and edited using Treeviewer version 2.2.0 (Bianchini and Sanchez-Baracaldo, 2024).

In addition, the online tool NetPhos-3.1 (https://services.healthtech.dtu.dk/service.php?NetPhos-3.1) was used to predict potential phosphorylation sites. The conserved domains of protein sequences were predicted by the Batch SMART plugin of TBtools (Toolbox for biologists, v.1.098652) software. For analysis of gene synteny, neighboring genes of *AjCTR*, *AjPDFR1* and *AjPDFR2* were found based on an *A. japonicus* chromosome-level genome assembly (Wang et al., 2022) and the corresponding genes in the starfish *Asterias rubens* and the sea urchin *Lytechinus variegatus* were also identified by performing BLASTp in the NCBI database. Specific primers for cloning of cDNAs encoding the candidate receptors are shown in the Key resources table and the details of the sequences used for constructing the phylogenetic tree are listed in Supplementary table 2.

4.4 Testing AjCT1 and AjCT2 as ligands for candidate receptors and exploration of downstream signaling pathways

AjCT1 and AjCT2 (both with a disulfide bridge between the two cysteine residues and with C-terminal amidation) were custom synthesized by GL Biochem Ltd. (Shanghai, China) with >95% purity. To test candidate receptors for CT-type neuropeptides and investigate their downstream activation mechanisms the following assays were used to measure cAMP signaling or Ca^{2+} signaling: i). direct measurement of cAMP levels using ELISA ii). indirect measurement of cAMP signaling using a cAMP response element-Luciferase (CRE-Luc) assay that measures cAMP-induced gene expression, iii). serum response element (SRE)-Luc assays that measure Ca^{2+}-induced gene expression, iv). receptor translocation assays and v).

Western blotting.

AjCTR, *AjPDFR1* and *AjPDFR2* incorporating enhanced green fluorescent protein (EGFP) were constructed respectively according to the method described by Li *et al.* (2022). Briefly, the complete ORFs of candidate receptors were cloned and sequenced. Then, the PCR products were digested with EcoRI and BamHI (TaKaRa, Kusatsu, Japan) and then incorporated into the pEGFP-N1 vector (YouBio, Changsha, China) that was subject to the same double-digestion. Finally, the constructed plasmid with correct sequences was transfected into HEK293T cells seeded on glass coverslips in 12-well plates. After incubation with AjCT1 (10^{-6} M), AjCT2 (10^{-6} M) or serum-free DMEM (Biosharp, Hefei, China) for 15 min, cells were washed with PBS (Biosharp, Hefei, China) and fixed with 4% PFA for 10 min. Finally, cell nuclei were stained with DAPI (G-CLONE, Beijing, China) for 5 min and an Olympus bright field light microscope was used for image capture. The pcDNA 3.1(+) vectors (YouBio, Changsha, China) comprising the complete ORF of the three candidate receptors were also constructed as described by Li *et al.* (2022). Then, they were co-transfected with the cAMP reporter pCRE-Luc (YouBio, Changsha, China) or Ca^{2+} signaling reporter pSRE-Luc plasmid including a PKC reporter gene (YouBio, Changsha, China) into HEK293T cells. Incubation was carried out with AjCT1 (10^{-6} M), AjCT2 (10^{-6} M) or serum-free DMEM (CO, negative control) for 4 h at 37 °C. Finally, luciferase activity was tested using the firefly luciferase assay kit (MK, Shanghai, China). When required, transfected cells described above were co-incubated with H89 (PKA inhibitor) (Absin, Shanghai, China), FR900359 (Gαq protein inhibitor) (Cayman Chemical, Ann Arbor, Michigan) or Gö 6983 (PKC inhibitor) (Cayman Chemical, Ann Arbor, Michigan) before the experiment to explore the potential signaling pathways. To confirm the concentration of intracellular cAMP after stimulation, HEK293T cells expressing pcDNA 3.1(+)/*AjCTR*, pcDNA 3.1(+)/*AjPDFR2* or pcDNA 3.1(+)/*AjPDFR1* were treated with AjCT1 or AjCT2 (10^{-9} – 10^{-5} M), respectively, for 15 min after 2 h starvation in serum-free medium. Subsequently, cAMP was measured using an ELISA-based cAMP assay kit (R&D systems, USA&Canada) following the manufacturer's instruction. HEK293T cells transfected

with empty pcDNA3.1(+) were used as a negative control. The specific primers used for constructing plasmids are listed in Key resources table.

Western blotting was performed as described previously (Li et al., 2022). Briefly, HEK293T cells transfected with the constructed pcDNA 3.1(+) plasmid were starved in serum-free medium for 2 h, and then incubated with AjCT1 or AjCT2 (10^{-6} M). PVDF membranes containing proteins were blocked with 5% BSA (G-CLONE, Beijing, China) and incubated overnight with antibodies to phosphorylated ERK1/2 kinases (CST, Boston, China). After that, goat anti-rabbit horseradish peroxidase-conjugated secondary antibody (Absin, Shanghai, China) was applied and incubated, followed by the addition of Omni-ECL™ Femto Light Chemiluminescence reagents (EpiZyme, Shanghai, China). Finally, RVL-100-G (ECHO, America) was applied for visualization of the PVDF membrane. When required, transfected cells were co-incubated with PKA or PKC inhibitor before the experiment to identify signaling pathways that activate downstream ERK1/2 cascade.

4.5 Total RNA extraction and Quantitative Real-Time PCR (qRT-PCR) detection

qRT-PCR was employed to detect *AjCTR*, *AjPDFR1*, *AjPDFR2*, *AjCTP1* and *AjCTP2* transcript expression in five tissues from *A. japonicus*, including the intestine, longitudinal muscle, respiratory tree, gonad and circumoral nervous system, and the circumoral nervous system was selected as the control group. Because it was difficult to design specific primers for *AjCTP1* and *AjCTP2* (Zheng et al., 2022), total transcript expression levels for *AjCTP1/2* (*AjCTP1* + *AjCTP2*) were investigated. Total RNA was extracted from the collected tissues using Trizol RNA isolation reagent (Vazyme, Nanjing, China) and Hifair® 1st Strand cDNA Synthesis SuperMix (YEASEN, Shanghai, China) was used to remove genomic DNA and synthesize cDNA according to manufacturer's instructions. For qRT-PCR, amplification was performed in 20 μL volume reactions based on Hieff UNICON Universal Blue qPCR SYBR Green Master Mix (YEASEN, Shanghai, China) and expression levels were assessed by a Corbett Rotoe-Gnen Q (Qiagen, Germany). β-actin (GenBank accession number: PIK61412.1) and β-tubulin (GenBank accession

number: PIK51093) were used as house-keeping genes for normalization (Zhao et al., 2014). The $2^{-\Delta\Delta CT}$ method was applied to analyze the relative expression levels. Specific sequences of primers used for qRT-PCR are listed in Key resources table.

4.6 Localization of CT-type neuropeptide expression in A. japonicus using immunohistochemistry

Juvenile specimens of *A. japonicus* (~15 mm in length) were fixed for 24 hours at room temperature or for 48 hours at 4 ^{o}C in Bouin's fixative (75 mL saturated picric acid in seawater, 25 mL 37% formaldehyde, 5 mL acetic acid) days and then washed in water before being transferred to 50% ethanol followed by 70% ethanol. The fixed specimens were in wrapped in tissue paper soaked in 70% ethanol and then transported from China to the UK. Following dehydration through 90% and 100% ethanol and clearing in xylene, specimens were embedded in paraffin wax and then sectioned (9 or 10 μm) transversely or longitudinally using a Leica RM2145 microtome. Sections were mounted on chrome alum-gelatin coated glass slides and then after incubation in xylene to remove wax followed by 100% ethanol, slides were incubated in 1% hydrogen peroxide in phosphate buffered saline (PBS, pH 7.3) to quench endogenous peroxidases. After using an ethanol series to rehydrate sections, slides were blocked in 5% goat serum in PBS containing 0.1% Tween-20 (PBST). Then slides were incubated overnight at 4 ^{o}C with the ArCT antiserum diluted to 1:2000, 1:3000 or 1:4000 in PBST. Following washing in PBST, slides were incubated with Peroxidase-AffiniPure Goat Anti-Rabbit IgG (H + L) conjugated to Horseradish Peroxidase (RRID: AB_2313567; Jackson ImmunoResearch, West Grove, PA) diluted 1:1000 in 2% goat serum/PBST for 3 h. Bound antibodies were revealed using a solution of 0.05% diaminobenzidine (VWR Chemicals, UK), 0.05% nickel chloride (Sigma-Aldrich, Gillingham, UK), 0.015% hydrogen peroxide (VWR Chemicals, UK) diluted in PBS. When staining was observed, slides were washed in water and dehydrated through an ethanol series into xylene and mounted with coverslips over DPX mounting medium (Thermo Fisher Scientific). The specificity of immunstaining was assessed by pre-absorption of the ArCT antiserum (at 1:100

dilution) for 1 h at room temperature with the ArCT antigen peptide (25 μM) prior to testing on sections at 1:3000 dilution. Images of stained sections were taken using a QIClich CCD Colour Camera (Qimaging, UK) linked to a DMRAI light microscope (Leica Microsystems, UK) with Volocity v. 6.3.1 image analysis software (Perkin-Elmer, USA) running on an iMac computer (27 inch with OS Yosemite, v. 10.10). Montages of images were prepared and labelled using GIMP (version 3.0.2) and Adobe Photoshop (version 26.7) running on a MacBook Pro laptop (OS Sequoia 15.5).

4.7 Analysis of the in vitro activity of AjCT1 and AjCT2 on preparations from A. japonicus

Longitudinal muscles and intestines (20 mm in length) from *A. japonicus* were dissected and then suspended in a 50 mL glass organ bath containing 20 mL sterilized seawater. Both ends of the preprations were tied with cotton ligatures and then one end was tied to a metal hook and the other end was connected with a High Grade Isotonic Transducer (ADinstruments MLT0015, Oxford, UK). Before testing, the preparation was stabilized for about 20 min, and the resting tension was adjusted to 1.0 g. Informed by previous findings from Cai et al. (2018), we investigated if AjCT1 and AjCT2 caused relaxation of preparations. First, acetylcholine (ACh) was applied to induce the contraction of preparations and then when a stable state of contraction was achieved, 20 uL AjCT1 or AjCT2 at a range of concentrations was added and relaxation responses were recorded. Output signal (cm) from PowerLab data acquisition hardware (ADinstruments PowerLab 4/26, Oxford, UK) was calculated using LabChart (v8.0.7) software.

4.8 Investigation of the in vivo pharmacological effects of AjCT1 and AjCT2 in A. japonicus

A total of 150 adult sea cucumbers were randomly assigned to five groups (30 individuals per group), including two high concentration groups (CT1H and CT2H, 5×10^{-1} mg/ml), two low concentration groups (CT1L and CT2L, 5×10^{-3} mg/ml) and the control group (CO, sterilized seawater), with each group consisting of three

parallel experiments comprising ten animals. Before the experiments, sea cucumbers were starved for a day to normalize their physiological status and their wet weights were measured. AjCT1 and AjCT2 were dissolved in sterilized seawater and then injected through the peristome at noon every other day (1 μl/g wet weight) and the CO group were injected in the same way but with sterilized seawater (1 μl/g wet weight). Feces and residual bait were collected and weighed after drying every day. After 24 days, wet weights of sea cucumbers were measured again. Then, WGR and SGR were calculated to assess their feeding and growth conditions. Formulas are as follows: WGR = $100*(W_t-W_0)/W_0$, SGR = $100*(\ln W_t-\ln W_0)/D$. In the formula, W_0 represents the initial wet body weight (g), W_t represents the final wet body weight (g), D represents the feeding days. Subsequently, animals were dissected and intestines were collected for detecting the expression levels of the three receptor genes (*AjCTR*, *AjPDFR1*, *AjPDFR2*) and several growth factors, including multiple epidermal growth factor 6 (*AjMegf6*, GenBank accession number: MG018199.1), insulin-like growth factor (*AjIgf*, GenBank accession number: PIK50518.1) and growth and differentiation factor-8 (*AjGDF-8*, GenBank accession number: KP100064.1) (Li et al., 2016; Wang et al., 2018). The specific primers for qRT-PCR analysis are listed in the Key resources table.

4.9 Loss-of-function experiments by RNA interference (RNAi)

To investigate how receptor expression is affected by knock-down of AjCTP expression, an RNAi experiment was carried out. It was difficult to design *AjCTP1*- and *AjCTP2*- specific interference oligonucleotides and therefore, we designed and customized generic interference oligonucleotides targeting both *AjCTP1* and *AjCTP2* (si*AjCTP1/2*-1 and si*AjCTP1/2*-2, containing the extra 2′ ome modification) (Beijing Tsingke Biotech Co., Ltd. China). Meanwhile, a negative control siRNA (siNC) was also customized for the experiment (Key resources table), which does not target genes in *A. japonicus*. The si*AjCTP1/2*-1, si*AjCTP1/2*-2 or siNC dry powder was diluted to 20 μM with DEPC water following the manufacturer's instruction, then 60 μl sterilized seawater was mixed with 20 μl si*AjCTP1/2*-1, si*AjCTP1/2*-2 or siNC, and

20 μl Lipo6000 transfection reagent (Beyotime, Shanghai, China) as the transfection solution. Eighteen sea cucumbers were randomly divided into three groups and injected with three different transfection solutions respectively. The mixed solutions were injected through the peristome once a day (1 μl/g wet weight) and intestines were dissected and frozen in liquid nitrogen 3 days after injection. The expression level of *AjCTP1/2* was investigated by qRT-PCR and the interference rate was calculated using ($1 - 2^{-\Delta\Delta CT}$) to determine the inhibition efficiency of siRNAs. Finally, the relative expression levels of *AjCTR*, *AjPDFR1* and *AjPDFR2* were investigated using the selected *A. japonicus* intestines.

To assess the effects of CT-type signaling inhibition on feeding and growth in *A. japonicus*, a 24-day RNAi experiment was conducted following the methodology outlined in Section 4.8. Sea cucumbers were randomly allocated into two groups: the negative control group received siNC injections, while the experimental group was injected with si*AjCTP1/2*-1 (effectively targeting *AjCTP1/2*). Throughout the experiment, the dry weight of remaining bait and excrement, along with the wet weight of individual sea cucumbers, were recorded. Subsequently, WGR and SGR, as indices of feeding efficiency and growth performance, were calculated. In addition, the expression levels of the three growth factors (*AjMegf6*, *AjIgf* and *AjGDF-8*) in the intestinal tissue were tested by qPCR.

To investigate the potential mediation of CT-type signaling effects on feeding and growth by AjPDFR2 in *A. japonicus*, an RNAi experiment targeting *AjPDFR2* was performed following the same knockdown protocol established for *AjCTP*. Briefly, the effective siRNA targeting *AjPDFR2* (si*AjPDFR2*-1 or si*AjPDFR2*-2) was selected by testing *AjPDFR2* expression in the intestines of injected sea cucumbers using qRT-PCR and calculating the interference rate efficiency. Subsequently, the validated siRNA was then employed in a 24-day RNAi experiment. The dry weight of remaining bait and excrement, as well as the wet weight of the sea cucumbers were measured, enabling calculation of WGR and SGR. Furthermore, the expression levels of three key growth factors (*AjMegf6*, *AjIgf* and *AjGDF-8*) in the intestinal tissue were

analyzed via qPCR.

4.10 Statistical analysis

Statistical analyses were carried out using GraphPad Prism 8.0. Significant differences between groups were determined by one-way analysis of variance (ANOVA) followed by a Tukey's multiple comparisons test. Statistical significance thresholds were defined as follows: $p < 0.05$ (*) for significant differences and $p < 0.01$ (**) for highly significant differences, with annotations directly marked on the figures. All data were presented as mean ± SEM from at least three independent biological replicates. Non-linear regression analysis was performed using a four-parameter logistic equation with automatic outlier exclusion to fit the dose-response curve. The half maximal effective concentration (EC_{50}) was derived from the fitted curves through built-in algorithms in GraphPad Prism 8.0.

Competing Interests

The authors declare that no competing interests exist.

Funding

This research was supported by National Natural Science Foundation of China [grant number 42276103] and Biotechnology and Biological Sciences Research Council (UK; grant numbers BB/M001644/1 and BB/X001024/1).

Author Contributions

Xiao Cong, Data curation, Formal analysis, Investigation, Methodology, Software, Visualization, Writing—original draft preparation; Huachen Liu, Investigation, Methodology, Validation; Lihua Liu, Methodology, Validation; Nayeli Escudero-Castelán, Investigation, Methodology, Visualization, Writing—review & editing; Kite Jones, Investigation, Methodology, Visualization, Writing—review & editing; Michaela Egertová, Investigation, Methodology, Visualization; Maurice R. Elphick, Formal analysis, Funding acquisition, Resources, Supervision, Validation, Visualization, Writing—review & editing; Muyan Chen, Conceptualization, Formal analysis, Funding acquisition, Methodology, Project administration, Resources, Supervision, Validation, Visualization, Writing—review & editing

References:

Aleotti A, Wilkie I C, Yañez-Guerra L A, et al. Discovery and functional characterization of neuropeptides in crinoid echinoderms. Frontiers in Neuroscience, 2022, 16: 1006594. doi: 10.3389/fnins.2022.1006594.

Amara S G, Jonas V, Rosenfeld M G, et al. Alternative RNA processing in calcitonin gene expression generates mRNAs encoding different polypeptide products. Nature, 1982, 298(5871): 240-244. doi: 10.1038/298240a0.

Andreassen K V, Hjuler S T, Furness S G, et al. Prolonged calcitonin receptor signaling by salmon, but not human calcitonin, reveals ligand bias. PloS one, 2014, 9(3): e92042. doi: 10.1371/journal.pone.0092042.

Arrowsmith S, Wray S. Oxytocin: its mechanism of action and receptor signaling in the myometrium. Journal of neuroendocrinology, 2014, 26(6): 356-369. dio: 10.1111/jne.12154.

Bauknecht P, Jékely G. Large-Scale Combinatorial Deorphanization of Platynereis Neuropeptide GPCRs. Cell reports, 2015, 12(4), 684–693. doi: 10.1016/j.celrep.2015.06.052.

Beets I, Zels S, Vandewyer E, Demeulemeester J, et al. System-wide mapping of peptide-GPCR interactions in *C. elegans*. Cell reports, 2023, 42(9), 113058. doi: 10.1016/j.celrep.2023.113058.

Bianchini G, Sánchez-Baracaldo P. TreeViewer: Flexible, modular software to visualise and manipulate phylogenetic trees. Ecology and evolution, 2024, 14(2), e10873. doi: 10.1002/ece3.10873.

Bomberger J M, Parameswaran N, Spielman W S. Regulation of GPCR trafficking by RAMPs. Adv. Exp. Med. Biol, 2012, 744: 25-37. doi: 10.1007/978-1-4614-2364-5_3.

Bourlat S J, Juliusdottir T, Lowe C J, et al. Deuterostome phylogeny reveals monophyletic chordates and the new phylum Xenoturbellida. Nature, 2006, 444(7115): 85-88. doi: 10.1038/nature05241

Bromham L D, Degnan B M. Hemichordates and deuterostome evolution: robust molecular phylogenetic support for a hemichordate+ echinoderm clade. Evolution & development, 1999, 1(3): 166-171. doi: 10.1046/j.1525-142x.1999.99026.x

Burke R D, Angerer L M, Elphick M R, et al. A genomic view of the sea urchin nervous system. Developmental biology, 2006, 300(1): 434-460. doi: 10.1016/j.ydbio.2006.08.007.

Cai W, Kim C H, Go H J, et al. Biochemical, anatomical, and pharmacological characterization of calcitonin-type neuropeptides in starfish: discovery of an ancient role as muscle relaxants. Frontiers in Neuroscience, 2018, 12: 382. doi: 10.3389/fnins.2018.00382.

Capella-Gutiérrez S, Silla-Martínez J M, Gabaldón T. trimAl: a tool for automated alignment trimming in large-scale phylogenetic analyses. Bioinformatics (Oxford, England), 2009, 25(15), 1972–1973. doi: 10.1093/bioinformatics/btp348.

Cardoso J C, Mc Shane J C, Li Z, et al. Revisiting the evolution of Family B1 GPCRs and ligands: Insights from mollusca. Molecular and cellular endocrinology, 2024, 586, 112192. doi: 10.1016/j.mce.2024.112192.

Changeux J P. Allosteric receptors: from electric organ to cognition. Annual review of pharmacology and toxicology, 2010, 50(1): 1-38. doi: 10.1146/annurev.pharmtox.010909.105741.

Chen M, Talarovicova A, Zheng Y, et al. Neuropeptide precursors and neuropeptides in the sea cucumber *Apostichopus japonicus*: a genomic, transcriptomic and proteomic analysis. Scientific Reports, 2019, 9(1): 8829. doi: 10.1038/s41598-019-45271-3.

Chen Y, Shyu J F, Santhanagopal A, et al. The calcitonin receptor stimulates Shc tyrosine phosphorylation and Erk1/2 activation: involvement of Gi, protein kinase C, and calcium[J]. Journal of Biological Chemistry, 1998, 273(31): 19809-19816. doi: 10.1074/jbc.273.31.19809.

Cong X, Liu H, Zheng Y, et al. A Putative Role of Vasopressin/Oxytocin-Type Neuropeptide in Osmoregulation and Feeding Inhibition of *Apostichopus japonicus*. International Journal of Molecular Sciences, 2023, 24(18): 14358. doi: 10.3390/ijms241814358.

Conner A C, Simms J, Hay D L, et al. Heterodimers and family-B GPCRs: RAMPs, CGRP and adrenomedullin. Biochemical Society Transactions, 2004, 32(5): 843-846. doi: 10.1042/BST0320843.

Conzelmann M, Williams E A, Krug K, et al. The neuropeptide complement of the marine annelid *Platynereis dumerilii*. BMC genomics, 2013, 14: 1-15. doi:10.1186/1471-2164-14-906.

Copp D H, Cameron E C, Cheney B A, et al. Evidence for calcitonin—a new hormone from the parathyroid that lowers blood calcium. Endocrinology, 1962, 70(5): 638-649. doi: 10.1210/endo-70-5-638.

Del Prete E, Schade B, Riediger T, et al. Effects of amylin and salmon calcitonin on feeding and drinking behavior in pygmy goats. Physiology & behavior, 2002, 75(4): 593-599. doi: 10.1016/s0031-9384(02)00655-8.

Deribe Y L, Wild P, Chandrashaker A, et al. Regulation of epidermal growth factor receptor trafficking by lysine deacetylase HDAC6. Science signaling, 2009, 2(102): ra84-ra84. doi: 10.1126/scisignal.2000576.

Dunn C W, Hejnol A, Matus D Q, et al. Broad phylogenomic sampling improves resolution of the animal tree of life. Nature, 2008, 452(7188): 745-749. doi: 10.1038/nature06614

Edgar R C. Muscle5: High-accuracy alignment ensembles enable unbiased assessments of sequence homology and phylogeny. Nature communications, 2022, 13(1), 6968. doi: 10.1038/s41467-022-34630-w.

Edvinsson L, Goadsby P J, Uddman R. Amylin: localization, effects on cerebral arteries and on local cerebral blood flow in the cat. The scientific world journal, 2001, 1: 168-180. doi: 10.1100/tsw.2001.23.

Furuya K, Milchak R J, Schegg K M, et al. Cockroach diuretic hormones: characterization of a calcitonin-like peptide in insects. Proceedings of the National Academy of Sciences, 2000, 97(12): 6469-6474. doi: 10.1073/pnas.97.12.6469.

Garelja M L, Bower R L, Brimble M A, et al. Pharmacological characterisation of mouse calcitonin and calcitonin receptor□like receptors reveals differences compared with human receptors. British journal of pharmacology, 2022, 179(3): 416-434. doi: 10.1111/bph.15628.

Goda T, Umezaki Y, Alwattari F, et al. Neuropeptides PDF and DH31 hierarchically regulate free-running rhythmicity in Drosophila circadian locomotor activity. Scientific reports, 2019, 9(1): 838. doi:10.1038/s41598-018-37107-3.

Golpon H A, Puechner A, Welte T, et al. Vasorelaxant effect of glucagon-like peptide-(7-36) amide and amylin on the pulmonary circulation of the rat. Regulatory peptides, 2001, 102(2-3): 81-86. doi: 10.1016/s0167-0115(01)00300-7.

Gorn A H, Lin H Y, Yamin M, et al. Cloning, characterization, and expression of a human calcitonin receptor from an ovarian carcinoma cell line. The Journal of clinical investigation, 1992, 90(5), 1726–1735. doi: 10.1172/JCI116046.

Guindon S, Dufayard J F, Lefort V, et al. New algorithms and methods to estimate maximum-likelihood phylogenies: assessing the performance of PhyML 3.0. Systematic biology, 2010, 59(3), 307–321. doi: 10.1093/sysbio/syq010.

Guindon S, Gascuel O. A simple, fast, and accurate algorithm to estimate large phylogenies by maximum likelihood. Systematic biology, 2003, 52(5), 696–704. doi: 10.1080/10635150390235520.

Guo K, Su L, Wang Y, et al. Antioxidant and anti-aging effects of a sea cucumber protein hydrolyzate and bioinformatic characterization of its composing peptides. Food & Function, 2020, 11(6): 5004-5016. doi: 10.1039/d0fo00560f.

Hay D L, Conner A C, Howitt S G, et al. The pharmacology of adrenomedullin receptors and their relationship to CGRP receptors. Journal of Molecular Neuroscience, 2004, 22: 105-113. doi: 10.1385/JMN:22:1-2:105.

Hay D L, Garelja M L, Poyner D R, et al. Update on the pharmacology of calcitonin/CGRP family of peptides: IUPHAR Review 25. British journal of pharmacology, 2018, 175(1): 3-17. doi: 10.1111/bph.14075.

Hoang D T, Chernomor O, von Haeseler A, et al. UFBoot2: Improving the Ultrafast Bootstrap Approximation. Molecular biology and evolution, 2018, 35(2), 518–522. doi: 10.1093/molbev/msx281.

Huang D, Zhang B, Han T, et al. Genome-wide prediction and comparative transcriptomic analysis reveals the G protein-coupled receptors involved in gonadal development of *Apostichopus japonicus*. Genomics, 2021, 113(1): 967-978. doi: 10.1016/j.ygeno.2020.10.030.

Huang T, Su J, Wang X, et al. Functional Analysis and Tissue-Specific Expression of Calcitonin and CGRP with RAMP-Modulated Receptors CTR and CLR in Chickens. Animals: an open access journal from MDPI, 2024, 14(7), 1058. doi: 10.3390/ani14071058.

Jékely G. Global view of the evolution and diversity of metazoan neuropeptide signaling. Proceedings of the National Academy of Sciences, 2013, 110(21): 8702-8707. doi: 10.1073/pnas.1221833110.

Johnson E C, Shafer O T, Trigg J S, et al. A novel diuretic hormone receptor in Drosophila: evidence for conservation of CGRP signaling. Journal of Experimental Biology, 2005, 208(7): 1239-1246. doi: 10.1242/jeb.01529.

Kandilci H B, Gumusel B, Lippton H. Intermedin/adrenomedullin-2 (IMD/AM2) relaxes rat main pulmonary arterial rings via cGMP-dependent pathway: role of nitric oxide and large conductance calcium-activated potassium channels (BKCa). Peptides, 2008, 29(8): 1321-1328. doi: 10.1016/j.peptides.2008.04.008.

Katafuchi T, Yasue H, Osaki T, et al. Calcitonin receptor-stimulating peptide: Its evolutionary and functional relationship with calcitonin/calcitonin gene-related peptide based on gene structure. Peptides, 2009, 30(9): 1753-1762. doi: 10.1016/j.peptides.2009.06.012.

Kuwasako K, Kitamura K, Nagata S, et al. Shared and separate functions of the RAMP-based adrenomedullin receptors. Peptides, 2011, 32(7): 1540-1550. doi: 10.1016/j.peptides.2011.05.022.

Li C, Zheng Y, Cong X, et al. Molecular and functional characterization of the luqin-type neuropeptide signaling system in the sea cucumber *Apostichopus japonicus*. Peptides, 2022, 155: 170839. doi: 10.1016/j.peptides.2022.170839.

Li S, Zhou Z, Dong Y, et al. Molecular characterization, expression analysis of the myostatin gene and its association with growth traits in sea cucumber (*Apostichopus japonicus*). Comparative Biochemistry and Physiology Part B: Biochemistry and Molecular Biology, 2016, 201: 12-20. doi: 10.1016/j.cbpb.2016.06.005.

Martins R, Vieira F A, Power D M. Calcitonin receptor family evolution and fishing for function using in silico promoter analysis. General and Comparative Endocrinology, 2014, 209: 61-73. doi: 10.1016/j.ygcen.2014.04.025.

Mathiesen D S, Lund A, Vilsbøll T, et al. Amylin and calcitonin: potential therapeutic strategies to reduce body weight and liver fat. Frontiers in Endocrinology, 2021, 11: 617400. doi: 10.3389/fendo.2020.617400.

Mayorova T D, Tian S, Cai W, Semmens D C. Odekunle E A, Zandawala M, Badi Y, Rowe M L, Egertová M, Elphick M R. (2016). Localization of neuropeptide gene expression in larvae of an echinoderm, the starfish *Asterias rubens*. Front. Neurosci. 10:553. doi: 10.3389/fnins.2016.00553.

McLatchie L M, Fraser N J, Main M J, et al. RAMPs regulate the transport and ligand specificity of the calcitonin-receptor-like receptor. Nature, 1998, 393(6683): 333-339. doi: 10.1038/30666.

Mendel H C, Kaas Q, Muttenthaler M. Neuropeptide signalling systems–an underexplored target for venom drug discovery. Biochemical pharmacology, 2020, 181: 114129. doi: 10.1016/j.bcp.2020.114129.

Mertens I, Vandingenen A, Johnson E C, et al. PDF receptor signaling in Drosophila contributes to both circadian and geotactic behaviors. Neuron, 2005, 48(2): 213-219. doi: 10.1016/j.neuron.2005.09.009.

Minh B Q, Schmidt H A, Chernomor O, et al. IQ-TREE 2: New Models and Efficient Methods for Phylogenetic Inference in the Genomic Era. Molecular biology and evolution, 2020, 37(5), 1530–1534. doi: 10.1093/molbev/msaa015.

Mirabeau O, Joly J S. Molecular evolution of peptidergic signaling systems in bilaterians. Proceedings of the national academy of sciences, 2013, 110(22): E2028-E2037. doi: 10.1073/pnas.1219956110.

Møller L N, Stidsen C E, Hartmann B, et al. Somatostatin receptors. Biochimica et Biophysica Acta (BBA)-Biomembranes, 2003, 1616(1): 1-84. doi: 10.1016/s0165-6147(97)89535-x.

Morris H R, Panico M, Etienne T, et al. Isolation and characterization of human calcitonin gene-related peptide. Nature, 1984, 308(5961): 746-748. doi: 10.1038/308746a0.

Nakamura M, Nomura S, Yamakawa T, et al. Endogenous calcitonin regulates lipid and glucose metabolism in diet-induced obesity mice. Scientific Reports, 2018, 8(1): 17001. Endogenous calcitonin regulates lipid and glucose metabolism in diet-induced obesity mice

Nguyen L T, Schmidt H A, von Haeseler A, et al. IQ-TREE: a fast and effective stochastic algorithm for estimating maximum-likelihood phylogenies. Molecular biology and evolution, 2015, 32(1), 268–274. doi: 10.1093/molbev/msu300.

Pangestuti R, Arifin Z. Medicinal and health benefit effects of functional sea cucumbers. Journal of traditional and complementary medicine, 2018, 8(3): 341-351. doi: 10.1016/j.jtcme.2017.06.007.

Párrizas M, LeRoith D. Insulin-like growth factor-1 inhibition of apoptosis is associated with increased expression of the bcl-xL gene product. Endocrinology, 1997, 138(3): 1355-1358. doi: 10.1210/endo.138.3.5103.

Perlow M J, Freed W J, Carman J S, et al. Calcitonin reduces feeding in man, monkey and rat. Pharmacology Biochemistry and Behavior, 1980, 12(4): 609-612. doi: 10.1016/0091-3057(80)90196-3.

Pinto A, Sekizawa K, Yamaya M, et al. Effects of adrenomedullin and calcitonin gene□related peptide on airway and pulmonary vascular smooth muscle in guinea□pigs. British journal of pharmacology, 1996, 119(7): 1477-1483. doi: 10.1111/j.1476-5381.1996.tb16061.x.

Pondel M. Calcitonin and calcitonin receptors: bone and beyond. International journal of experimental pathology, 2000, 81(6): 405-422. doi: 10.1046/j.1365-2613.2000.00176.x.

Purdue B W, Tilakaratne N, Sexton P M. Molecular pharmacology of the calcitonin receptor. Receptors and Channels, 2002, 8(3-4): 243-255. doi: 10.3109/10606820213681

Rowe M L, Achhala S, Elphick M R. Neuropeptides and polypeptide hormones in echinoderms: new insights from analysis of the transcriptome of the sea cucumber *Apostichopus japonicus*. General and Comparative Endocrinology, 2014, 197: 43-55. doi: 10.1016/j.ygcen.2013.12.002.

Rowe M L, Elphick M R. The neuropeptide transcriptome of a model echinoderm, the sea urchin *Strongylocentrotus purpuratus*. General and comparative endocrinology, 2012, 179(3): 331-344. doi: 10.1016/j.ygcen.2012.09.009.

Schwartz J, Réalis-Doyelle E, Dubos M P, et al. Characterization of an evolutionarily conserved calcitonin signaling system in a lophotrochozoan, the Pacific oyster (*Crassostrea gigas*). Journal of Experimental Biology, 2019, 222(13): jeb201319. doi: 10.1242/jeb.201319.

Sekiguchi T, Kuwasako K, Ogasawara M, et al. Evidence for conservation of the calcitonin superfamily and activity-regulating mechanisms in the basal chordate *Branchiostoma floridae*: insights into the molecular and functional evolution in chordates. Journal of Biological Chemistry, 2016, 291(5): 2345-2356. doi: 10.1074/jbc.M115.664003.

Sekiguchi T, Suzuki N, Fujiwara N, et al. Calcitonin in a protochordate, *Ciona intestinalis*–the prototype of the vertebrate calcitonin/calcitonin gene□related peptide superfamily. The FEBS Journal, 2009, 276(16): 4437-4447. doi: 10.1111/j.1742-4658.2009.07151.x.

Sekiguchi T. Evolution of calcitonin/calcitonin gene-related peptide family in chordates: identification of CT/CGRP family peptides in cartilaginous fish genome. General and Comparative Endocrinology, 2022, 328: 114123. doi: 10.1016/j.ygcen.2022.114123.

Semmens D C, Mirabeau O, Moghul I, Pancholi M R, Wurm Y, and Elphick M R (2016). Transcriptomic identification of starfish neuropeptide precursors yields new insights into neuropeptide evolution. Open Biol. 6:150224. doi: 10.1098/rsob.150224.

Shafer O T, Kim D J, Dunbar-Yaffe R, et al. Widespread receptivity to neuropeptide PDF throughout the neuronal circadian clock network of Drosophila revealed by real-time cyclic AMP imaging. Neuron, 2008, 58(2): 223-237. doi: 10.1016/j.neuron.2008.02.018.

Smith M K, Wang T, Suwansa-Ard S, et al. The neuropeptidome of the Crown-of-Thorns Starfish, *Acanthaster planci*. Journal of proteomics, 2017, 165: 61-68. doi: 10.1016/j.jprot.2017.05.026.

Steiner D F, Ohagi S, Nagamatsu S, et al. Is islet amyloid polypeptide a significant factor in pathogenesis or pathophysiology of diabetes?. Diabetes, 1991, 40(3): 305-309. doi: 10.2337/diab.40.3.305.

Suwansa-Ard S, Chaiyamoon A, Talarovicova A, et al. Transcriptomic discovery and comparative analysis of neuropeptide precursors in sea cucumbers (Holothuroidea). Peptides, 2018, 99: 231-240. doi: 10.1016/j.peptides.2017.10.008.

Toribio R E, Kohn C W, Leone G W, et al. Molecular cloning and expression of equine calcitonin, calcitonin gene-related peptide-I, and calcitonin gene-related peptide-II. Molecular and cellular endocrinology, 2003, 199(1-2): 119-128. doi: 10.1016/s0303-7207(02)00289-7.

Tsurumaki T, Muraoka O, Yamaguchi T, et al. Neuropeptide Y-induced contraction and its desensitization through the neuropeptide Y receptor subtype in several rat veins. Journal of Cardiovascular Pharmacology, 2003, 41: S23-S27.

Walker C S, Conner A C, Poyner D R, et al. Regulation of signal transduction by calcitonin gene-related peptide receptors. Trends in pharmacological sciences, 2010, 31(10): 476-483. doi: 10.1016/j.tips.2010.06.006.

Wang Y, Yang Y, Li Y, et al. Identification of sex determination locus in sea cucumber *Apostichopus japonicus* using genome-wide association study. BMC genomics, 2022, 23(1): 391. doi: 10.1186/s12864-022-08632-3.

Wang Z, Cui J, Song J, et al. Comparative transcriptome analysis reveals growth-related genes in juvenile Chinese sea cucumber, Russian sea cucumber, and their hybrids. Marine biotechnology, 2018, 20: 193-205. doi: 10.1007/s10126-018-9796-6.

Wong A H C, Buckle C E, Van Tol H H M. Polymorphisms in dopamine receptors: what do they tell us? European journal of pharmacology, 2000, 410(2-3): 183-203. doi: 10.1016/s0014-2999(00)00815-3.

Yoshimoto R, Mitsui□Saito M, Ozaki H, et al. Effects of adrenomedullin and calcitonin gene□related peptide on contractions of the rat aorta and porcine coronary artery. British journal of pharmacology, 1998, 123(8): 1645-1654. doi: 10.1038/sj.bjp.0701805.

Zandawala M, Moghul I, Yañez Guerra L A, et al. Discovery of novel representatives of bilaterian neuropeptide families and reconstruction of neuropeptide precursor evolution in ophiuroid echinoderms. Open biology, 2017, 7(9): 170129. doi: 10.1098/rsob.170129.

Zandawala M. Calcitonin-like diuretic hormones in insects. Insect biochemistry and molecular biology, 2012, 42(10): 816-825. doi: 10.1016/j.ibmb.2012.06.006.

Zhao Y, Chen M, Wang T, et al. Selection of reference genes for qRT-PCR analysis of gene expression in sea cucumber *Apostichopus japonicus* during aestivation. Chinese Journal of Oceanology and Limnology, 2014, 32(6): 1248-1256. doi: 10.1007/s00343-015-4004-2

Zheng Y, Cong X, Liu H, et al. Nervous system development and neuropeptides characterization in embryo and larva: insights from a non-chordate deuterostome, the sea cucumber *Apostichopus japonicus*. Biology, 2022, 11(10): 1538. doi: 10.3390/biology11101538.

Zheng Y, Liu H, Cong X, et al. A potential feeding regulation strategy during aestivation: Relaxation of intestine mediated by pedal peptide/orcokinin-type neuropeptides in sea cucumber *Apostichopus japonicus*. Aquaculture, 2024, 579: 740150. doi:10.1016/j.aquaculture.2023.740150.

Supplementary figures

Figure 1-figure supplement 1. Calcitonin-type (CT-type) neuropeptide precursors in *A. japonicus*. (A) *AjCTP1* comprises two putative CT-type neuropeptides, AjCT1 and AjCT2, whereas *AjCTP1* generated by alternative splicing comprises only AjCT2. The predicted signal peptide is shown in blue, the predicted cleavage sites (KR or KK) are shown in green, CT-type neuropeptides are shown in red and C-terminal glycines that are potential substrates for amidation are shown in orange. Predicted disulfide bridges in AjCT1 and AjCT2 are formed between the two underlined cysteines. (B) Nucleotide sequences encoding CT-type neuropeptide precursors and the deduced amino acid sequences in *A. japonicus*. 3'UTR and 5'UTR are shown in lowercase and the ORF is shown in uppercase. Blue uppercase labels the predicted signal peptide, the green uppercase shows the predicted cleavage site, AjCT1 and AjCT2 are shown in red and the putative substrate for amidation is shown in orange.

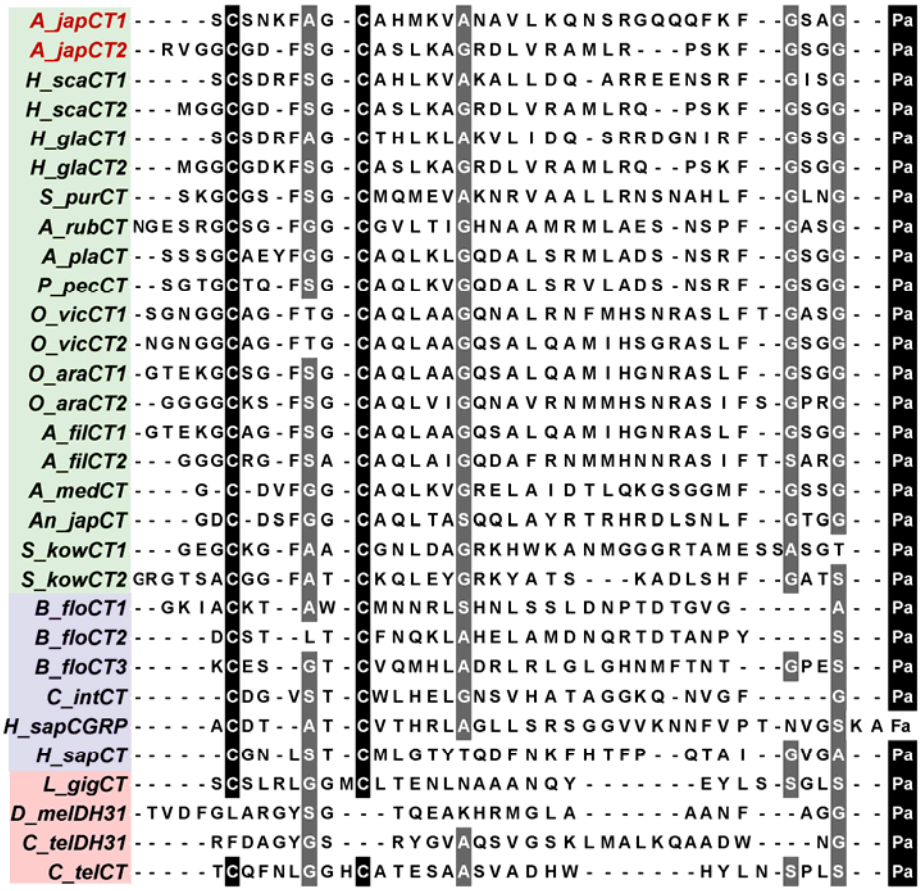

Figure 1-figure supplement 2. Comparison of the sequences CT-type neuropeptides from Bilateria: deuterostomes-ambulacraria (green), deuterostomes-chordates (purple) and protostomes (pink). The conserved residues are shown with white lettering highlighted in gray and black. The accession numbers or citations are shown in the Supplementary table 1.

A

AjCTR

```
  1 cagaatcctttcaccggacctctgcagctgaaatcaaagtcgaattcaggagtggtggat
  1                                           M  Q  E  N  D  G  G  G
 61 gtcaaaacggacactggcagtacgaaaggatatcgaaaATGCAGGAGAACGATTCATATT

  9  F  S  F  G  G  L  G  N  D  P  G  C  G  E  E  F  E  D  F  D
121 ATTTCAGCTTTGGTTCCCTTTACAACGACCCGAGTTGCTCTGAAGAATTTGAAGACTTTG

 29  P  L  A  G  A  D  Q  I  D  E  W  R  R  R  R  D  G  C  C  E
181 ACCCGCTTGCTACAGCTGACCAAATAGACGAATGGAGGAGAAGGCGAGATTCTTGTTGCG

 49  R  I  E  N  E  G  P  P  D  E  P  H  C  G  L  V  W  D  T  W
241 AAAGAATTGAAAACGAGAGCCCTCCTGACGAGCCGCATTGCACGCTTGTATGGGATACGT

 69  D  C  W  N  W  T  G  P  G  D  G  L  V  Q  P  C  P  W  W  V
301 GGGATTGTTGGAACTGGACTACACCCGGAGATACCCTGGTTCAACCATGCCCATGGTGGG

 89  P  Q  V  N  P  N  K  D  A  M  K  G  C  M  P  D  G  G  W  F
361 TTCCACAAGTTAATCCGAACAAAGATGCCATGAAAACATGCATGCCTGATGGGACGTGGT

109  K  H  P  D  T  N  G  T  W  G  N  G  G  N  C  G  A  G  Q  S
421 TCAAACATCCCGACACTAATTATACCTGGACCAACTACTCTAATTGCGGCGCATCACAGA

129  G  I  H  V  A  I  F  Y  T  G  Y  G  V  G  V  I  S  L  C  L
481 GCACTATCCATGTGGCCATATTCTACACCGGATACAGTGTTTCAGTTATATCACTCTGCT

149  A  L  F  I  F  G  Y  F  Q  S  L  G  C  P  R  V  G  I  H  K
541 TAGCCCTCTTCATATTCACATACTTTCAGAGCCTTGGATGCCCGAGGGTTACCATCCACA

169  N  L  F  I  S  F  I  L  G  C  I  S  N  I  T  W  H  I  T  I
601 AAAATCTGTTCATCTCCTTCATCTTGAGCTGCATATCAAACATCACGTGGCATATCACCA

189  I  A  S  A  E  G  K  Q  E  T  A  C  R  I  G  H  I  I  A  Q
661 TCATTGCATCAGCGGAGAGCAAACAGGAGACGGCATGTCGAATAACTCATATCATTGCGC

209  F  F  V  L  C  N  Y  F  W  M  L  G  E  G  L  G  L  H  G  V
721 AGTTTTTTGTCCTTTGCAACTACTTTTGGATGCTAAGTGAGGGATTATACCTACATACGG

229  I  V  V  A  V  F  S  E  N  H  N  L  L  L  Y  Y  I  V  G  W
781 TGATAGTGGTTGCAGTCTTCTCGGAAAATCATAATCTCCTTCTCTATTATATCGTCGGAT

249  V  I  P  L  V  P  A  G  V  F  L  S  L  L  L  T  Q  D  G  G
841 GGGTGATTCCATTGGTGCCAGCAAGTGTTTTCCTCAGCTTGTTATTAACACAAGATGGTG

269  R  C  W  G  N  A  N  E  I  E  W  V  V  G  G  G  I  I  A  V
901 GAAGGTGTTGGACGAACGCTAATGAGATCGAATGGGTCGTGGGTGGAACTATTATTGCAG

289  L  L  T  N  A  A  L  L  L  N  I  V  R  V  L  V  G  K  L  R
961 TATTATTGACAAACGCTGCTCTTCTCCTTAACATAGTACGCGTTTTAGTCACGAAGCTTA

309  A  T  P  S  Q  G  A  R  T  Y  V  R  A  V  R  A  T  I  I  L
1021 GGGCAGCACCAGCCCAAGGTGCAAGAACATACGTAAGAGCTGTTCGAGCGGCCATTATTC

329  L  P  L  M  G  L  H  G  I  I  V  P  V  R  P  G  D  N  H  V
1081 TGCTTCCTCTGATGGGCCTCCATTATATCATCGTTCCAGTGAGGCCAAGTGATAACCATG

349  A  E  V  I  G  D  C  I  V  A  F  L  I  S  F  Q  G  L  F  V
1141 TAGCCGAAGTTATTTACGATTGTATCGTCGCTTTCTTAATTTCATTTCAGGGCCTTTTCG

369  A  C  I  F  C  F  F  N  G  E  V  K  M  Q  I  R  R  K  W  L
1201 TAGCCTGCATATTTTGTTTCTTCAATGGCGAGGTAAAGATGCAGATCAGGAGAAAATGGC

389  G  N  W  Q  F  R  R  G  G  D  F  R  S  R  H  G  G  G  G  V
1261 TATCCAACTGGCAGTTCAGAAGAAGTGGTGACTTCCGGTCACGACACACCACTACTACTG

409  G  E  A  V  G  T  G  P  P  L  G  V  N  L  H  G  E  K  D  L
1321 TAACCGAAGCTGTATCCACTACACCACCTCTGAGTGTCAATCTTCATTCGGAGAAAGATT

429  D  N  G  I  N  H  P  I  K  G  K  N  G  I  N  G  D  N  G  K
1381 TGGATAACTACATCAATCATCCTATCAAGACAAAGAATGGGATTAACGGGGACAATGGGA

449  G  K  K  G  V  G  F  T  E  A  T  I  A  N  D  M  E  G  R  K
1441 AGAGTAAAAAATCGGTCGGATTTACAGAGGCGACGATTGCTAACGACATGGAAAGTCGAA

469  P  L  M  G  G  K  D  A  A  E  D  P  D  K  G  T  V  V  *
1501 AACCATTGATGACAGGGAAAGATGCGGCCGAAGATCCAGATAAAACAACGGTAGTTTAAa
1561 atgggaggaaggaaggatgaatgaatgacttcttgagagcccggcgtttcatctctggga
1621 tgtaaaagggggacggatggatatccccatatatatctacattatgtgtactctacaactt
1681 gcttcggacgacacttcttgacatctagacatcggttactactattgcctcaaattttgg
1741 ccaaatgacgcaagaagaagaagacatatcagagactttagaaaattgattttccattc
1801 tgcaaattttgacatcaagttacagtatctgttgttgccttcgcactgtctatgtaccaa
1861 acccagtttggtaacagctcttttgtagctctgttttgtcatgcaatgttgttgaaaaat
1921 agttatcaccgtcctcaacagtcttaacaatttaacgttgtagaaaatgatgaacaggac
1981 ttacatttgacaatatctataaaattactgtgctcaatgtgaatttctgttttccatttg
2041 gttttaagggttatttctgtaatctacggcagatacattccaaacgtagtttgtggaaga
2101 ctacgataacttgaggtagatgaaagcgaattgatctagtctcgttttgctggaactaga
2161 gatttgaagaaaaaaaaaatcattatattatgtttgtatcgtaaattgtaagcaaagtct
2221 cacttacattataacttctcagatatgatccagctcatgcaagaacagaggtagatagaa
2281 agtttagagcatggaagtattttagtcgtcatattttatagttcaagaataaaggcaaaa
2341 ctgagtgaaagtgatgtttccaaaggtgatgagattttcgtgatattcagctagaaaaca
2401 tgctaaaactctggaaatgctcctttggggctaacttgatgatgaggtctgaacctcagc
2461 gtggcctaaatgttattgttaatccaataggtttcaaatttatgaaagtataccttatatat
2521 atatgtttttgtatatatatatatatacgcgtttatatatatatatatata
```

B

AjPDFR1

```
  1 agagagagaggtggagagagagagagtattcttatcagccaatcgggtggtaatttcaat
 61 ccgtttaaagttgcgcgctgtctttccgattcctatagaagtcagttggttgtgatggga
121 acataccggatgcatggttcatgagcaaccattgcacaagatctgtaaagcctacagtcg
181 gtggtctcgtagtaatgtttaccggcatgatatactgtcatattaaactcatagtatgat
241 agtcatgggtgactgccattacaagtaacttgaacacaaatttcgctctagttggtttgt
301 tatttttcattattctttcaggagcatttctttggaattgtaaaacgtaaacggtttggg
361 ttgtgctttgcgcagtgagctttaagtgttctgtttactacgattgatcatattcctacc
  1                                       M  G  V  G  N  V  P  C  P  D  N
421 gtaactcaacaatatataactgcgcaacaATGAGTGTCGGGAACGTACCCTGCCCTGACA

 12  S  R  G  G  I  I  P  Y  D  V  T  G  M  T  L  F  C  P  E  T
481 ATTCCAGGAGCAGTATTATTCCTTATGACGTCACAGGTATGACTTTGTTCTGTCCCGAGA

 32  G  D  G  T  L  C  W  P  D  G  P  P  N  T  T  V  H  I  D  C
541 CCTATGACTCTACTCTCTGCTGGCCAGATACACCACCGAACACGACAGTGCATATAGATT

 52  P  I  F  P  W  N  A  G  I  D  I  D  A  Q  A  H  R  R  C  G
601 GCCCGATTTTTCCATGGAACGCTGGAATTGACATTGATGCCCAGGCACATCGTCGGTGTG

 72  A  D  G  F  W  E  Q  H  V  G  E  D  C  G  Q  I  G  P  P  G
661 GGGCTGATGGATTCTGGGAACAGCATGTCTACGAAGATTGCTCGCAGATAGGACCACCTG

 92  T  V  P  P  G  N  H  E  D  D  L  K  F  Y  G  K  V  I  N  G
721 GAACTGTTCCTCCTGGATATACAGAGGATGATCTTAAGTTTTATAGCAAAGTAATAAATG

112  A  K  I  L  E  V  I  G  I  T  M  G  L  M  A  V  L  V  A  L
781 GTGCCAAGATCCTGGAGGTGATTGGGATAACTATGTCTCTTATGGCGGTGCTGGTAGCAT

132  Y  I  F  H  G  F  R  G  L  R  N  H  R  G  R  I  H  Q  H  L
841 TGTACATATTCCATTCTTTCAGGAGTTTGCGCAATCATCGTACTCGAATACATCAACATC

152  F  L  A  F  L  I  R  L  G  L  D  V  I  F  M  I  N  R  F  K
901 TGTTTCTAGCCTTCCTTATCCGACTCACTCTCGATGTTATATTCATGATTAACAGGTTCA

172  K  K  A  G  D  G  L  E  P  V  G  I  N  K  F  P  P  L  V  K
961 AAAAGAAAGCCTCAGATTCTTTGGAACCAGTTGGCATCAACAAATTTCCACCATTGGTGA

192  V  M  E  L  C  R  E  Y  A  R  L  C  G  F  T  W  M  F  V  E
1021 AAGTAATGGAACTTTGCCGAGAATATGCCCGATTGTGTACGTTTACGTGGATGTTTGTGG

212  G  I  G  L  N  G  L  L  G  G  A  V  F  R  K  P  N  F  L  W
1081 AAGGCATATACCTGAACAGTCTTTTATCAACCGCCGTCTTCAGAAAACCAAACTTCCTCT

232  Y  Y  L  I  G  W  A  S  P  I  P  F  V  L  A  F  C  I  A  M
1141 GGTACTATCTCATTGGCTGGGCCTCACCGATACCATTTGTGCTAGCATTTTGCATTGCGA

252  Q  K  T  S  G  N  G  G  W  H  I  G  T  E  S  N  Y  G  V  F
1201 TGCAAAAGACATCTTCAAATGGCTATTGGCATATATACACTGAATCAAATTATTACGTAT

272  F  I  E  G  P  R  N  I  I  V  V  M  N  V  F  L  L  L  N  I
1261 TTTTCATTGAGGGACCAAGAAACATTATCGTCGTGATGAATGTGTTCCTCCTCCTGAACA

292  I  R  V  L  I  G  K  L  R  E  G  Q  T  G  E  G  K  Q  V  R
1321 TTATCAGAGTCTTGATAACAAAACTGAGGGAAAGCCAAACCAGCGAGACGAAACAAGTCA

312  K  A  G  K  A  C  I  V  L  L  P  L  L  G  T  A  N  L  V  W
1381 GGAAGGCAACCAAGGCCTGTATCGTATTACTGCCTCTGCTGGGTACTGCTAATCTTGTTT

332  I  P  K  V  P  E  P  G  K  G  G  R  F  Y  F  A  S  Y  Y  Y
1441 GGATTCCGAAAGTTCCAGAGCCTGGCAAATCGTCTCGGTTTTACTTTGCTAGTTACTACT

352  V  V  L  F  L  D  A  Y  Q  G  F  F  L  A  L  L  Y  C  F  L
1501 ACGTGGTTCTATTCCTGGATGCTTACCAAGGTTTCTTCCTGGCATTATTGTATTGCTTCT

372  N  I  D  V  R  V  G  I  K  R  K  W  Q  G  W  M  N  A  R  N
1561 TAAACATTGATGTCCGAGTTACGATAAAAAGAAAATGGCAAGGTTGGATGAACGCCAGAA

392  P  Y  R  A  H  G  G  V  V  T  G  G  T  D  V  R  M  G  G  L
1621 ATCCTTATCGAGCTCATGGATCTGTGGTTACTACGACAACCGATGTACGGATGTCATCTT

412  D  N  N  D  G  E  W  G  G  K  *
1681 TGGATAACAATGACAGTGAGTGGGGTGGGAAATGAagtcaaatatgatggcgctattgaa
1741 ctaattttatctttgcaattggtatccaggtgtggttaactagacgtgtatgtatcctta
1801 acaacatgtattcggcaacttgctcgcacattgttctggtcaccgataacctaatttcac
1861 ccaatgcatatcaccaatagagtttcaatacctatatatccatgcagtgaacgattttgt
1921 acgaatgtgtataagtgccatgcttgacaatttaaactttgtactatactcgttttaaga
1981 cgtcgaattgatctgtttgttgttaacaaagtaatcatttgctattacgaattggtaaat
2041 tttctcaaaagtatatttgataaaatgatcacatatgtatagcagaaaaagataaaaaaa
2101 aagtactctgcgttgatac
```

1270

1271

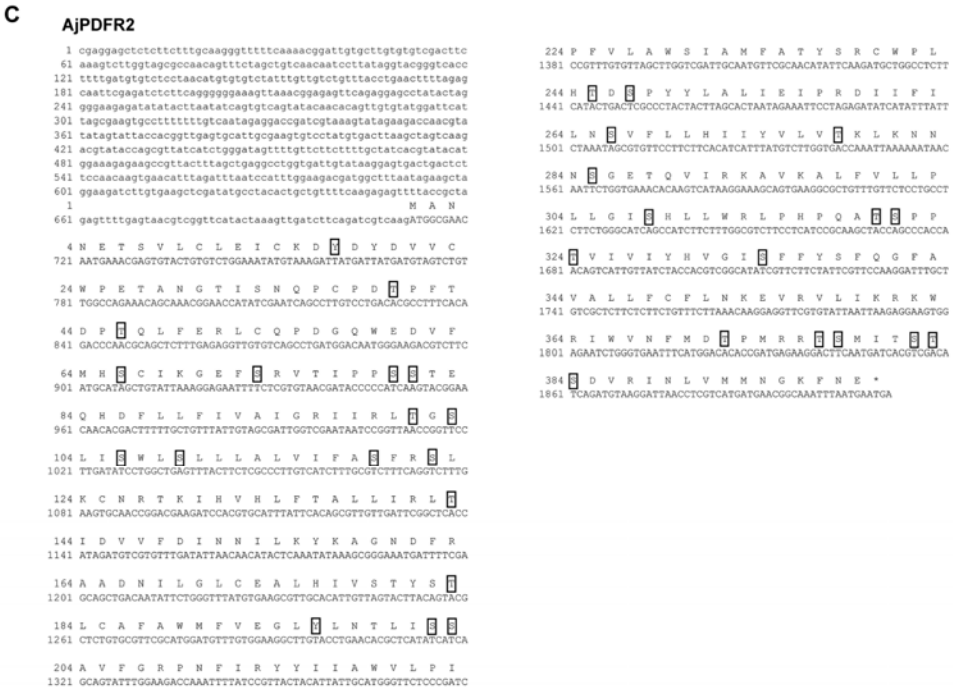

Figure 2-figure supplement 1. Amino acid sequences and phosphorylation sites of AjCTR, AjPDFR1 and AjPDFR2 in *A. japonicus*. (A), (B) and (C) show the cDNA sequences encoding the receptors and their deduced amino acid sequences. ORFs are shown in uppercase; 3'UTR and 5'UTR are shown in lowercase. The stop codon is shown by the asterisk (*). Predicted potential phosphorylation sites are shown with squares.

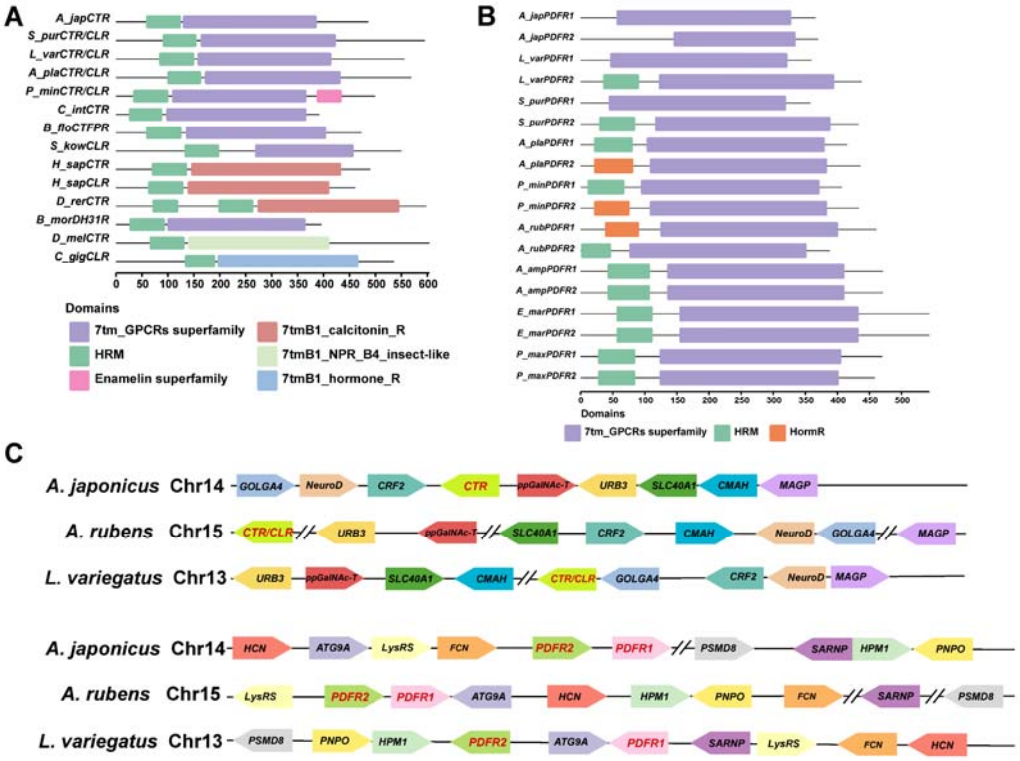

Figure 2-figure supplement 2. Characterization of AjCT1 and AjCT2 receptors (AjCTR, AjPDFR1 and AjPDFR2). (A) Conserved domains of CTR/CLR-type protein sequences. Black line represents the length of proteins and different domains are represented by rectangles. (B) Conserved domains of PDFRs in Bilateria. Black line represents the length of proteins and different domains are represented by rectangles. (C) Synteny analysis of AjCT1 and AjCT2 receptors (AjCTR, AjPDFR1 and AjPDFR2). The chromosomal locations of AjCT1 and AjCT2 receptor genes from *A. rubens*, *L. variegatus* and *A. japonicus* are shown, with different colors used to mark neighboring genes and with their transcriptional direction shown by arrows. *GOLGA4*, golgin subfamily A member 4; *NeuroD*, neurogenic differentiation factor; *CRF2*, corticotropin-releasing factor receptor 2; *CTR*, calcitonin type receptor; *CLR*, calcitonin gene-related peptide type 1 receptor; *ppGalNAc-T*, polypeptide N-acetylgalactosaminyltransferase; *URB3*, E3 ubiquitin-protein ligase ubr3; *SLC40A1*, solute carrier family 40 member 1; *CMAH*, cytidine monophosphate-N-acetylneuraminic acid hydroxylase; *MAGP*, microfibril-associated glycoprotein; *HCN*, hyperpolarization-gated and cyclic nucleotide regulated channel; *ATG9A*, autophagy-related protein 9A-like; *lysRS*, lysine--tRNA ligase; *FCN*, ficolin; *PDFR1*, pigment-dispersing factor receptor 1; *PDFR2*, pigment-dispersing factor receptor 2; *PSMD8*, 26S proteasome regulatory subunit 8; *SARNP*, SAP domain-containing ribonucleoprotein; *HPM1*, histidine protein methyltransferase 1; *PNPO*, pyridoxine-5'-phosphate oxidase.

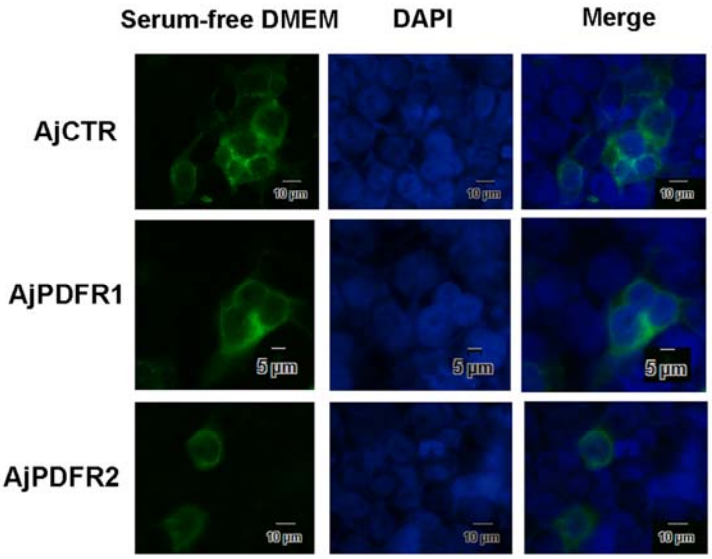

Figure 4-figure supplement 1. Negative control for analysis of AjCTR, AjPDFR1 and AjPDFR2 internalization. The images show the localization of AjCTR, AjPDFR1 and AjPDFR2 in HEK293T cells without AjCT1 or AjCT2 stimulation. Green fluorescence represents the localization of pEGFP-N1/receptors in cell membrane. Cell nucleus probe (DAPI) was applied for cell nucleus staining. All pictures are representative of three independent experiments.

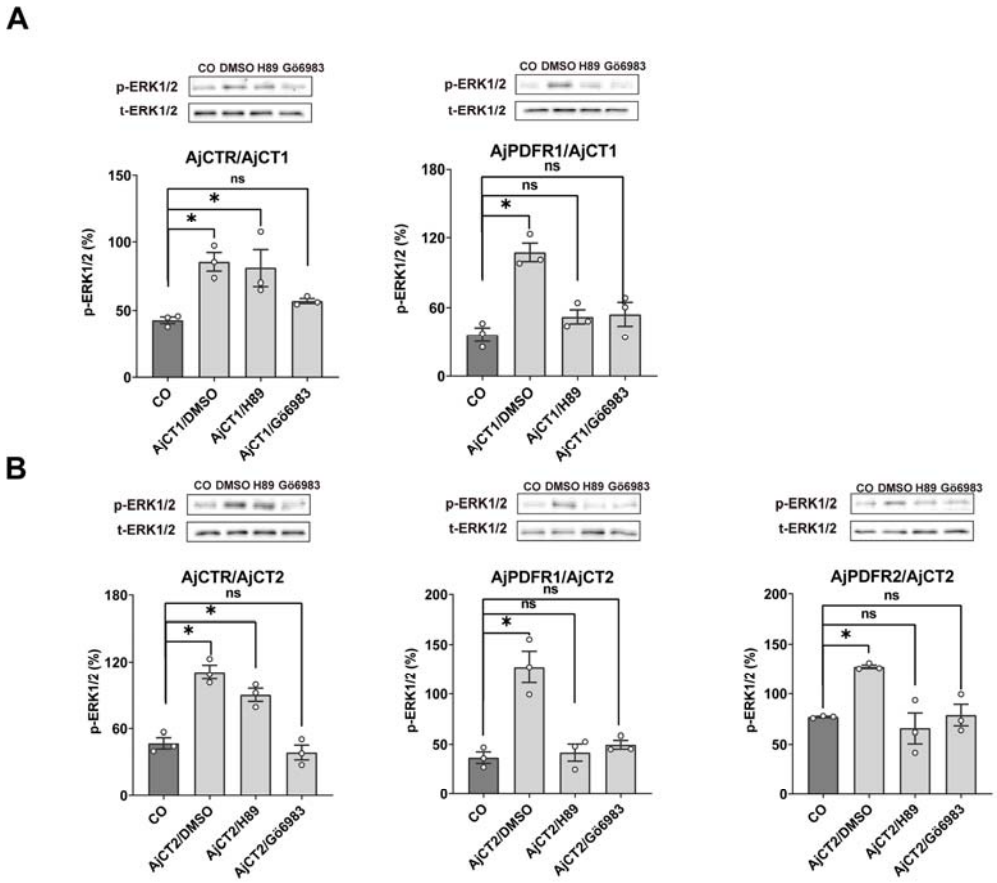

Figure 5-figure supplement 1. Effects of PKA or PKC inhibitor on AjCT1 or AjCT2 stimulated ERK1/2 phosphorylation in AjCTR, AjPDFR1 or AjPDFR2 expressing HEK293T cells. (A) ERK1/2 phosphorylation, activated by AjCT1, is blocked by PKC inhibitor Gö 6983 in AjCTR expressing HEK293T cells and is blocked by PKA inhibitor H89 and PKC inhibitor in AjPDFR1 expressing HEK293T cells. (B) ERK1/2 phosphorylation, activated by AjCT2, is blocked by PKC inhibitor in AjCTR expressing HEK293T cells and is blocked by PKA inhibitor and PKC inhibitor in AjPDFR1 and AjPDFR2 expressing HEK293T cells. Serum-starved HEK293 cells were pre-treated with DMSO, PKA inhibitor, or PKC inhibitor before AjCT1 or AjCT2 stimulation. All images are representative of three independent experiments. Error bars represent SEM for three independent experiments. Statistically significant differences are indicated as follows: *: $p < 0.05$, ns: no significant.

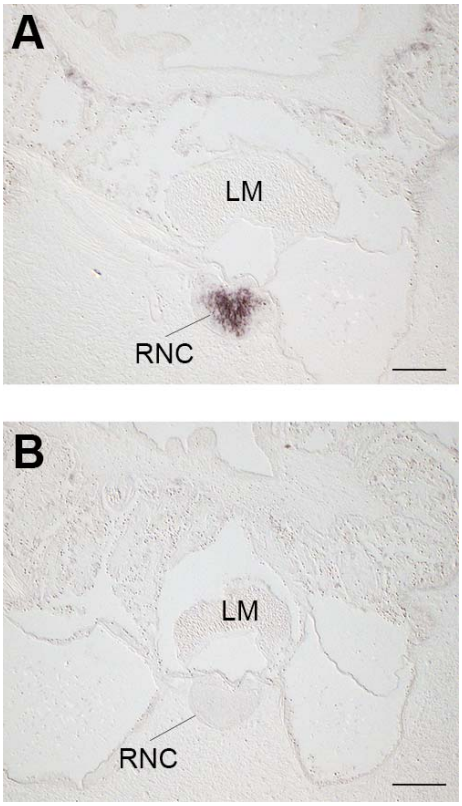

Figure 7–figure supplement 1. Immunostaining in the radial nerve cord of *A. japonicus* is abolised by pre-absorption of ArCT antiserum with the ArCT antigen peptide. (A) Transverse section of a juvenile specimen of *A. japonicus* showing immunostaining in the radial nerve cord revealed by an antiserum to the starfish calcitonin-type neuropeptide ArCT, as also shown in Figure 7A. (B) A transverse section neighbouring the section shown in A was incubated with ArCT antiserum that had been pre-absorbed with the ArCT antigen peptide; note the absence of immunostaining in the radial nerve cord, demonstrating the specificity of the immunostaining in A. Abbreviations: LM, longitudinal muscle; RNC, radial nerve cord. Scale is 100 µm.

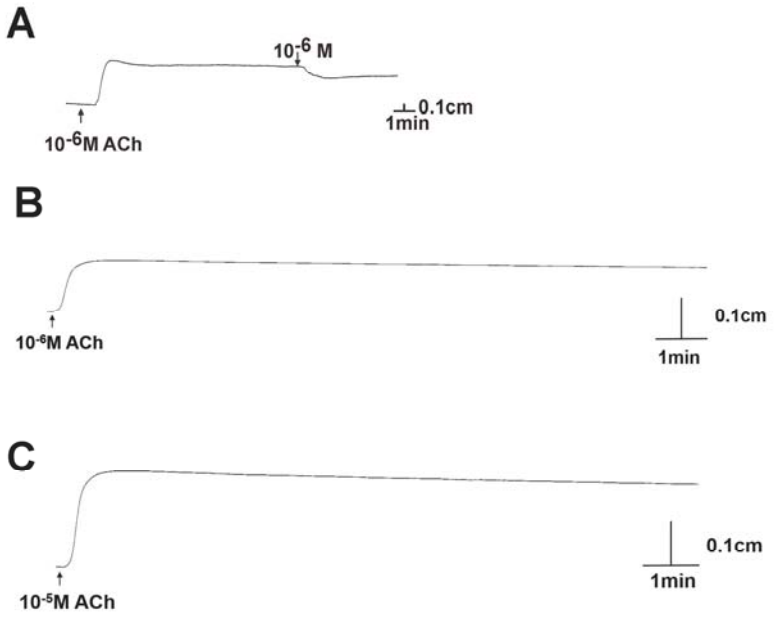

Figure 8-figure supplement 1. Positive control on experimental tissues and pharmacological effects of 10^{-6} M AjCT2 on longitudinal muscle from *A. japonicus*. (A) shows a recording of the relaxing effect of AjCT2 (10^{-6} M) on a longitudinal muscle preparation. (B) and (C) respectively are recordings of the contracting effects of ACh on longitudinal muscle and intestine preparations, showing that the effect of ACh persists for at least 15 minutes. All recordings shown are representative of three independent experiments.

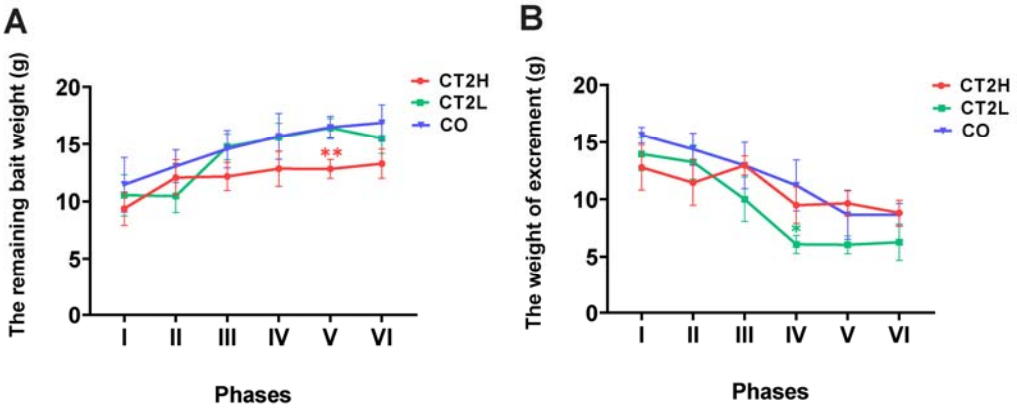

Figure 9A-figure supplement 1. Measurement of the mass of remaining bait and excrement for AjCT2-treated and control animals. (A) Remaining bait mass in different phases. (B) The mass of excrement in different phases. The 24-day experiment was divided into six phases (I-VI), with each phase comprising four days for statistical analysis. CO: control group (sterilized seawater); CT2L: AjCT2 low concentration group (5×10^{-3} mg/mL); CT2H: AjCT2 high concentration group (5×10^{-1} mg/mL). Values are means ± SEM (n = 3, representing three parallel experiments of each group). Asterisks represent the significant difference as follows: *: $p < 0.05$, **: $p < 0.01$.

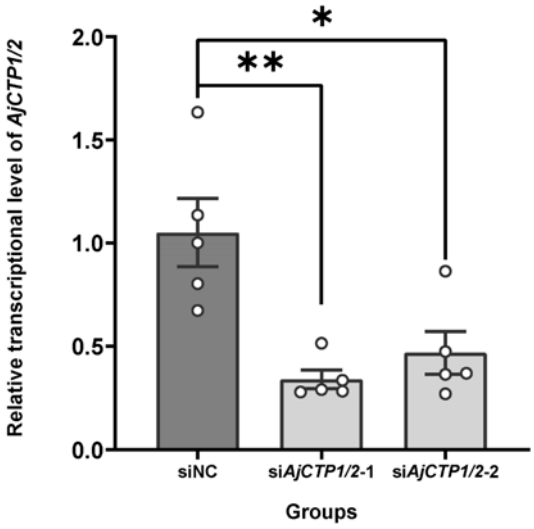

Figure 10-figure supplement 1. The relative expression level of *AjCTP1/2* in siNC, si*AjCTP1/2*-1 and si*AjCTP1/2*-2. siNC: negative control group; si*AjCTP1/2*-1 and si*AjCTP1/2*-2: experimental groups targeting *AjCTP1/2*. Values are means ± SEM (n = 5). Asterisks represent the significant differences as follows: *: $p < 0.05$, **: $p < 0.01$.

Supplementary tables

Supplementary table 1. Accession numbers or citations of calcitonin-type family peptides or precursors in Bilateria

Abbreviation	Species Names	Accession Numbers And/or Citations
H_sapCTP	*Homo sapiens*	GI:179819
H_sapCGRPP	*Homo sapiens*	NP_001029125.1
T_rubCTP	*Takifugu rubripes*	GenBank: CAC81278.1
T_rubCGRPP	*Takifugu rubripes*	GenBank: CAC81277.1
C_intCTP	*Ciona intestinalis*	GenBank: BAI63095.1
B_floCTP1	*Branchiostome floridae*	GI:260826569
B_floCTP2	*Branchiostome floridae*	GI:260826567
B_floCTP3	*Branchiostome floridae*	GI:260826573
S_kowCTP	*Saccoglossus kowalevskii*	GI:187217193
A_japCTP1	*Apostichopus japonicus*	GenBank: AWU78769.1
A_japCTP2	*Apostichopus japonicus*	GenBank: AWU78770.1
A_rubCTP	*Asterias rubens*	GenBank: KT601715.1
P_pecCTP	*Patiria pectinifera*	GenBank: AWX63418.1
A_plaCTP	*Acanthaster planci*	Smith et al. (2017)
S_purCTP	*Strongylocentrotus purpuratus*	GI:115767208
O_vicCTP1	*Ophionotus. victoriae*	GenBank: ASK86238.1
O_vicCTP2	*Ophionotus. victoriae*	GenBank: ASK86238.1
O_araCTP1	*Ophiopsila aranea*	Zandawala et al. (2017)
O_araCTP2	*Ophiopsila aranea*	
A_filCTP1	*Amphiura filiformis*	
A_filCTP2	*Amphiura filiformis*	
H_scaCTP1	*Holothuria scabra*	Suwansa-Ard et al. (2018)

H_scaCTP2	*Holothuria scabra*	
H_glaCTP1	*Holothuria glaberrima*	
H_glaCTP2	*Holothuria glaberrima*	
A_medCTP	*Antedon mediterranea*	Aleotti et al., (2022)
An_japCTP	*Anneissia japonica*	
L_gigCTP	*Lottia gigantea*	GI:163526287
D_melDH31P	*Drosophila melanogaster*	NP_523514.1
L_migDH31P	*Locusta migratoria*	GenBank: AKN21237.1
C_telCTP	*Capitella teleta*	GI: 161220966
C.telDH31P	*Capitella teleta*	Rowe et al. (2014)

Supplementary table 2. Accession numbers of CT-type, PDF-type and CRH-type receptor families in Bilateria

Species	Protein ID	Gene code	Species code
Amphiura filiformis	XP_072029112.1	CRHR	Afil
Amphiura filiformis	XP_072021544.1	CTR	Afil
Amphiura filiformis	XP_072029557.1	PDFR1	Afil
Amphiura filiformis	XP_072028436.1	PDFR2	Afil
Anneissia japonica	XP_033108182.1	CRHR	Anja
Anneissia japonica	XP_033104142.1	CTR	Anja
Anneissia japonica	XP_033104113.1	PDFR	Anja
Apis mellifera	XP_006564466.1	DH31R	Amel
Apis mellifera	XP_016768833.2	PDFR	Amel
Aplysia californica	XP_012938918.2	CRHR	Acal
Aplysia californica	XP_005089839.2	CTR	Acal
Aplysia californica	XP_005093780.3	DH31R	Acal
Apostichopus japonicus	XP_071811976.1	CRHR	Ajap
Apostichopus japonicus	PIK36177.1	CRHR	Ajap
Apostichopus japonicus	XP_071811994.1	CRHR	Ajap
Apostichopus japonicus	PIK41405.1	CRHR	Ajap
Apostichopus japonicus	XP_071812618.1	CTR	Ajap
Apostichopus japonicus	XP_071811731.1	PDFR1	Ajap
Apostichopus japonicus	XP_071812243.1	PDFR2	Ajap
Asterias rubens	ENSASRP00000008640.1	CRHR	Arub
Asterias rubens	ENSASRP00000013963.1	CRHR	Arub
Asterias rubens	ENSASRP00000014061.1	CRHR	Arub
Asterias rubens	ENSASRP00000011186.1	CTR	Arub
Asterias rubens	ENSASRP00000010309.1	PDFR1	Arub
Asterias rubens	ENSASRP00000010166.1	PDFR2	Arub
Bombus impatiens	ENSBIMP00000009704.1	CRHR	Bimp
Bombus impatiens	ENSBIMP00000023653.1	DH31R	Bimp
Bombus impatiens	ENSBIMP00000026387.1	PDFR	Bimp
Branchiostoma floridae	XP_035687893.1	CRHR	Bflo
Branchiostoma floridae	XP_035687894.1	CRHR	Bflo
Branchiostoma floridae	XP_035689670.1	CRHR	Bflo
Branchiostoma floridae	XP_035689671.1	CRHR	Bflo
Branchiostoma floridae	XP_035687895.1	CTR*	Bflo
Caenorhabditis elegans	NP_001122749.1	SEB2*	Cele
Ciona intestinalis	XP_002122381.1	CRHR	Cint
Ciona intestinalis	XP_009858716.1	CRHR	Cint
Drosophila melanogaster	NP_725278.1	DH31R*	Dmel

Drosophila melanogaster	NP_001285174.1	HECTOR	Dmel
Drosophila melanogaster	CAB72288.1	PDFR	Dmel
Gallus gallus	ENSGALP00010018855.1	CLR*	Ggal
Gallus gallus	ENSGALP00010039362.1	CRHR	Ggal
Gallus gallus	ENSGALP00010039367.1	CRHR	Ggal
Gallus gallus	ENSGALP00010033414.1	CRHR	Ggal
Gallus gallus	ENSGALP00010004560.1	CTR*	Ggal
Gekko gecko	ENSEGEP00000030211.1	CLR	Ggec
Gekko gecko	ENSEGEP00000005175.1	CRHR	Ggec
Gekko gecko	ENSEGEP00000009950.1	CRHR	Ggec
Gekko gecko	ENSEGEP00000001898.1	CTR	Ggec
Homo sapiens	ENST04850112052.1	CLR*	Hsap
Homo sapiens	ENST04850047995.1	CRHR	Hsap
Homo sapiens	ENST04850093643.1	CRHR	Hsap
Homo sapiens	ENST04850217190.1	CTR*	Hsap
Hypsibius exemplaris	OQV19025.1	CRHR	Hexe
Hypsibius exemplaris	OQV18662.1	CRHR	Hexe
Hypsibius exemplaris	OWA52582.1	CTR	Hexe
Hypsibius exemplaris	OWA52579.1	DH31Ra	Hexe
Hypsibius exemplaris	OQV24416.1	DH31Rb	Hexe
Hypsibius exemplaris	OQV13187.1	PDFR	Hexe
Lepisosteus oculatus	XP_015199664.1	CLRa	Locu
Lepisosteus oculatus	XP_015214520.1	CLRb	Locu
Lepisosteus oculatus	XP_015209811.1	CRHR	Locu
Lepisosteus oculatus	XP_015217722.1	CRHR	Locu
Lepisosteus oculatus	XP_006636078.2	CTR	Locu
Limulus polyphemus	XP_013771881.1	CRHR	Lpol
Limulus polyphemus	XP_022240360.1	CRHR	Lpol
Limulus polyphemus	XP_013775447.1	CRHR	Lpol
Limulus polyphemus	XP_013791145.1	CRHR	Lpol
Limulus polyphemus	XP_013791446.1	CRHR	Lpol
Limulus polyphemus	XP_022240480.1	CTRa	Lpol
Limulus polyphemus	XP_022240470.1	CTRb	Lpol
Limulus polyphemus	XP_022254242.1	CTRc	Lpol
Limulus polyphemus	XP_022237602.1	CTRd	Lpol
Limulus polyphemus	XP_022246293.1	DH31Ra	Lpol
Limulus polyphemus	XP_022235154.1	DH31Rb	Lpol
Limulus polyphemus	XP_022235431.1	DH31Rc	Lpol
Limulus polyphemus	XP_022239928.1	DH31Rd	Lpol
Limulus polyphemus	XP_022248891.1	DH31Re	Lpol
Limulus polyphemus	XP_022255301.1	PDFR	Lpol
Lineus longissimus	ENSLLNP00015009405.1	CRHR	Llon
Lineus longissimus	ENSLLNP00015009422.1	CRHR	Llon
Lineus longissimus	ENSLLNP00015009434.1	CRHR	Llon
Lineus longissimus	ENSLLNP00015009638.1	CTRa	Llon
Lineus longissimus	ENSLLNP00015008640.1	CTRb	Llon
Lineus longissimus	ENSLLNP00015012550.1	CTRc	Llon
Lineus longissimus	ENSLLNP00015013093.1	DH31R	Llon
Lineus longissimus	ENSLLNP00015009635.1	PDFR	Llon
Lumbricus terrestris	ENSVPPP00000022107.1	CTRa	Lter

Lumbricus terrestris	ENSVPPP00000011858.1	CTRb	Lter
Lumbricus terrestris	ENSVPPP00000018690.1	CTRc	Lter
Lumbricus terrestris	ENSVPPP00000033159.1	CTRd	Lter
Lumbricus terrestris	ENSVPPP00000030225.1	DH31Ra	Lter
Lumbricus terrestris	ENSVPPP00000022149.1	DH31Rb	Lter
Lumbricus terrestris	ENSVPPP00000003533.1	PDFR	Lter
Magallana gigas	NP_001292279.1	CTR1*	Mgig
Magallana gigas	XP_034310675.2	CTR2*	Mgig
Magallana gigas	XP_011442634.2	CTR3	Mgig
Magallana gigas	XP_011442636.3	CTR4	Mgig
Magallana gigas	XP_065929766.1	CTR5	Mgig
Magallana gigas	XP_065923133.1	CTR6	Mgig
Magallana gigas	XP_052684037.1	CTR7	Mgig
Magallana gigas	XP_034317823.1	PDFR	Mgig
Magallana gigas	XP_034310400.1		Mgig
Owenia fusiformis	CAC9666549.1	CRHR	Ofus
Owenia fusiformis	CAC9666335.1	CTRa	Ofus
Owenia fusiformis	CAC9673671.1	CTRb	Ofus
Owenia fusiformis	CAC9666125.1	DH31R	Ofus
Owenia fusiformis	CAC9578850.1	PDFR	Ofus
Paramacrobiotus metropolita	XP_055352663.1	CRHR	Pmet
Paramacrobiotus metropolita	XP_055352664.1	CRHR	Pmet
Paramacrobiotus metropolita	XP_055329231.1	CTR	Pmet
Paramacrobiotus metropolita	XP_055329233.1	DH31R	Pmet
Paramacrobiotus metropolita	XP_055331530.1	PDFR	Pmet
Pecten maximus	XP_033762144.1	CRHR	Pmax
Pecten maximus	XP_033762006.1	CTRa	Pmax
Pecten maximus	XP_033762916.1	CTRb	Pmax
Pecten maximus	XP_033762874.1	CTRc	Pmax
Pecten maximus	XP_033762263.1	CTRd	Pmax
Pecten maximus	XP_033762155.1	DH31Ra	Pmax
Pecten maximus	XP_033762946.1	DH31Rb	Pmax
Pecten maximus	XP_033729115.1	DH31Rc	Pmax
Pecten maximus	XP_033762294.1	PDFR	Pmax
Platynereis dumerilii	AKQ63006.1	DH31R-1*	Pdum
Platynereis dumerilii	WOE99345.1	PDFR	Pdum
Priapulus caudatus	XP_014664111.1	DH31Ra	Pcau
Priapulus caudatus	XP_014661438.1	DH31Rb	Pcau
Rotaria socialis	CAF3356201.1	PDFRa	Rsoc
Rotaria socialis	CAF3546535.1	PDFRb	Rsoc
Saccoglossus kowalevskii	NP_001161520.1	CRHR	Skow
Saccoglossus kowalevskii	XP_006818813.1	CTR	Skow
Saccoglossus kowalevskii	XP_006825104.1	PDFRa	Skow
Saccoglossus kowalevskii	XP_006825103.1	PDFRb	Skow
Schmidtea mediterranea	SMEST051050001	CRHR	Smed
Schmidtea mediterranea	SMEST064388001	CRHR	Smed
Schmidtea mediterranea	SMEST049048003	CRHR	Smed
Schmidtea mediterranea	SMEST080399003	CTRa	Smed
Schmidtea mediterranea	SMEST042095002	CTRb	Smed
Schmidtea mediterranea	SMEST006966001	DH31Ra	Smed

Schmidtea mediterranea	SMEST027375002	DH31Rb	Smed
Schmidtea mediterranea	SMEST023013001	DH31Rc	Smed
Schmidtea mediterranea	SMEST035956002	PDFR	Smed
Sepioteuthis lessoniana	ENSUKOP00000023564.1	CRHR	Sles
Sepioteuthis lessoniana	ENSUKOP00000009609.1	CTRa	Sles
Sepioteuthis lessoniana	ENSUKOP00000023956.1	CTRc	Sles
Sepioteuthis lessoniana	ENSUKOP00000023961.1	CTRd	Sles
Sepioteuthis lessoniana	ENSUKOP00000005365.1	DH31Ra	Sles
Sepioteuthis lessoniana	ENSUKOP00000007960.1	DH31Rb	Sles
Sepioteuthis lessoniana	ENSUKOP00000030254.1	PDFR	Sles
Strongylocentrotus purpuratus	XP_003725174.2	CRHR	Spur
Strongylocentrotus purpuratus	XP_030845739.1	CRHR	Spur
Strongylocentrotus purpuratus	XP_030846612.1	CRHR	Spur
Strongylocentrotus purpuratus	XP_030846621.1	CTR	Spur
Strongylocentrotus purpuratus	XP_030845952.1	PDFR1	Spur
Strongylocentrotus purpuratus	XP_030845953.1	PDFR2	Spur
Styela clava	XP_039255657.1	CRHR	Scla
Tribolium castaneum	XP_008198347.1	CRHR	Tcas
Tribolium castaneum	XP_008192711.1	CRHR	Tcas
Tribolium castaneum	XP_064212169.1	CTR	Tcas
Tribolium castaneum	XP_008193920.1	DH31Ra	Tcas
Tribolium castaneum	XP_064210831.1	DH31Rb	Tcas
Tribolium castaneum	XP_064212793.1	PDFR	Tcas
Xenopus tropicalis	ENSXETP00000114756.1	CLR	Xtro
Xenopus tropicalis	ENSXETP00000109962.1	CRHR	Xtro
Xenopus tropicalis	ENSXETP00000101014.1	CRHR	Xtro
Xenopus tropicalis	ENSXETP00000060302.3	CTR	Xtro

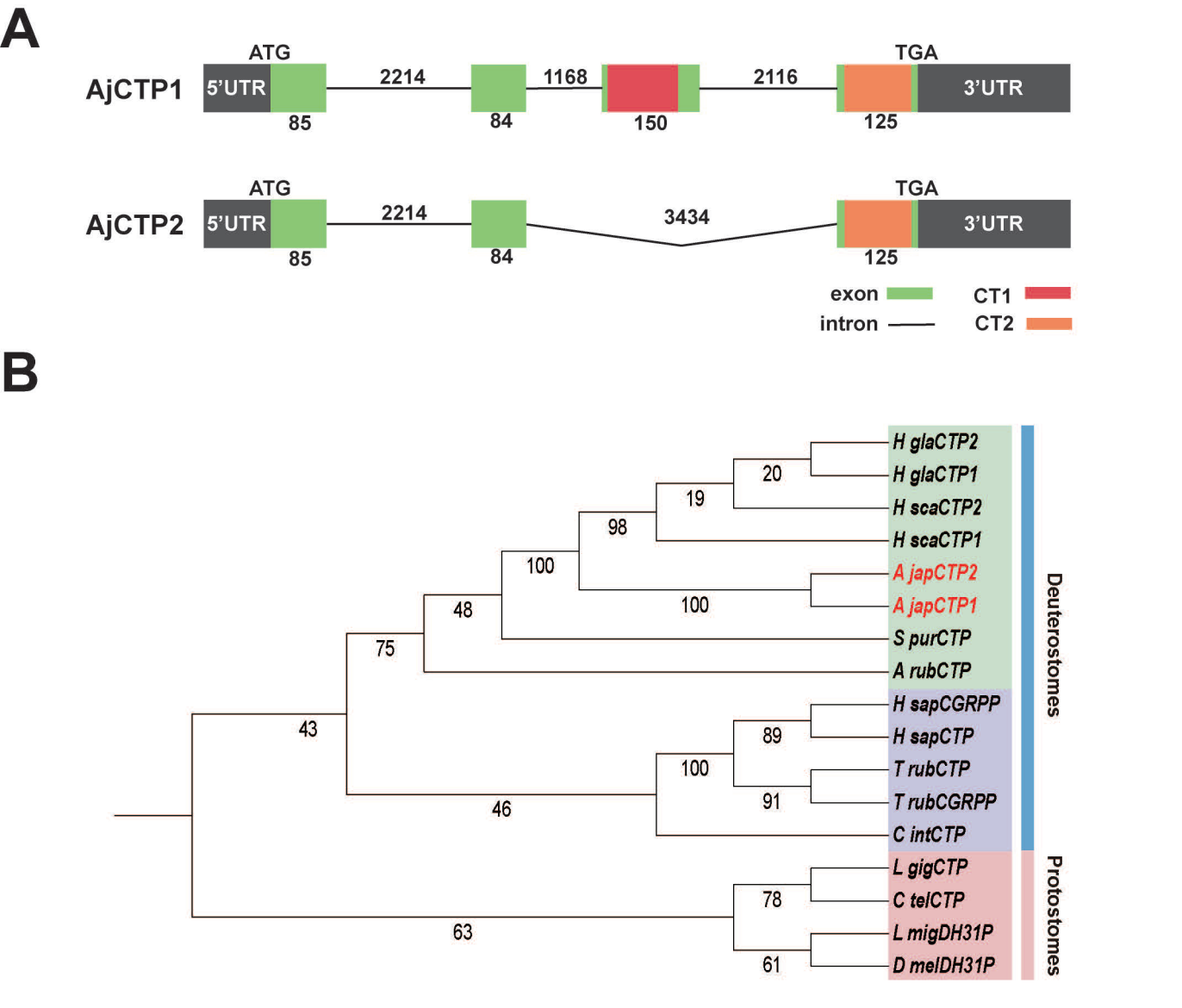
A
AjCTP1
ATG
5'UTR
85
2214
84
1168
150
2116
TGA
125
3'UTR
AjCTP2
ATG
5'UTR
85
2214
84
3434
TGA
125
3'UTR
exon
intron
CT1
CT2
B
H glaCTP2
H glaCTP1
H scaCTP2
H scaCTP1
A japCTP2
A japCTP1
S purCTP
A rubCTP
H sapCGRPP
H sapCTP
T rubCTP
T rubCGRPP
C intCTP
L gigCTP
C telCTP
L migDH31P
D melDH31P
20
19
98
100
100
48
75
43
89
100
91
46
78
63
61
Deuterostomes
Protostomes

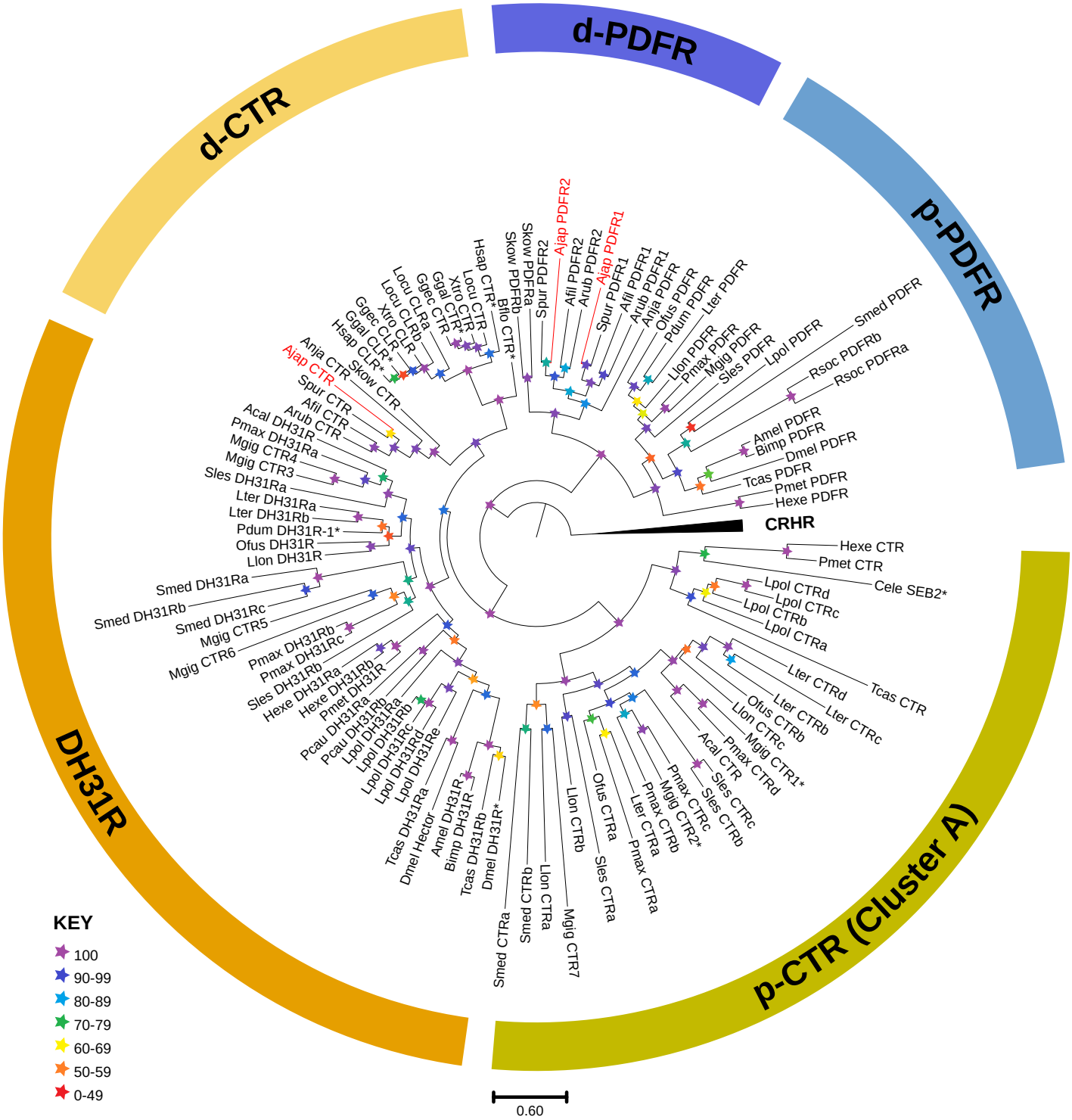
d-CTR
d-PDFR
p-PDFR
DH31R
p-CTR (Cluster A)
CRHR
Ajap PDFR2
Ajap PDFR1
Ajap CTR
Hsap CTR*
Skow PDFRb
Skow PDFRa
Skow PDFR2
Spur PDFR2
Afil PDFR2
Arub PDFR2
Spur PDFR1
Afil PDFR1
Arub PDFR1
Anja PDFR
Ofus PDFR
Pdum PDFR
Lter PDFR
Llon PDFR
Pmax PDFR
Mgig PDFR
Sles PDFR
Lpol PDFR
Smed PDFR
Rsoc PDFRb
Rsoc PDFRa
Amel PDFR
Bimp PDFR
Dmel PDFR
Tcas PDFR
Pmet PDFR
Hexe PDFR
Hexe CTR
Pmet CTR
Cele SEB2*
Lpol CTRd
Lpol CTRc
Lpol CTRb
Lpol CTRa
Tcas CTR
Lter CTRd
Lter CTRc
Lter CTRb
Ofus CTRb
Llon CTRc
Mgig CTR1*
Pmax CTRd
Acal CTR
Sles CTRc
Sles CTRb
Pmax CTRc
Mgig CTR2*
Pmax CTRb
Lter CTRa
Pmax CTRa
Ofus CTRa
Sles CTRa
Llon CTRb
Mgig CTR7
Llon CTRa
Smed CTRb
Smed CTRa
Dmel DH31R*
Tcas DH31Rb
Bimp DH31R
Amel DH31R
Dmel Hector
Tcas DH31Ra
Lpol DH31Re
Lpol DH31Rd
Lpol DH31Rc
Lpol DH31Rb
Lpol DH31Ra
Pcau DH31Rb
Pcau DH31Ra
Pmet DH31R
Hexe DH31Rb
Sles DH31Ra
Pmax DH31Rc
Pmax DH31Rb
Mgig CTR6
Smed DH31Rc
Smed DH31Rb
Smed DH31Ra
Mgig CTR5
Llon DH31R
Ofus DH31R
Pdum DH31R-1*
Lter DH31Rb
Lter DH31Ra
Sles DH31Ra
Mgig CTR3
Mgig CTR4
Pmax DH31Ra
Acal DH31R
Arub CTR
Afil CTR
Spur CTR
Anja CTR
Skow CTR
Hsap CLR*
Ggal CLR*
Ggec CLR
Xtro CLR
Locu CLRb
Locu CLRa
Ggec CTR
Ggal CTR*
Xtro CTR
Locu CTR
Bflo CTR*
KEY
100
90-99
80-89
70-79
60-69
50-59
0-49
0.60

A

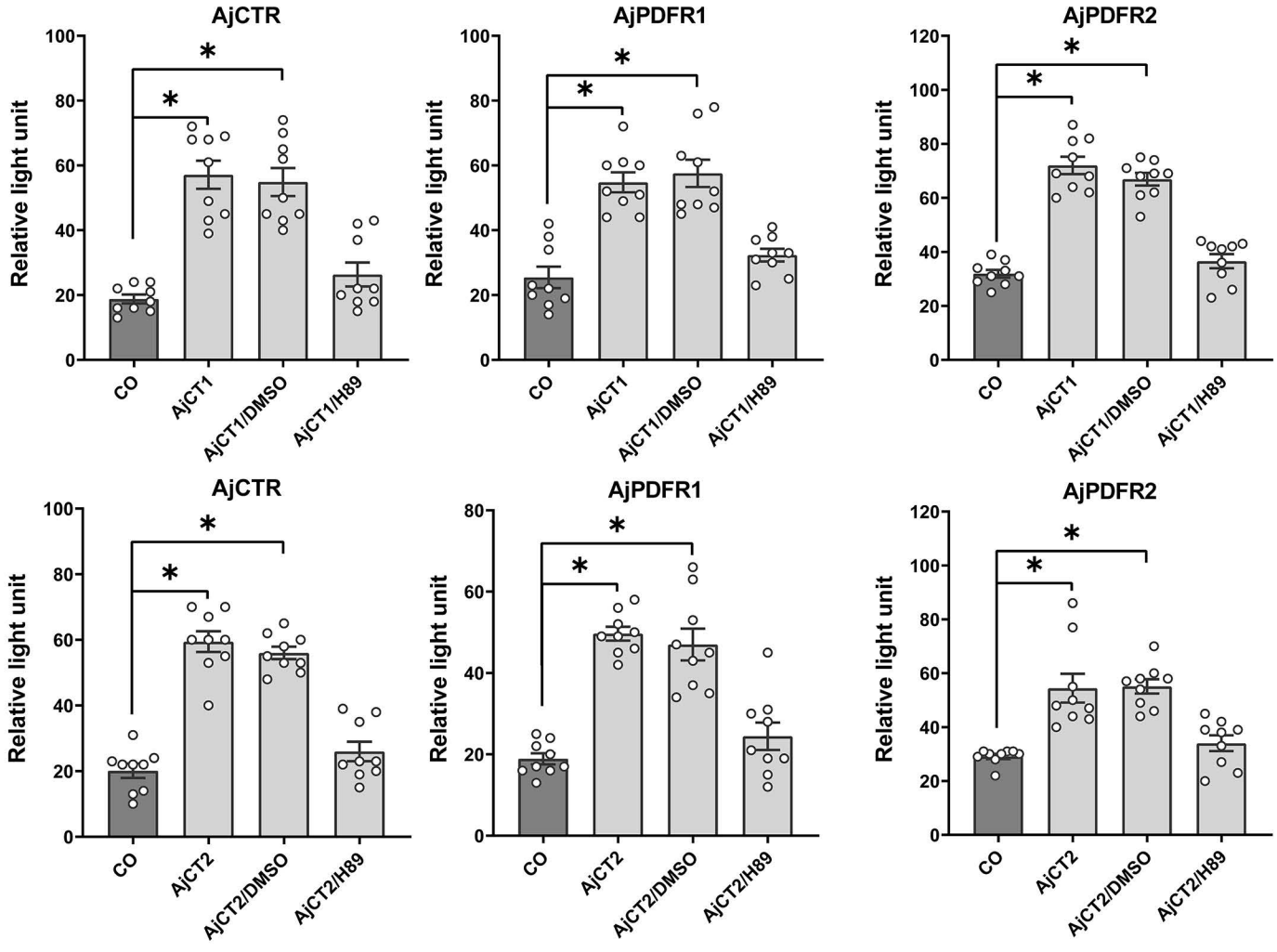
AjCTR
AjPDFR1
AjPDFR2
Relative light unit
CO
AjCT1
AjCT1/DMSO
AjCT1/H89
AjCT2
AjCT2/DMSO
AjCT2/H89
*

B

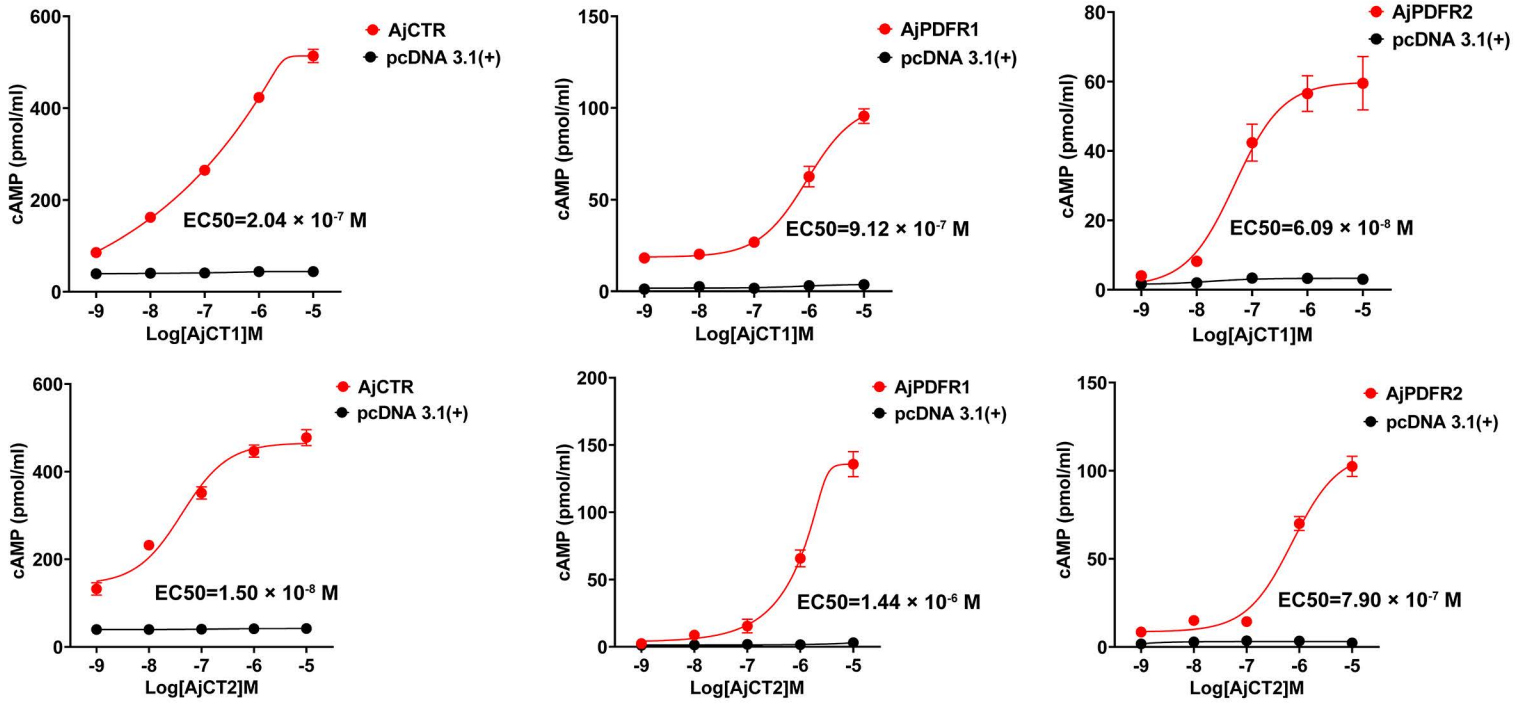
AjCTR
AjPDFR1
AjPDFR2
pcDNA 3.1(+)
cAMP (pmol/ml)
Log[AjCT1]M
Log[AjCT2]M
EC50=2.04 × 10-7 M
EC50=9.12 × 10-7 M
EC50=6.09 × 10-8 M
EC50=1.50 × 10-8 M
EC50=1.44 × 10-6 M
EC50=7.90 × 10-7 M

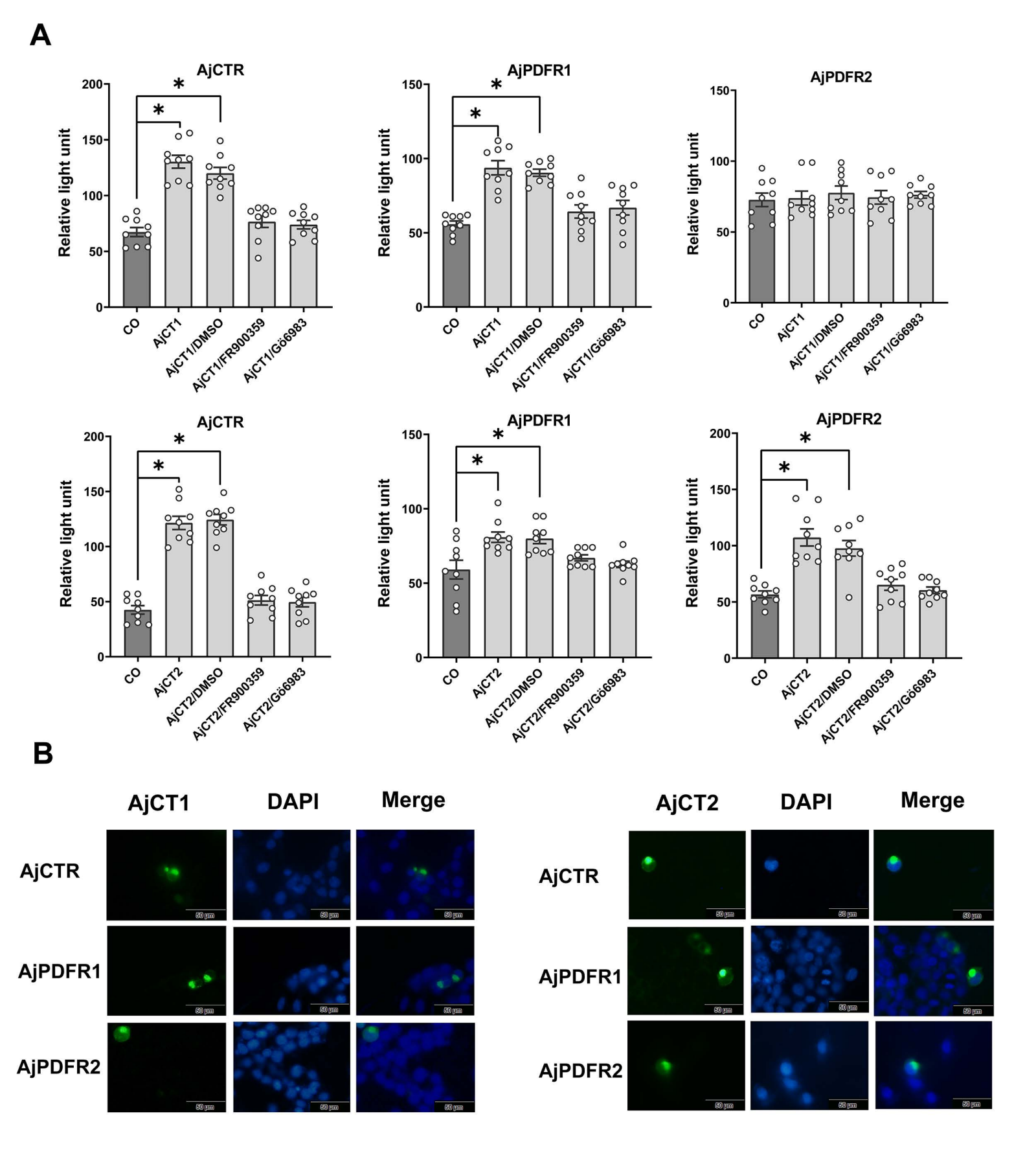
A
AjCTR
AjPDFR1
AjPDFR2
Relative light unit
CO
AjCT1
AjCT1/DMSO
AjCT1/FR900359
AjCT1/Gö6983
AjCT2
AjCT2/DMSO
AjCT2/FR900359
AjCT2/Gö6983
B
AjCT1
DAPI
Merge
AjCT2
AjCTR
AjPDFR1
AjPDFR2
50 μm

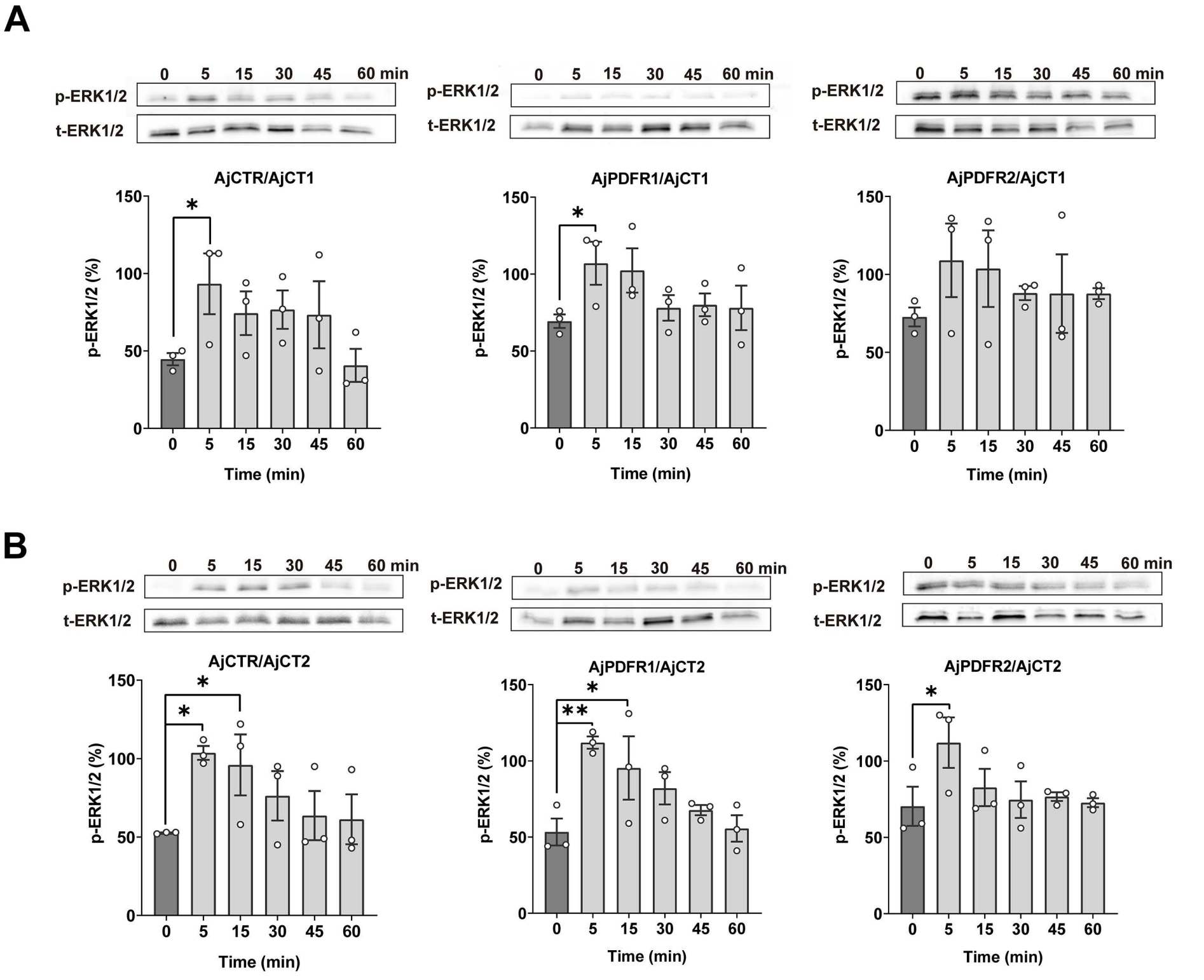
A
0 5 15 30 45 60 min
p-ERK1/2
t-ERK1/2
AjCTR/AjCT1
AjPDFR1/AjCT1
AjPDFR2/AjCT1
p-ERK1/2 (%)
Time (min)
B
AjCTR/AjCT2
AjPDFR1/AjCT2
AjPDFR2/AjCT2

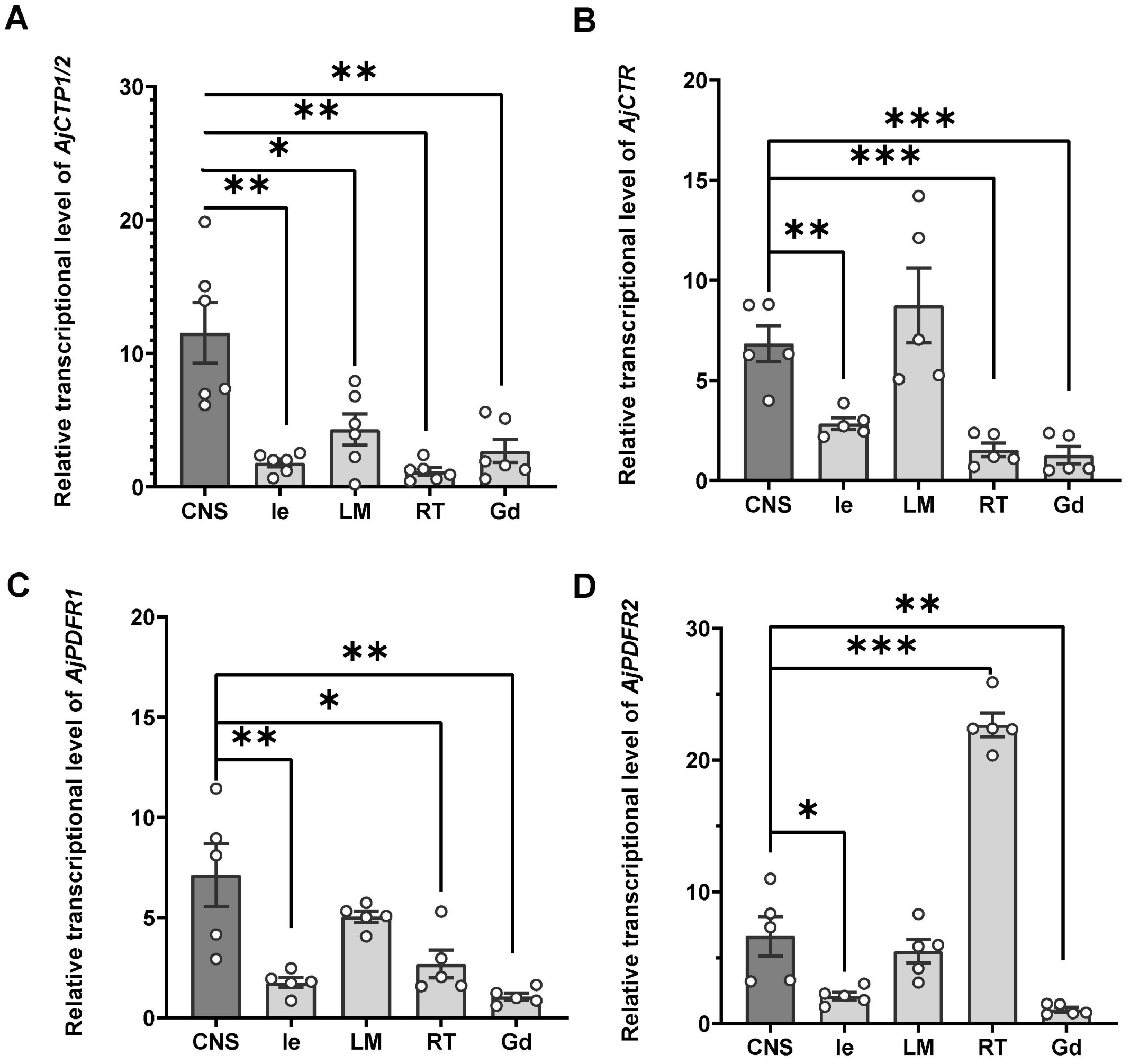
A
Relative transcriptional level of AjCTP1/2
30
20
10
0
**
**
*
**
CNS
Ie
LM
RT
Gd
B
Relative transcriptional level of AjCTR
20
15
10
5
0
***
***
**
CNS
Ie
LM
RT
Gd
C
Relative transcriptional level of AjPDFR1
20
15
10
5
0
**
*
**
CNS
Ie
LM
RT
Gd
D
Relative transcriptional level of AjPDFR2
30
20
10
0
**
***
*
CNS
Ie
LM
RT
Gd

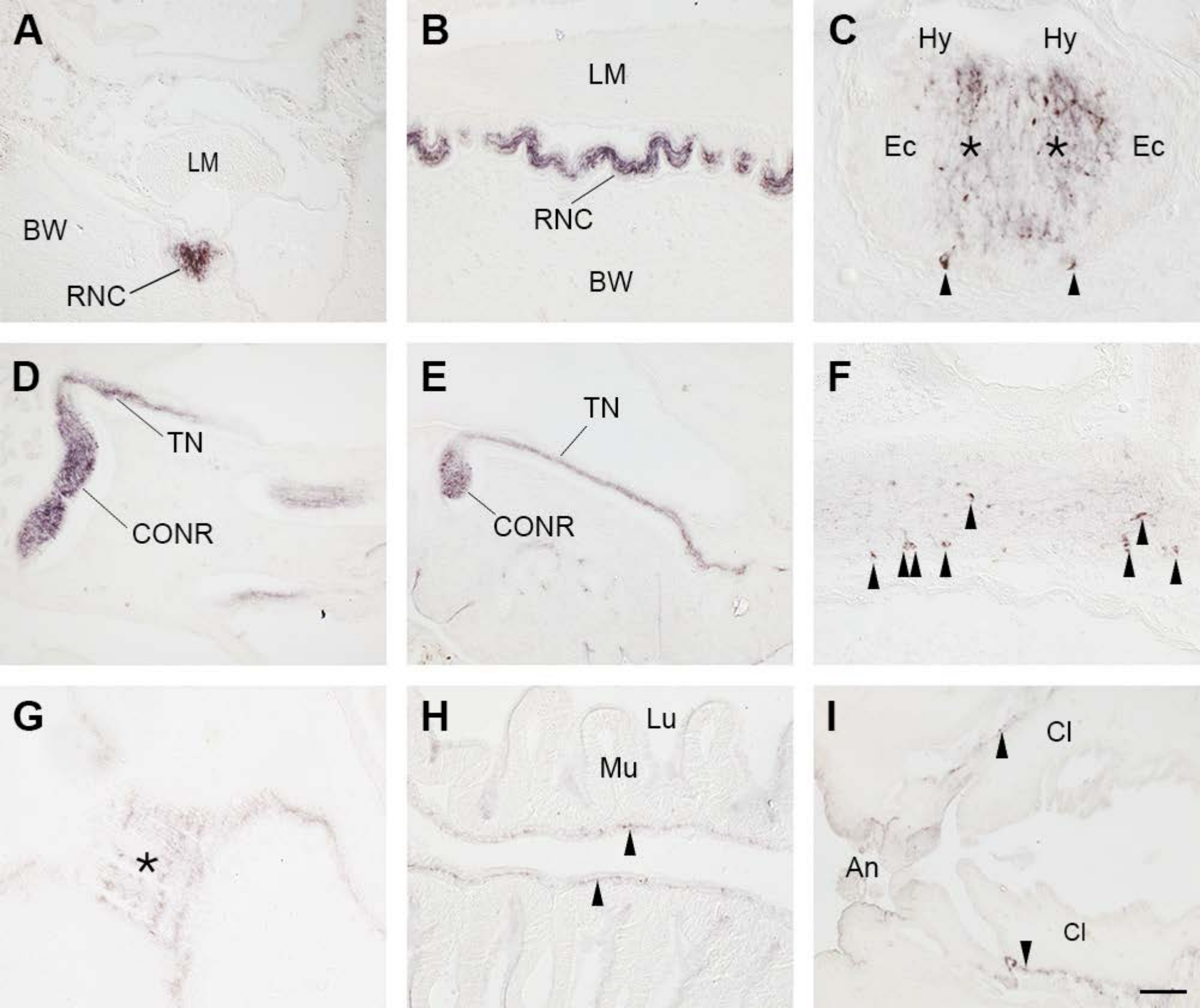
A
LM
BW
RNC
B
LM
RNC
BW
C
Hy
Hy
Ec
Ec
D
TN
CONR
E
TN
CONR
F
G
H
Lu
Mu
I
Cl
An
Cl

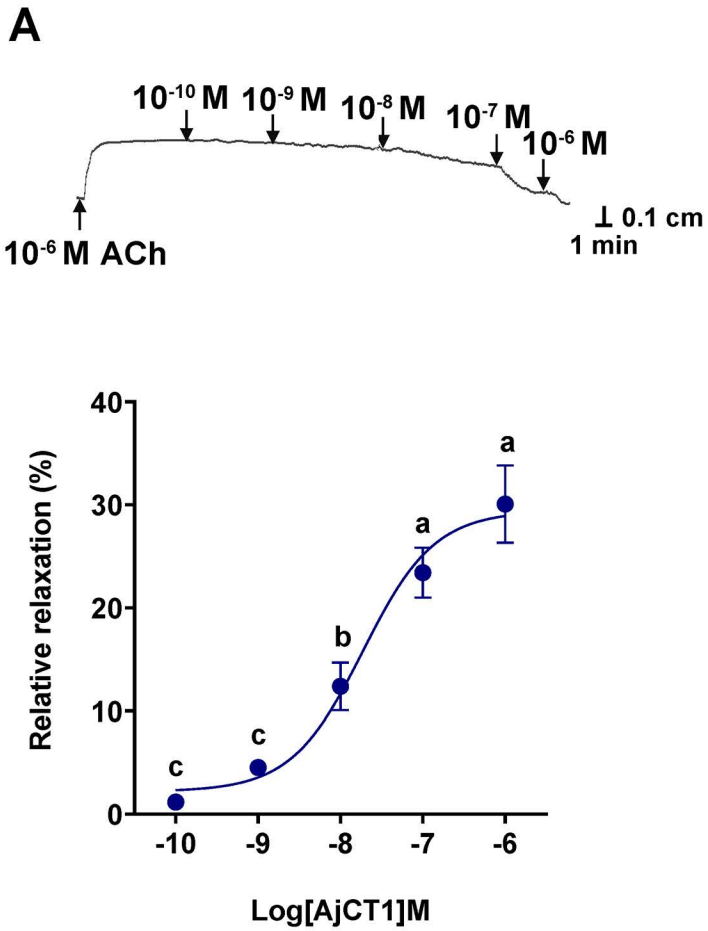
A
10-10 M
10-9 M
10-8 M
10-7 M
10-6 M
10-6 M ACh
0.1 cm
1 min
Relative relaxation (%)
Log[AjCT1]M
c
c
b
a
a

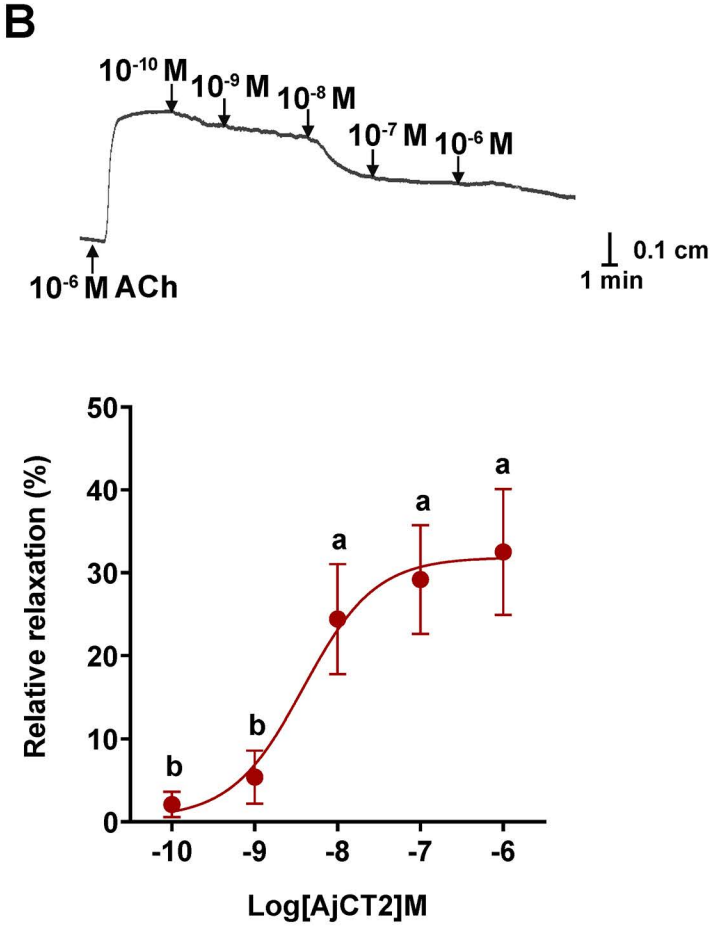
B
10-10 M
10-9 M
10-8 M
10-7 M
10-6 M
10-6 M ACh
0.1 cm
1 min
Relative relaxation (%)
Log[AjCT2]M
b
b
a
a
a

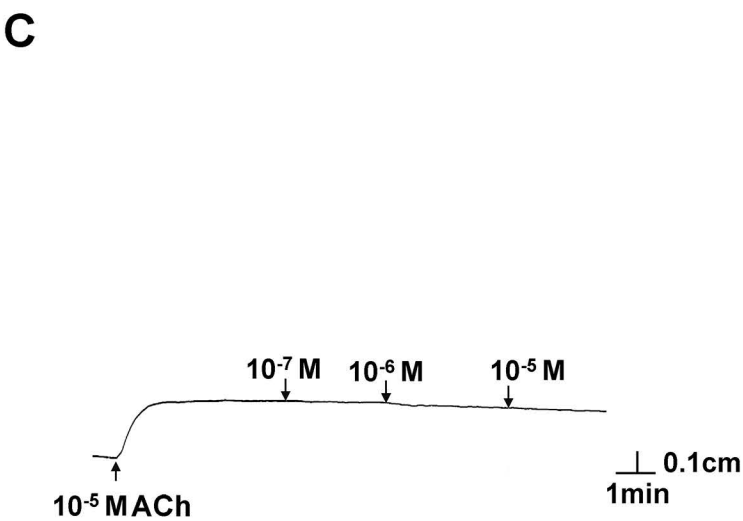
C
10-7 M
10-6 M
10-5 M
10-5 M ACh
0.1cm
1min

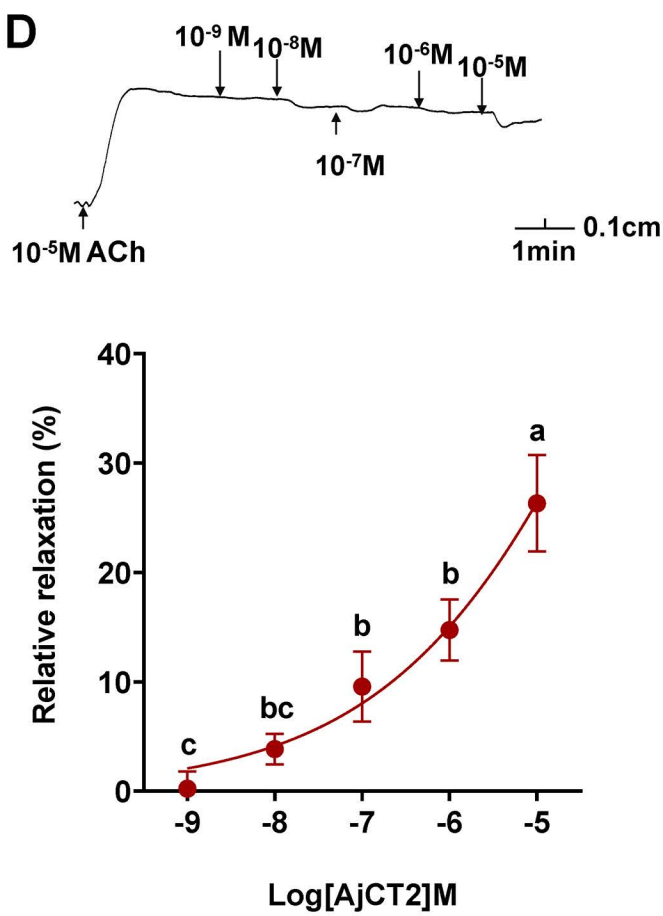
D
10-9 M
10-8M
10-6M
10-5M
10-7M
10-5M ACh
0.1cm
1min
Relative relaxation (%)
Log[AjCT2]M
c
bc
b
b
a

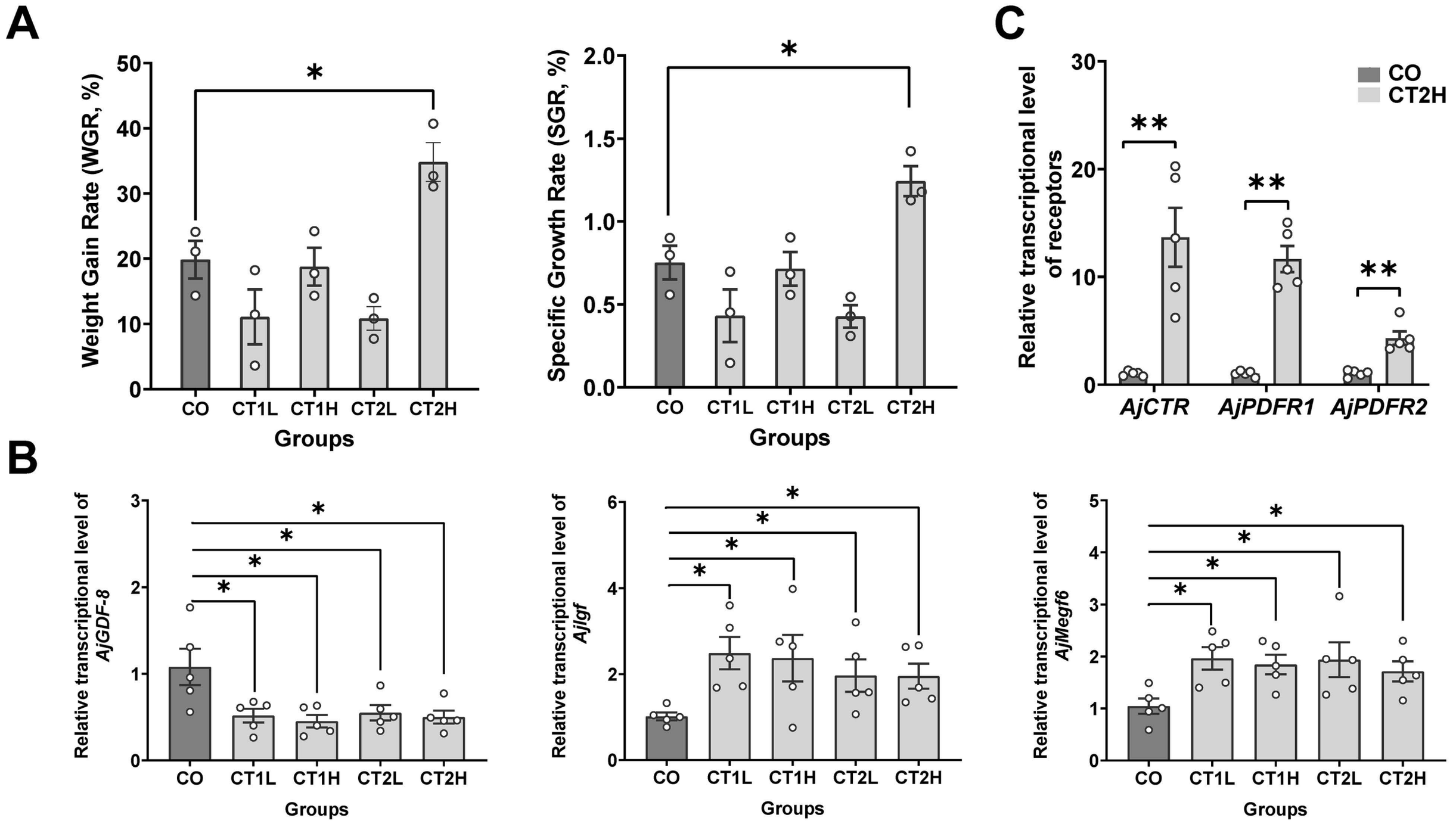
A
Weight Gain Rate (WGR, %)
50
40
30
20
10
0
*
CO
CT1L
CT1H
CT2L
CT2H
Groups
Specific Growth Rate (SGR, %)
2.0
1.5
1.0
0.5
0.0
*
CO
CT1L
CT1H
CT2L
CT2H
Groups
C
Relative transcriptional level of receptors
30
20
10
0
CO
CT2H
**
**
**
AjCTR
AjPDFR1
AjPDFR2
B
Relative transcriptional level of AjGDF-8
3
2
1
0
*
*
*
*
CO
CT1L
CT1H
CT2L
CT2H
Groups
Relative transcriptional level of Ajlgf
6
4
2
0
*
*
*
*
CO
CT1L
CT1H
CT2L
CT2H
Groups
Relative transcriptional level of AjMegf6
5
4
3
2
1
0
*
*
*
*
CO
CT1L
CT1H
CT2L
CT2H
Groups

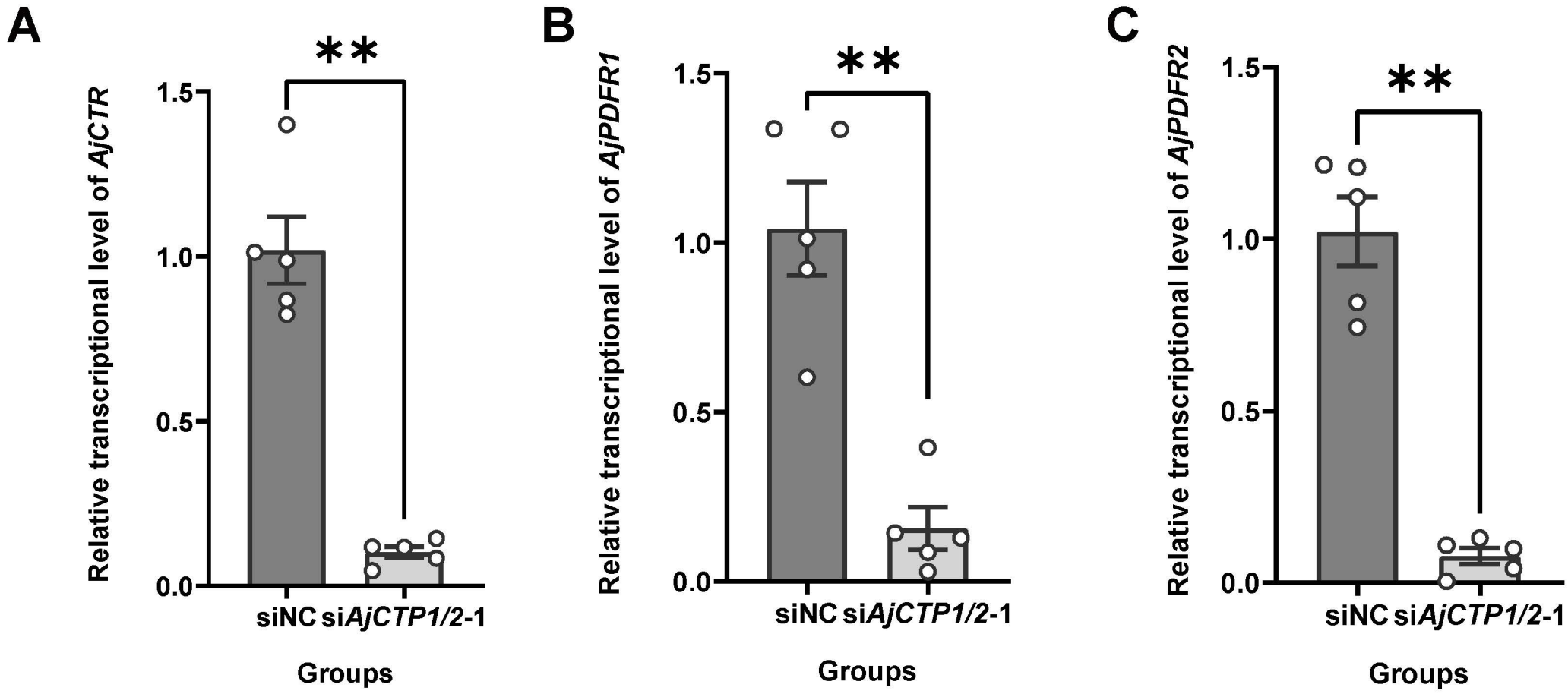
A
**
Relative transcriptional level of AjCTR
1.5
1.0
0.5
0.0
siNC
siAjCTP1/2-1
Groups
B
**
Relative transcriptional level of AjPDFR1
1.5
1.0
0.5
0.0
siNC
siAjCTP1/2-1
Groups
C
**
Relative transcriptional level of AjPDFR2
1.5
1.0
0.5
0.0
siNC
siAjCTP1/2-1
Groups

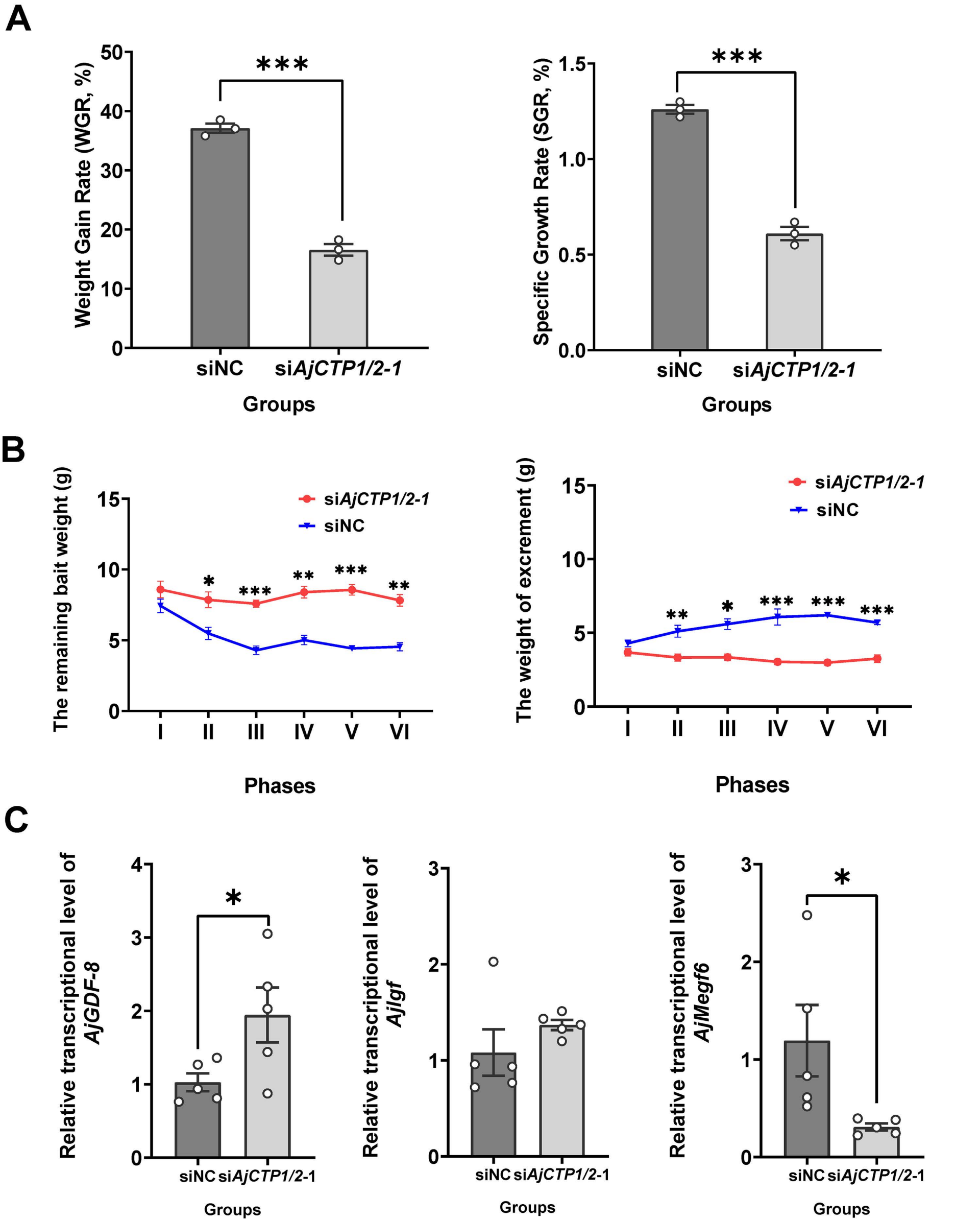
A
Weight Gain Rate (WGR, %)
50
40
30
20
10
0
***
siNC
siAjCTP1/2-1
Groups
Specific Growth Rate (SGR, %)
1.5
1.0
0.5
0.0
***
siNC
siAjCTP1/2-1
Groups
B
The remaining bait weight (g)
15
10
5
0
siAjCTP1/2-1
siNC
*
***
**
***
**
I
II
III
IV
V
VI
Phases
The weight of excrement (g)
15
10
5
0
siAjCTP1/2-1
siNC
**
*
***
***
***
I
II
III
IV
V
VI
Phases
C
Relative transcriptional level of AjGDF-8
4
3
2
1
0
*
siNC
siAjCTP1/2-1
Groups
Relative transcriptional level of AjIgf
3
2
1
0
siNC
siAjCTP1/2-1
Groups
Relative transcriptional level of AjMegf6
3
2
1
0
*
siNC
siAjCTP1/2-1
Groups

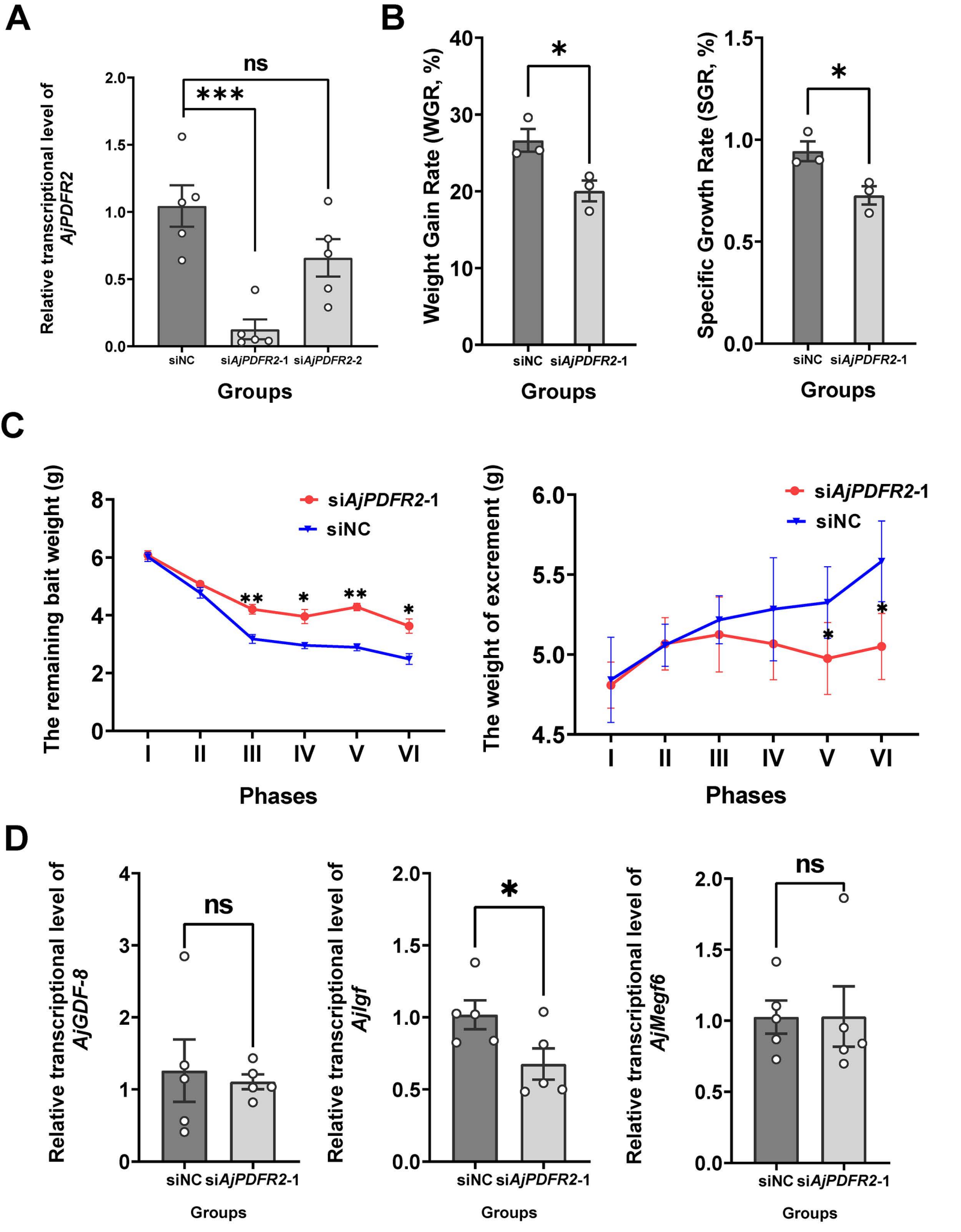
A
ns
***
Relative transcriptional level of AjPDFR2
2.0
1.5
1.0
0.5
0.0
siNC
siAjPDFR2-1
siAjPDFR2-2
Groups
B
*
Weight Gain Rate (WGR, %)
40
30
20
10
0
siNC
siAjPDFR2-1
Groups
*
Specific Growth Rate (SGR, %)
1.5
1.0
0.5
0.0
siNC
siAjPDFR2-1
Groups
C
The remaining bait weight (g)
8
6
4
2
0
siAjPDFR2-1
siNC
**
*
**
*
I
II
III
IV
V
VI
Phases
The weight of excrement (g)
6.0
5.5
5.0
4.5
siAjPDFR2-1
siNC
*
*
I
II
III
IV
V
VI
Phases
D
Relative transcriptional level of AjGDF-8
4
3
2
1
0
ns
siNC
siAjPDFR2-1
Groups
Relative transcriptional level of Ajlgf
2.0
1.5
1.0
0.5
0.0
*
siNC
siAjPDFR2-1
Groups
Relative transcriptional level of AjMegf6
2.0
1.5
1.0
0.5
0.0
ns
siNC
siAjPDFR2-1
Groups

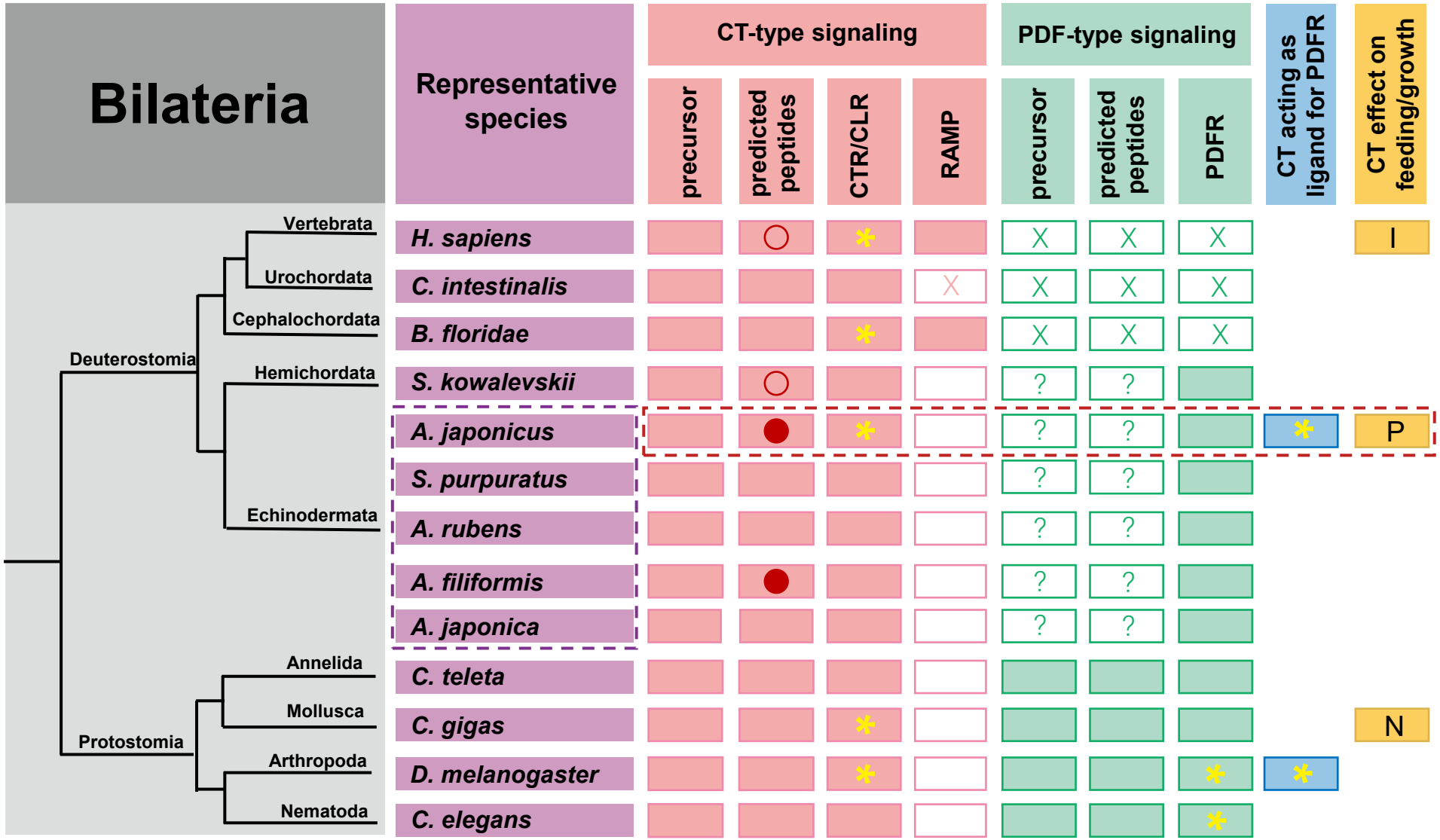
Bilateria
Representative species
CT-type signaling
PDF-type signaling
precursor
predicted peptides
CTR/CLR
RAMP
precursor
predicted peptides
PDFR
CT acting as ligand for PDFR
CT effect on feeding/growth
Deuterostomia
Vertebrata
Urochordata
Cephalochordata
Hemichordata
Echinodermata
Protostomia
Annelida
Mollusca
Arthropoda
Nematoda
H. sapiens
C. intestinalis
B. floridae
S. kowalevskii
A. japonicus
S. purpuratus
A. rubens
A. filiformis
A. japonica
C. teleta
C. gigas
D. melanogaster
C. elegans
I
P
N